

Dissertation zur Erlangung des Doktorgrades
der Fakultät für Biologie
der Ludwig-Maximilians-Universität München

The novel sumoylation enhancer RSUME is implicated in pituitary tumor pathogenesis



Shan, Bing

From Zhengzhou, P. R. China

August, 2010

Erstgutachter: Prof. Rainer Landgraf
Zweitgutachter: Prof. Elisabeth Weiß
Tag der mündlichen Prüfung: 02-12-2010

Table of Contents

1	Introduction	1
1.1	Pituitary gland	1
1.1.1	Anatomy of Pituitary gland	1
1.1.2	Blood supply and vascularization of pituitary gland	4
1.2	Pituitary adenomas	6
1.2.1	Prolactinomas	7
1.2.2	Somatotroph adenomas	8
1.2.3	Corticotroph adenomas	9
1.2.4	Thyrotroph adenomas	9
1.2.5	Gonadotroph adenomas	10
1.2.6	Non-functioning adenomas	10
1.2.7	Plurihormonal adenomas	11
1.2.8	Pituitary carcinomas	12
1.3	Pathogenesis of pituitary adenomas	12
1.3.1	Genetic abnormalities of proto-oncogenes and anti-proliferative signals	12
1.3.2	Over-expression of proto-oncogenes and proliferative signals	13
1.3.3	Down-regulation of tumor suppressors and inhibitory signals	14
1.3.4	Endocrine specific mechanisms	14
1.4	General overview of angiogenesis	15
1.5	Angiogenesis in pituitary adenomas	17
1.6	Sumoylation and RSUME	18
1.7	Hypoxia-inducible factor 1 (HIF-1) α	21
1.8	VEGF	25
2	Aim of this study	27
3	Materials and methods	28
3.1	Reagents	28
3.2	Solutions	30
3.3	Human pituitary and pituitary adenoma tissues	32
3.3.1	Tissues used for investigation of HIF-1 α , VEGF and RSUME mRNA expression	32
3.3.2	Tissues used for primary cell culture	33

3.4	RNA isolation	34
3.5	Reverse Transcriptase- Polymerase Chain Reaction	35
3.6	Cell culture and stimulation experiments	36
3.7	Cell counting	37
3.8	Transfection of siRNA against RSUME	37
3.8.1	Transfection of siRNA against mouse RSUME in pituitary cell lines	38
3.8.2	Transfection of siRNA against human RSUME in primary human pituitary adenoma cells	39
3.9	Western blot analysis	39
3.10	Immunofluorescence assay	41
3.11	Enzyme-Linked Immunosorbent Assay (ELISA)	43
3.12	Proliferation assay	44
3.13	Apoptosis detection	44
3.14	Statistics	46
4	Results	48
4.1	HIF-1 α , VEGF and RSUME mRNA expression in human normal pituitaries and pituitary adenomas	48
4.2	Effect of hypoxia mimicking conditions on RSUME mRNA expression	49
4.3	Effect of hypoxia mimicking conditions on HIF-1 α protein expression	51
4.4	Effect of hypoxia mimicking conditions on VEGF expression	53
4.5	Effect of RSUME knockdown on HIF-1 α and VEGF production	55
4.5.1	In mouse pituitary cell lines	55
4.5.2	In primary human pituitary tumor cell cultures	61
4.6	Effect of RSUME knockdown on proliferation and apoptosis in mouse pituitary cell lines	63
5	Discussion	67
6	Summary	76
7	References	78
8	Abbreviations	98
9	Acknowledgements	101
	Curriculum Vitae	103

1 Introduction

1.1 Pituitary gland

1.1.1 Anatomy of Pituitary gland

The pituitary gland is a small (pea-sized in humans) endocrine gland, lies in close proximity to the hypothalamus at the base of brain, and is protected by a bony cavity structure of the sphenoid bone called sella turcica (also known as Turkish saddle) (Figure 1). The pituitary gland is regulated by the central nervous system to control normal homeostasis through neuroendocrine pathways involving the hypothalamus. By feedback effects from peripheral target gland hormones, the hypothalamus secretes stimulatory and inhibitory hormones to regulate pituitary gland function. Under control of hypothalamus, the pituitary gland is a central regulator, responsible for the producing trophic hormones, and these hormones affect peripheral endocrine glands which are essential for growth, reproduction, metabolism, development, adaptation to external environmental changes, and stress.

The pituitary gland is composed of three compartments which are anterior (adenohypophysis), posterior (neurohypophysis) and intermediate lobe. The anterior pituitary arises from a depression in the dorsal wall of the pharynx (stomodial part) known as Rathke's pouch (Kelberman and Dattani 2007). It consists of two anatomical regions known as the pars tuberalis and pars distalis. The pars distalis represents the majority of the anterior pituitary and is where the pituitary hormone production occurs. The function of the anterior pituitary is to synthesize and secrete important endocrine hormones, such as adrenocorticotrophic hormone (ACTH), thyroid-stimulating hormone (TSH), prolactin (PRL), growth hormone (GH), follicle-stimulating hormone (FSH), and luteinizing hormone (LH). These hormones are produced by specific types of endocrine cells, and work on target glands or tissues, regulating corresponding release of hormones and several processes of human physiology (Table 1). The anterior pituitary itself is regulated by hypothalamic hormones which are transported from hypothalamus by a system of blood vessels called hypothalamo-hypophyseal portal system.

Table 1. Anterior pituitary hormones and their control (Nussey and Whitehead 2001)

Hormone	Target organs	Effect	Secretory cell types (% of pituitary cell population)	Hypothalamic hormone	Predominant hypothalamic nucleus of synthesis
Adrenocorticotrophic hormone (ACTH)	Adrenal gland	Stimulates glucocorticoids; induces stress response	Corticotroph (15%-20%)	CRH (+)	Paraventricular, supraoptic
Growth hormone (GH)	Liver; adipose tissue	Stimulates IGF-1; promotes bone and muscle growth; lipid and carbohydrate metabolism	Somatotroph (40%-50%)	GHRH (+) Somatostatin (-)	Arcuate, anterior periventricular
Prolactin (PRL)	Ovary, mammary gland	Stimulates estrogens/progesterone; milk production	Lactotroph (10%-25%)	TRH (+) Dopamine (-)	Arcuate, paraventricular
Luteinizing hormone (LH) Follicle-stimulating hormone (FSH)	Gonads	Stimulates sex hormones; regulates the development, growth, pubertal maturation of the reproductive system	Gonadotroph (10-15%)	GnRH (+)	Arcuate
Thyroid-stimulating hormone (TSH)	Thyroid gland	Stimulates thyroid hormone; regulates thyroid function	Thyrotroph (3%-5%)	TRH (+) Somatostatin (-)	Paraventricular, anterior periventricular

CRH, Corticotropin-releasing hormone; GHRH, growth-hormone-releasing hormone; TRH, Thyrotropin-releasing hormone; GnRH, Gonadotropin-releasing hormone. (+), stimulatory; (-), inhibitory.

Among the endocrine cells scattered pluripotent progenitor cells, stem cells, and folliculostellate cells (FS cells) (Landolt, et al. 2006). FS cells are of neuro-ectodermal origin, and represent 5% of anterior pituitary cell population (Landolt, et al. 2006). They are immunopositive for S-100 protein and glial fibrillary acidic protein (GFAP), and are characterized by their star-like morphology and their ability of forming follicles (Allaerts and Vankelecom 2005; Jin, et al. 2001; Kagayama 1965; Rinehart and Farquhar 1953). They not only act as supporting cells for the endocrine cells, but also offer an intrapituitary communication system through gap junctions and their long cytoplasmic processes surround the neighboring endocrine cells (Acosta, et al. 2010; Fauquier, et al. 2001; Inoue, et al. 1999; Morand, et al. 1996). FS cells do not produce hormones but express interleukin-6 (IL-6), basic fibroblast growth factor (bFGF), vascular endothelial growth factor (VEGF), transforming growth factor-beta (TGF- β), platelet-derived growth factor-A (PDGF-A), PDGF-B and some cytokine and hormone receptors, suggesting that they are implicated in regulation of hormone secretion, angiogenesis promotion, formation and permeability of blood vessels by auto- and paracrine manner (Inoue, et al. 1999; Kowarik, et al. 2010; Lohrer, et al. 2001; Lohrer, et al. 2000; Renner, et al. 2009; Renner, et al. 2002; Vlotides, et al. 2009).

The posterior pituitary gland develops by the evagination of neural tissue from the floor of the third ventricle (Mehta and Dattani 2008). It is mainly composed of the terminals of the distal axons which extend from the magnocellular neurons of supraoptic and paraventricular nuclei in hypothalamus. Besides axons, the posterior pituitary also contains glial cells called pituicytes which surround the axon projections. Two hormones named oxytocin and arginine vasopressin (AVP) are produced by the hypothalamus and these hormones are transported through extended axons to the posterior pituitary where they are stored and released as required under hypothalamic control (di Iorgi, et al. 2009). Pituicytes were reported to regulate the release of these two hormones by morphological changes (Rosso and Mienville 2009; Theodosis 2002). Oxytocin increases the uterine contraction during labor and stimulates lactation, and recently, some studies have shown the implication of oxytocin in social memory and attachment, sexual and maternal behavior, human bonding and trust, and aggression (Lee, et al. 2009). AVP is involved in regulating body's retention of water. Additionally, AVP has primarily been implicated in male-typical social behaviors, including aggression and pair-bond formation, and in stress-responsiveness (Heinrichs, et al. 2009).

The intermediate lobe, which is the part between anterior pituitary and posterior pituitary, is derived from oral ectoderm together with the anterior pituitary (Mehta and Dattani 2008). It mainly contains melanotroph cells, which produce pro-opiomelanocortin (POMC) and release processed POMC products such as β -endorphin and α -melanocyte stimulating hormone (α -MSH) (Bicknell 2008; Saland 2001). In humans, in contrast to the mouse, the intermediate lobe largely disappears during embryogenesis, and fuses with the anterior lobe soon after birth, thought to be represented in the adult by cysts at the junction of anterior and posterior lobes (Kelberman, et al. 2009; McNicol 1986; Rasmussen 1930). The function of the intermediate lobe as defined in animals has no discrete anatomical location within human pituitary gland (McNicol 1986).

The pituitary stalk is the bridge between hypothalamus and pituitary gland, carrying neural and vascular connections, responsible for delivering hypothalamic hormones to the anterior pituitary and neural tracts from the hypothalamic nuclei to the posterior pituitary (Kelberman, et al. 2009; Mehta and Dattani 2008).

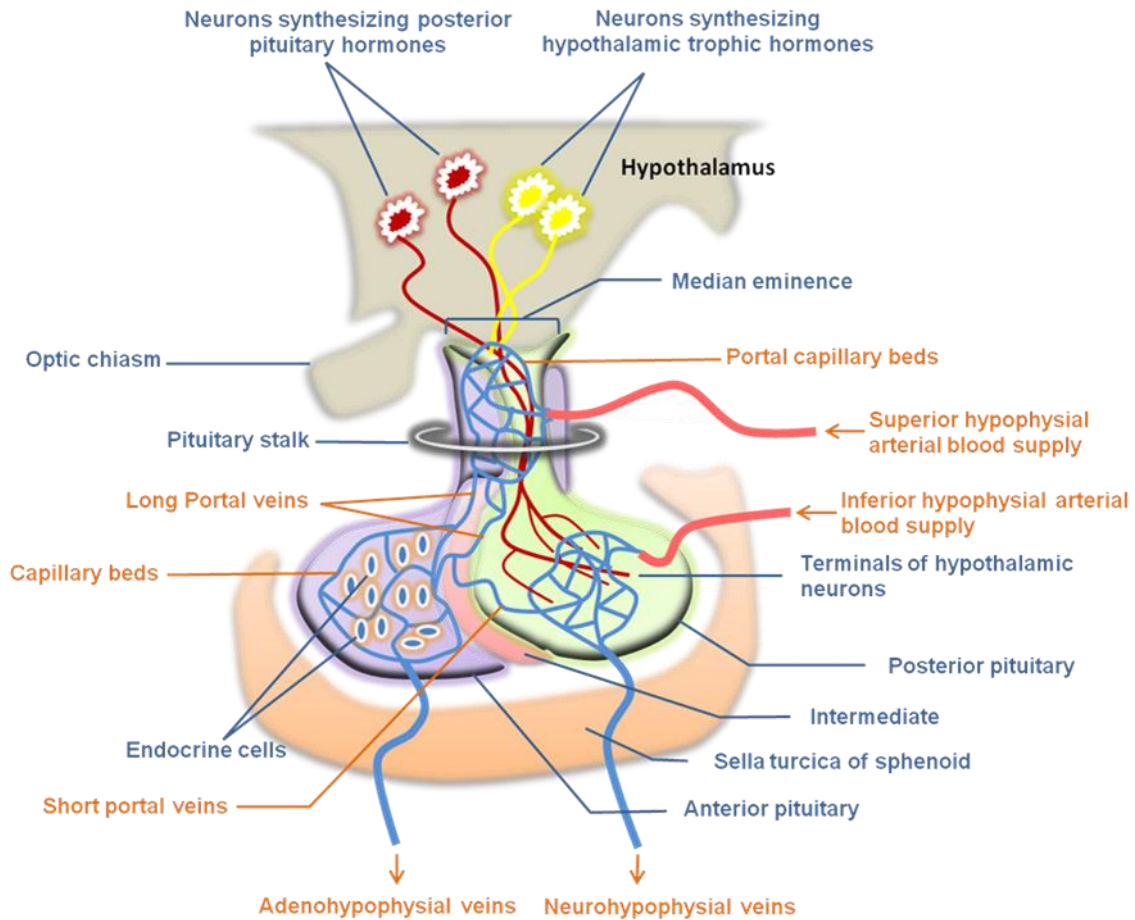


Figure 1. Anatomy and blood supply of pituitary gland. The pituitary gland is located below the hypothalamus, sitting in the sella turcica of sphenoid bone. It contains three parts: anterior, posterior and intermediate lobe. The hypothalamic trophic hormones which target endocrine cells in the anterior pituitary are produced by neurosecretory cells in the hypothalamus. The terminals of these neurosecretory cell axons reach to the median eminence capillaries, where the hormones are transported to and released into the anterior pituitary by portal blood system. The posterior hormones are produced by the magnocellular neurons in the hypothalamus and are released into the posterior pituitary through the extending magnocellular neuron axons. The secreted pituitary hormones diffuse into the systemic blood circulation through capillaries network in the anterior and posterior pituitary.

1.1.2 Blood supply and vascularization of pituitary gland

The pituitary gland is highly vascularized and gains blood supply through the hypothalamo-hypophyseal portal system (Figure 1). The capillaries of the hypothalamo-hypophyseal portal system are characterized by fenestrated endothelia, improving the delivery and diffusion of hormones (Nussey and Whitehead 2001). A separate branch of the internal carotid artery called superior hypophysial artery, which ascends from cavernous sinus, delivers the arterial

blood into portal capillary beds in the median eminence, and then reaches the pars distalis of anterior pituitary through the long portal veins that descend along the pituitary stalk, and interconnect the portal capillary beds and capillary beds inside the pars distalis (Leclercq and Grisoli 1983). In addition, approximately 30% of the total blood supply to the anterior pituitary is from the venous blood draining from the posterior pituitary through the short portal veins (Gross, et al. 1993). The pars distalis of anterior pituitary receives little or no arterial blood supply from the internal carotid artery (Bergland and Page 1978; Leclercq and Grisoli 1983). Rapidly enhanced magnetic resonance images (dynamic MRI) showed in man that the perfusion sequence of arterial blood first reached the posterior pituitary and the median eminence, followed by venous drainage to the anterior pituitary (Yuh, et al. 1994). The venous blood drainage from the anterior pituitary flows into systemic circulation through the adenohypophysial veins (Bergland and Page 1978). This blood flow pattern allows anterior pituitary to collect both hypothalamic factors and posterior information. The posterior pituitary is fed by the inferior hypophyseal artery branches distributing in the cavernous sinus. The venous drainage from the posterior pituitary goes into the neurohypophysial veins besides the short portal veins, and then enters the venous circulation.

Some studies about activators contributing to the angiogenesis and vascularization of pituitary gland have been performed. VEGF, which is a well known angiogenic factor, has been localized mainly in corticotroph, somatotroph and folliculostellate cells (Lloyd, et al. 1999; Vidal, et al. 1999; Yamamoto, et al. 1999). A study in rat using FITC-labeled gelatin injection, immunohistochemistry and in-situ RT-PCR showed that VEGF is involved in development of primary capillaries in median eminence and vascularization of pars distalis (Nakakura, et al. 2006). Pituitary autotransplantation demonstrated that VEGF expression in pituitary is not critical under hypothalamic control and hypoxia may play a crucial role in the induction of VEGF expression in the non-tumorous pituitary (Lombardero, et al. 2006). Leptin, which was reported to have a significant role in induction of neovascularization, is also expressed in pituitary gland, suggesting that it could play a role in pituitary angiogenesis (Cao, et al. 2001; Lloyd, et al. 2001; Ribatti, et al. 2007a). The mouse pituitaries with Prop1 (Prophet of pituitary transcription factor 1) gene mutations are poorly vascularized and dysmorphic, with a striking elevation in apoptosis, indicating that Prop 1 is implicated in pituitary vascularization during the pituitary development (Ward, et al. 2006). bFGF, a stimulator of angiogenesis, has been shown to be localized in gonadotroph cells, FS cells and endothelial cells in the anterior pituitary, and is released by cellular disruption during pituitary vascular development in rats (Schechter, et al. 1996; Schechter, et al. 1993).

1.2 Pituitary adenomas

Pituitary adenomas, arising from adenohypophysial cells, are the most common tumors in the sella region. The majority of pituitary adenomas grow slowly, and are defined as benign because of the absence of metastases, but some exhibit a faster growth pace and can be highly invasive (Kovacs, et al. 2001). About 15–25% of cases demonstrate tumor invasion into the hypophysis or cavernous sinus at initial diagnosis (Yoshida and Teramoto 2007). Pituitary adenomas may cause serious health problems due to either compression of neighboring tissues (i.e. visual nerve) or major changes in endocrine homeostasis resulted from the hormone excess syndromes they cause. It is difficult to determine the true incidence of the pituitary adenomas, because they are often asymptomatic (Swearingen and Biller 2008b). They are present in approximately 16.9% of the general population, and represent up to 25% of all intracranial tumors (Ezzat, et al. 2004; Oberholtzer 1999). There are no significant differences in the frequency of pituitary adenomas between men and women, if the types are ignored and both surgically and autopsy obtained tissues are combined (Kovacs, et al. 2001). Although rarely diagnosed in prepubertal age, pituitary adenomas can be found in every age group, from infancy to senescence (Kovacs, et al. 2001). The prevalence, which increases with advancing age, is about 14% and 22% in postmortem and imaging studies, respectively (Swearingen and Biller 2008b).

Pituitary adenomas can be classified in various ways, such as functional, anatomic/radiologic, histologic, immunohistochemical, ultrastructural, and clinicopathologic (Asa and Ezzat 2009). The functional classification, based on hormonal activity, divides pituitary adenomas into six groups: ACTH-producing adenomas, linked to Cushing disease and Nelson's syndrome; GH-producing adenomas, linked to acromegaly and/or gigantism; PRL-producing adenomas, linked to hyperprolactinemia, TSH-producing tumors linked to thyroid dysfunction; rare clinically detectable gonadotroph adenomas, linked to hypogonadism due to paradoxical down-regulation of function; non-functioning adenomas, clinically endocrinologically inactive adenomas, unaccompanied with detectable hormone activity (Asa and Ezzat 2009; Kovacs, et al. 2001). The anatomic/radiologic classification is based on size and degree of local invasion. On the basis of their size, pituitary adenomas can be separated into macroadenomas with more than 10 mm in their largest diameter and microadenomas with less volume (Kovacs, et al. 2001). The histologic classification is based on the tinctorial characteristics of the cell cytoplasm, and separates pituitary adenomas into acidophilic, basophilic and chromophobic tumors (Asa and Ezzat 2009; Kovacs, et al. 2001). This classification has limited value, since it fails to take into consideration hormone production, cellular derivation and structure–function relationship, and has been largely abandoned (Kovacs, et al. 2001). The immunohistochemical classification is based on the detection of antigens in tissue, providing

the information primarily about hormone content, additionally about transcription factors and keratins (Asa and Ezzat 2009; Kovacs, et al. 2001). The ultrastructural classification with application of electron microscopy is based on subcellular features of cell differentiation. The electron microscopy provides conclusive information on the cellular composition and secretory activity of the tumor, and it's a very valuable tool for research. However, the ultrastructural investigation is time consuming, expensive and has difficulties in correct diagnosis (Asa and Ezzat 2009; Kovacs, et al. 2001). Clinicopathologic classification, based on both morphological and clinical features, is most effective and practical (Table 2).

Table 2. Clinicopathological classification of pituitary adenomas (Asa and Ezzat 2009)

Functioning adenomas	Non-functioning adenomas
GH-PRL-TSH family	
Adenomas causing GH excess	
Densely granulated somatotroph adenomas	
Sparsely granulated somatotroph adenomas	Silent somatotroph adenomas
Mammotroph adenomas	
Adenomas causing hyperprolactinemia	
Lactotroph adenomas	Silent lactotroph adenomas
Acidophil stem cell adenomas	
Adenomas causing TSH excess	
Thyrotroph adenomas	Silent thyrotroph adenomas
ACTH family	
Adenomas causing ACTH excess	
Densely granulated corticotroph adenomas	Silent corticotroph adenomas (Type I)
Sparsely granulated corticotroph adenomas	Silent corticotroph adenomas (Type II)
Gonadotroph family	
Adenomas causing gonadotropin excess	
Gonadotroph adenomas	Silent gonadotroph adenomas (null-cell adenomas, oncocyomas)
Unclassified adenomas	
Unusual plurihormonal adenomas	Immunonegative adenomas

ACTH, adrenocorticotropin; GH, growth hormone; PRL, prolactin; TSH, thyrotropin-stimulating hormone.

1.2.1 Prolactinomas

Prolactinomas (also known as lactotroph adenomas) are the most common type of pituitary adenomas. It arises from lactotroph cells of anterior pituitary, secreting prolactin (PRL). They comprise 45% of the clinical pituitary tumor cases with an incidence of 6 to 10 per million per year and a prevalence of 60 to 100 cases per million in clinical series (Ciccarelli, et al. 2005). Prolactinomas are the most frequent cause of PRL excess, and usually the most relevant clinical manifestations are infertility, gonadal and sexual dysfunction in both sexes (Gillam, et al. 2006; Schlechte 2003). The number of these tumors in surgical series is very low, due to the success of dopamine agonist therapy.

There are three variants of prolactinomas: sparsely granulated and densely granulated lactotroph adenomas and the rare, but aggressive, acidophil stem cell tumor (Asa and Ezzat 2009). The most common variant is sparsely granulated lactotroph adenomas which consist of chromophobic tumor cells (Asa and Ezzat 2009). Immunohistochemistry shows strong immunostaining for PRL with paranuclear globular pattern corresponding to the Golgi area (Asa and Ezzat 2009). Densely granulated lactotroph adenomas are much less common than the sparsely granulated variant (Asa and Ezzat 2009). Differing from the sparsely granulated adenomas, these tumors cells are acidophilic and show diffuse cytoplasmic positivity for PRL (Asa and Ezzat 2009). The acidophil stem cell adenomas are composed of oncocytic cells with large cytoplasmic vacuoles corresponding to giant mitochondria (Asa and Ezzat 2009). These tumors may have an unusual bihormonal profile with diffuse immunoreactivity for PRL and scant immunoreactivity for GH (Asa and Ezzat 2009).

1.2.2 Somatotroph adenomas

Somatotroph adenomas, which arise from GH-producing cells, account for 10~15% of pituitary adenomas (Asa and Ezzat 2009). GH hypersecreting tumors cause gigantism in young patients and acromegaly in adults (Asa and Ezzat 2009). The incidence of acromegaly is about 2 to 4 per million with a mean age at presentation of 40–50 years (Ciccarelli, et al. 2005). Morphologically, the majority of these tumors are macroadenomas and frequently have suprasellar growth and expansion to the lateral sellar wall (Swearingen and Biller 2008b).

The subtypes of these adenomas include densely granulated, sparsely granulated somatotroph adenomas and mammosomatotroph adenomas (Swearingen and Biller 2008b). Densely granulated somatotroph adenomas are the most common finding in adult acromegaly, and mammosomatotroph adenomas that produce both GH and PRL are the most frequent findings in childhood-onset gigantism and in young patients with acromegaly (Asa and Ezzat 2009). Both of these two types of adenomas express α -subunit, and resemble normal somatotroph and mammosomatotroph cells (Asa and Ezzat 2009). They are characterized by acidophilic and densely granulated cytoplasm, strong and diffuse cytoplasmic immunoreactivity for GH, and strong nuclear immunoreactivity for Pit-1 (pituitary transcription factor-1) (Asa and Ezzat 2009; Kovacs, et al. 2001). The immunohistochemistry shows that the low molecular weight cytokeratins (CAM 5.2) in densely granulated somatotroph adenomas cells are of diffuse cytoplasmic pattern (Asa and Ezzat 2009; Kovacs, et al. 2001; Swearingen and Biller 2008b). In contrast, the sparsely granulated somatotroph adenomas with chromophobic and less granular cytoplasm have weak and focal GH immunoactivity and the staining for α -subunit is not identified (Asa and Ezzat 2009; Swearingen and Biller 2008b). The immunostaining for CAM 5.2 shows dot-like juxtannuclear aggregates corresponding to the

fibrous body (Asa and Ezzat 2009; Swearingen and Biller 2008b). However, they are usually nuclear immunopositive for Pit-1 like densely somatotroph adenomas (Asa and Ezzat 2009).

1.2.3 Corticotroph adenomas

The corticotroph adenomas which arise from ACTH-producing corticotroph cells comprise about 10%~15% of clinical cases of pituitary adenomas (Asa and Ezzat 2009). ACTH is overproduced by corticotroph adenomas which cause an excessive release of adrenal glucocorticoids leading to the different symptoms of Cushing's disease. The majority of corticotroph adenomas are microadenomas, softer and paler than the normal gland (Swearingen and Biller 2008b). Three variants of corticotroph adenomas are known: densely granulated corticotroph adenomas, sparsely granulated corticotroph adenomas and Crooke's cell adenomas (Swearingen and Biller 2008b). Cushing's disease is mostly caused by densely granulated corticotroph adenomas, which have densely granulated basophilic cytoplasm apparent with the classical hematoxylin and eosin stain (Asa and Ezzat 2009; Swearingen and Biller 2008b). The cytoplasm is also strongly PAS (Periodic acid-Schiff stain)-positive (Swearingen and Biller 2008b). The macroadenomas with lower florid hormone excess in patients are less common, and have sparsely granulated chromophobic cytoplasm and are less PAS-positive (Asa and Ezzat 2009; Swearingen and Biller 2008b). They may be associated with Nelson's syndrome in patients who have undergone bilateral adrenalectomy as treatment for pituitary Cushing's disease without initial identification of a discrete lesion (Asa and Ezzat 2009). The Crooke's cell adenomas are rare. The normal corticotroph cells respond to high levels of glucocorticoids by developing Crooke's hyalinization corresponding to intracytoplasmic accumulation of cytokeratins 7 and 8, which are intermediate filaments on electron microscopy (Asa and Ezzat 2009; Swearingen and Biller 2008b). Usually the corticotroph adenomas don't have this marker of feedback suppression by glucocorticoids; however, the Crooke's adenomas have the same change as nontumorous corticotroph cells (Asa and Ezzat 2009; Kovacs and Horvath 1986; Swearingen and Biller 2008b). They can be associated with Cushing's disease as well (Asa and Ezzat 2009).

1.2.4 Thyrotroph adenomas

The thyrotroph adenomas are rare and make up to 1% of pituitary adenomas (Asa and Ezzat 2009). They can be associated with hyperthyroidism or hypothyroidism, but the majority are clinically nonfunctioning (Asa and Ezzat 2009; Swearingen and Biller 2008b). The thyrotroph adenomas in general are macroadenomas and invasive, and mass effects with visual-field disturbances are common (Asa and Ezzat 2009). The tumor cells are chromophobic and can have small cytoplasmic granules with PAS stain (Swearingen and Biller 2008b).

Immunohistochemistry shows positivity for TSH and variable staining for α -subunit; some also express GH and PRL (Swearingen and Biller 2008b). Characteristically, the tumor cells with significant nuclear pleomorphism have a polygonal or elongated shape and resemble nontumorous thyrotroph cells (Asa and Ezzat 2009).

1.2.5 Gonadotroph adenomas

The gonadotroph adenomas comprise the majority of clinically nonfunctioning adenomas (Swearingen and Biller 2008b), and clinical manifestations of gonadotropin excess are rare. The elevated serum FSH level induced by the gonadotroph adenomas led to ovarian enlargement in a 10-year old girl (Tashiro, et al. 1999). A case of clearly high circulating immunoreactive FSH due to a functioning FSH-secreting gonadotroph adenoma in a man with the MEN 1 syndrome was also reported (Sztal-Mazer, et al. 2008). The tumor cells exhibit strong nuclear staining with SF-1 (steroidogenic factor-1), but variable and often only focal positive reaction for α -subunit, β -FSH, and β -LH, and show variable degrees of differentiation (Asa and Ezzat 2009). Well-differentiated tumor cells are elongated, with the nucleus occupying one pole and secretory granules accumulating at the opposite pole (Asa and Ezzat 2009). In contrast, poorly differentiated cells are generally ovoid or polygonal and lack polarity (Asa and Ezzat 2009).

1.2.6 Non-functioning adenomas

The non-functioning adenomas lack detectable hormone activity, and cause no signs or symptoms secondary to hormonal hypersecretion by the tumor (Greenman and Stern 2009). They typically tend to be present with signs of mass effects such as headaches, visual field defects and hypopituitarism, when the tumor has reached the stage of a macroadenoma, and are usually large at the time of diagnosis (Greenman and Stern 2009; Snyder 1985). Non-functioning adenomas comprise roughly 50% of pituitary tumors in surgical series (Saeger, et al. 2007). The vast majority of these lesions are actually silent gonadotroph adenomas, accounting for 85% of non-functioning adenomas, and they are morphologically and pathogenetically identical to functioning gonadotroph adenomas (Asa and Ezzat 2009; Greenman and Stern 2009). They are positively stained with FSH, LH and their subunits (Greenman and Stern 2009). In a minority of patients, intact gonadotropins, mainly FSH, may be detected on basal conditions in vivo, but hormone-related symptoms are rare (Greenman and Stern 2009). Based on hormone and transcription factor staining, the non-functioning adenomas also include silent somatotroph adenomas, silent prolactinomas, silent thyrotroph adenomas and silent corticotroph adenomas (Table 3) (Greenman and Stern 2009). They may express hormones but do not secrete them, and their lack of clinical manifestation may be

attributable to reduced hormonal activity or to synthesis of nonfunctional hormone products (Asa and Ezzat 2009; Greenman and Stern 2009). The majority are the silent corticotroph adenomas which express ACTH (Greenman and Stern 2009). The silent type 3 adenomas may express several pituitary hormones and transcription factors (Greenman and Stern 2009). Poorly differentiated gonadotroph adenomas cells are often classified as null-cell or undifferentiated adenomas because of focal or weak immunoreactivity, but they are positive stained with SF-1 and can secrete gonadotropins *in vitro*, indicating their gonadotroph origin (Asa and Ezzat 2009; Greenman and Stern 2009). The truly null cell adenomas stain negatively both to pituitary hormones and transcription factors (Greenman and Stern 2009). Additionally, most oncocytomas represent silent gonadotroph adenomas with extensive oncocytic change (Asa and Ezzat 2009).

Table 3. Clinicopathological classification of non-functioning adenomas (Greenman and Stern 2009)

Tumor Type	Transcription factors	Hormone staining
Silent gonadotroph adenomas	SF-1, GATA-2, ER	β -FSH, β -LH, α -subunit
Silent somatotroph adenomas	Pit-1	GH
Silent prolactinomas	Pit-1, ER	PRL
Silent thyrotroph adenomas	Pit-1, TEF, GATA-2	β -TSH, α -subunit
Silent corticotroph adenomas	Tpit	ACTH
Null cell adenomas	None	None
Silent subtype 3 adenomas		Multiple

SF-1, steroidogenic factor-1; ER, estrogen receptor; Pit-1, pituitary transcription factor-1; TEF, thyrotropin embryonic factor; GATA-2, GATA binding protein-2; Tpit-1, T-box transcription factor.

1.2.7 Plurihormonal adenomas

Plurihormonal pituitary adenomas are capable of producing more than one hormone (Kovacs, et al. 2001). Morphologically, they can be divided into monomorphous and plurimorphous tumors (Kovacs, et al. 2001). Monomorphous plurihormonal adenomas consist of one cell population which produces two or more hormones, and they can not be explained by a common cellular origin (Kovacs, et al. 2001; Swearingen and Biller 2008b). Plurimorphous adenomas, representing mixed adenomas, are composed of two or more distinct cell types, each producing one hormone (Kovacs, et al. 2001). The 2004 WHO classification includes only monomorphous adenomas in the category of plurihormonal adenomas, which excludes adenomas with any combination of GH, PRL and TSH, or FSH and LH. By this definition these tumors are rare (Swearingen and Biller 2008b).

1.2.8 Pituitary carcinomas

Pituitary carcinomas are defined based on the presence of metastasis (Swearingen and Biller 2008b). In contrast to the high frequency of local invasion, pituitary adenomas only rarely metastasize to distant locations in the central nervous system, lymphnodes, and liver (Asa and Ezzat 2009). The pituitary carcinomas represent approximately only 0.2% of operated pituitary neoplasms (Swearingen and Biller 2008b). Microscopically, the tumors have different degrees of high cell density, pleomorphism, necrosis, and invasion, but all of these characteristics can also be found in benign pituitary adenomas (Swearingen and Biller 2008b).

1.3 Pathogenesis of pituitary adenomas

The pathogenesis of pituitary adenomas has been intensively studied, but the exact mechanisms involved in pituitary cell transformation and tumorigenesis is still unclear. X-chromosomal inactivation analysis demonstrated that pituitary adenomas arise from the replication of a single transformed pituitary cell, indicating that they are monoclonal neoplasms (Alexander, et al. 1990; Gicquel, et al. 1992; Herman, et al. 1990; Schulte, et al. 1991). This observation also suggests that the tumor formation results from the growth advantage characteristics of the monoclonal transformed pituitary cell with either activation of proto-oncogenes or inactivation of tumor-suppressor genes.

A lot of etiologic factors involved in pituitary tumor formation have been extensively studied, including genetic abnormalities in pituitary tumors, over-expression of proto-oncogenes and proliferative signals, down-regulation of tumor suppressor genes and inhibitory signals, and hormonal dysregulation.

1.3.1 Genetic abnormalities of proto-oncogenes and anti-proliferative signals

Many common genetic defects in proto-oncogenes which occur frequently in human malignancies are not identified in most of pituitary adenomas (i.e. abnormalities of the Ras-family).

The mutations in the gene encoding the α subunit of Gs (GNAS1) frequently appear in about 30–40% GH-secretion adenomas, leading to constitutively active cAMP-dependent pathway (Landis, et al. 1989; Vallar, et al. 1987). However, these mutations infrequently occur in other tumors, i.e., in about 10% of non-functioning pituitary adenomas and less than 5% of ACTH-secreting adenomas (Tordjman, et al. 1993; Williamson, et al. 1995).

The aberrant expression of an N-terminally truncated variant of fibroblast growth factor (FGF) receptor-4 (ptd-FGFR4) has been detected in 40% of pituitary adenomas, and ptd-FGFR4 is constitutively phosphorylated in the absence of ligand and transformation *in vitro* and *in vivo* (Ezzat, et al. 2002).

Germline mutations of the tumor suppressor gene *MEN1* with LOH (loss of heterozygosity) inactivate the normal allele in tumors, resulting in familial pituitary adenomas associated with multiple endocrine type 1 (MEN1) (Chandrasekharappa, et al. 1997). However, *MEN1* mutations rarely occur in sporadic pituitary adenomas (Prezant, et al. 1998; Wenbin, et al. 1999; Zhuang, et al. 1997), although LOH have been found in the region of *MEN1* gene in 10~30% of sporadic pituitary adenomas and the expression of Menin is down-regulated in high percentage of cases with or without LOH. Therefore, allelic loss may be responsible for the lower menin levels in some, but not all, cases with low menin expression, and post-transcriptional mechanisms may be involved (Tanaka, et al. 1998; Theodoropoulou, et al. 2004).

Germline Inactivating mutations in the aryl hydrocarbon receptor (AHR) interacting protein (AIP) gene with LOH of the normal allele in familial presentation of somatotroph adenomas and prolactinomas have been reported (Vierimaa, et al. 2006). However, *AIP* mutations have not been identified in sporadic pituitary adenomas (DiGiovanni, et al. 2007).

Germline mutations in protein kinase-A (PKA) regulatory subunit 1 gene *PRKAR1* are responsible for Carney's complex, an autosomal dominant disorder associated with somatotroph adenomas and other endocrine tumors (Kirschner, et al. 2000a; Kirschner, et al. 2000b). However, no mutations of this gene were found in sporadic pituitary adenomas, although significantly reduced protein expression of this gene was shown in non-functioning and somatotroph adenomas (Kaltsas, et al. 2002; Lania, et al. 2004; Mantovani, et al. 2005; Sandrini, et al. 2002; Yamasaki, et al. 2003).

1.3.2 Over-expression of proto-oncogenes and proliferative signals

Cyclin proteins are cell cycle regulators, which promote cell progression by activating cyclin-dependent kinases (CDKs). It has been shown that cyclin proteins, especially cyclin D1, are over-expressed in aggressive non-functioning adenomas without cyclin D1 gene (*CCND1*) amplification, indicating that additional mechanisms are involved in the deregulating of cyclin D1 expression in human pituitary tumorigenesis. Moreover, cyclin E is preferentially present in corticotroph adenomas (Hibberts, et al. 1999; Jordan, et al. 2000).

The pituitary tumor transforming gene (*PTTG*) which is an estrogen-inducible gene responsible for chromosomal separation and mitosis during the cell division is mostly over-expressed in adenomas with a more than 50% increase (up to a 10-fold increase in some cases) in non-functioning, GH-, PRL-, and ACTH-producing adenomas compared with normal pituitaries, suggesting that *PTTG* is indeed involved in some manner in pituitary tumorigenesis (Zhang, et al. 1999); however, specific mutation of *PTTG* has not been shown in sporadic pituitary adenomas (Dworakowska and Grossman 2009). *PTTG* mediates the estrogen-induced up-regulation of growth factors with potent mitogenic and angiogenic activity, such as

fibroblast growth factor-2 (FGF-2) (Zhang, et al. 1999). FGF-2 (also known as basic or bFGF) is over-expressed in pituitary tumor cells (Ezzat, et al. 1995).

Akt, the best-characterized phosphorylation target of phosphatidylinositol 3-kinase (PI3K), which enhances cell proliferation by activating the serine-threonine kinase mTOR (mammalian target of rapamycin) is over-expressed (at both mRNA and protein levels) as well as over-activated (through phosphorylation) in all pituitary tumors, especially non-functioning pituitary adenomas (Musat, et al. 2005; Volarevic and Thomas 2001).

1.3.3 Down-regulation of tumor suppressors and inhibitory signals

The retinoblastoma protein (pRb), coded by *Rb1* gene, is a main inhibitor of cell cycle progression between G1 and S phases. The phosphorylation of the pRb by cyclin/CDK complex leads to inactive pRb and thus allowing a cell cycle transit from G1 to S phase (Musat, et al. 2004). Additionally, CDK inhibitors (CDKI) including Ink4 family (p15, p16, p18, for CDK4 and 6) and Kip/cip family (p21, p27, p57 for CDK2) are involved in regulation of cell cycle (Musat, et al. 2004). The vast majority of pituitary adenomas (90%) display alterations of the pRb pathway. In particular, promoter hypermethylation (resulting in transcription silencing) of the p15 (INK4b), p16 (INK4a) and pRb genes was detected in 32~36%, 59~71% and 29~35% of pituitary tumors, respectively (Ogino, et al. 2005; Yoshino, et al. 2007). It has been demonstrated that p27 (Kip1) protein expression level is lower in all types of pituitary adenomas without changes of the mRNA levels compared with normal pituitaries, especially in corticotroph adenomas and pituitary carcinomas, suggesting enhanced p27 protein degradation (Lidhar, et al. 1999; Yoshino, et al. 2007).

The pituitary tumor apoptosis gene (PTAG) which is a differentially methylated chromosome 22 CpG island-associated gene (C22orf3) has been recently identified (Bahar, et al. 2004). It has been shown that 80% of the pituitary adenomas failed to express this gene compared with normal pituitaries, and in this group approximately 20% showed methylation of the CpG islands of the PTAG promoter (Bahar, et al. 2004). The methylation of the promoter was invariably associated with loss of transcript expression (Bahar, et al. 2004).

ZAC, a zinc-finger protein that induces apoptosis and cell cycle, is highly expressed in the anterior pituitary gland, and is strongly down-regulated at both mRNA and protein expression level in non-functioning adenomas (Pagotto, et al. 2000).

1.3.4 Endocrine specific mechanisms

The vast majority of sporadic pituitary adenomas do not show hyperplasia in the surrounding tissue, suggesting that hormonal stimulation is not a primary etiologic mechanism in pituitary adenomas; however, hormone dysregulation and impaired feedback inhibition may be involved in development of the pituitary adenomas, concerning that the differentiation,

proliferation and hormone release of the adeno-hypophysial cells are under the strict control of hypothalamic neurohormones and regulated by the feedback mechanisms (Asa and Ezzat 2009; Swearingen and Biller 2008a).

High levels of CRH and vasopressin V3 receptors have been detected in ACTH-secreting adenomas without identified mutational changes in the genes (de Keyzer, et al. 1998). Glucocorticoid hormones regulate corticotroph function through specific negative feedback loop, and loss of glucocorticoid feedback might cause Cushing's disease (Asa and Ezzat 2009). A germline mutation of glucocorticoid receptor (GR) which results in glucocorticoid resistance by diminished ligand binding has been implicated as the cause of pituitary Cushing's disease in a small number of patients (Karl, et al. 1996a). However, rare GR mutations have been found in sporadic pituitary corticotroph tumors (Karl, et al. 1996b).

GH auto-regulation and Insulin-like growth factor-1 (IGF-1) regulate GH secretion through negative feedback inhibition (Dworakowska and Grossman 2009). The decreased expression of the GH receptors and IGF receptors in 18 somatotroph tumors (both at the mRNA and protein level) may be the cause of the continuous secretion of GH from the tumor despite high circulation levels of IGF-1 and GH; However, no somatic mutations of GH receptor mRNA was detected in that group, indicating that decreased feedback inhibition of GH due to somatic mutations of the coding region of the GH receptor is unlikely to be a common factor in the pathogenesis of GH-producing adenomas (Kola, et al. 2003).

Dopamine inhibits prolactin secretion through dopamine 2 receptor (D2R). D2R-deficient mice develop lactotroph adenomas, suggesting that inactivating mutations of this receptor might contribute to the development of lactotroph adenomas (Asa, et al. 1999). However, no mutations in the D2R gene have been found in human prolactinomas, including those dopaminergic drug resistant prolactinomas which frequently show a reduction of D2R transcript (Caccavelli, et al. 1994; Friedman, et al. 1994). Inactivation of the nerve growth factor (NGF) receptor (p75) gene results in D2R loss in dopamine-responsive cells and prevents D2R expression by NGF in dopamine-nonresponsive cells, which may account for some dopamine resistant prolactinomas (Asa and Ezzat 2009; Fiorentini, et al. 2002).

The mutations in the thyroid hormone receptor β isoform (TR β) causing diminished T3 binding resulted in reduced inhibition of TSH secretion in two TSH-secreting adenomas (Ando, et al. 2001).

1.4 General overview of angiogenesis

Angiogenesis is the process of new capillary formation by sprouting or by splitting from pre-existing blood vessels (Risau 1997). Angiogenesis by vessel sprouting is a multistep process. Firstly, after a stimulatory signal, the basement membrane is degraded by the proteolytic

enzymes (such as matrix metalloproteinases (MMPs) and plasminogen activators) released by activated endothelial cells (ECs), which leads to the formation of tiny sprouts penetrating the perivascular stroma. Next, the ECs at the sprout tip migrate toward the angiogenic stimulus and proliferate, whereby the ECs form a tubular structure by cell adhesion molecules which establish the polarity, luminal versus abluminal, followed by the formation of capillary loops, which leads to the development of functioning circulatory network. Finally, the new vessels are stabilized, and this process requires the recruitment of pericytes and vascular smooth muscle cells (VSMCs), which is regulated by platelet-derived growth factor (PDGF) (Ribatti, et al. 2007a; Risau 1997). The non-sprouting angiogenesis is the process of splitting pre-existing vessels by transcapillary pillars or posts of extracellular matrix, first described in the embryonic lung (Patan, et al. 1996; Risau 1997).

Angiogenesis is controlled by the balance of proangiogenic and inhibitory stimuli (Ribatti, et al. 2007b). The quiescence of endothelial cells in the healthy adult organism is maintained by the dominant influence of endogenous angiogenesis inhibitors over angiogenic stimuli (Ribatti, et al. 2007a). Negative regulators may be particularly important in endocrine organs that are very vascular, and down-regulation of inhibitor production may be required to activate the angiogenic switch (Hanahan and Folkman 1996). Angiogenesis involves a large number of endogenous proangiogenic factors including VEGF, FGF-2, IL-8, TGF- β , PDGF, angiopoietins, matrix metalloproteinases, which play important roles in endothelial cell proliferation, vascular stabilization, recruitment of inflammatory cells releasing angiogenic factors, or extracellular matrix degradation (Li, et al. 2003; Ribatti, et al. 2007a). In addition to metabolic factors such as hypoxia, the process of angiogenesis is also regulated by some hormones such as estrogen, GH, IGH-1 and TSH through promoting endothelial cell proliferation or increasing VEGF production (Hellstrom, et al. 1999; Hyder, et al. 2000; Smith, et al. 1999). Gene mutations or down-regulation of tumor suppressor genes such as *p53* and *VHL* facilitate tumor angiogenesis by inactivating angiogenesis inhibitors or enhancing angiogenic factors (Dameron, et al. 1994; Levine 1997; Teodoro, et al. 2007; Turner, et al. 2002). The endogenous inhibitors of angiogenesis include thrombospondin-1, angiostatin, endostatin and so on, which inhibit endothelial cell proliferation or matrix metalloproteinases (Ribatti, et al. 2007a). In pathological situations angiogenesis may be triggered not only by the overproduction of proangiogenic factors, but also by the down-regulation of inhibitory factors (Ribatti, et al. 2007a). Pathogenic angiogenesis may occur in several diseases such as atherosclerosis (O'Brien, et al. 1994), rheumatoid arthritis (Colville-Nash and Scott 1992), diabetic retinopathy (Sharp 1995) and psoriasis (Nickoloff, et al. 1994).

A large number of studies have firmly demonstrated that angiogenesis plays an essential role in tumorigenesis, tumor development and progression, besides in physiological processes such as embryogenesis, wound healing and the normal menstrual cycle. It is well known that

tumors require neovascularization to supply themselves with nutrients, oxygen and also give the metabolites access to blood circulation if they are to grow beyond 2 mm³ (Jugenburg, et al. 1997). It is proposed that increased tumor diameter require a corresponding increase in vascularization (Folkman 1972). Tumor invasion of surrounding structures and tumor metastasis may occur due to the degradation of extracellular matrix during angiogenesis, and the new blood vessels provide a way for metastatic tumor cells to enter the systemic circulation (Folkman 1990; Gasparini and Harris 1995). The acquisition of angiogenic capability can be regarded as a milestone of progression from neoplastic transformation to tumor growth and metastasis (Ribatti, et al. 2007a). Many studies have shown the relationship between angiogenesis and tumor behavior; for example, increased angiogenesis has been shown to be associated with the development of metastases, poor prognosis, and reduced survival in breast, prostate and stomach malignancies (Horak, et al. 1992; Maeda, et al. 1995; Turner, et al. 2003; Weidner, et al. 1993; Weidner, et al. 1992; Weidner, et al. 1991). Angiogenesis is measured as microvessel density using antibodies against different endothelial markers on both frozen and paraffin-embedded sections. Antibodies that are most commonly used are against the endothelial antigens factor eight-related antigen (F8), CD31 (platelet endothelial cell adhesion molecule), CD34, and the lectin ulex europaeus agglutinin 1 (UEA1) (Turner, et al. 2003).

1.5 Angiogenesis in pituitary adenomas

The pituitary, as a central endocrine organ, is highly-vascularized, and in contrast to other tumor types such as prostate and breast tumors, which are more vascularized than respective normal tissue, pituitary adenomas have been shown of less vascular density compared with normal pituitary specimens as measured by different endothelial markers (Horak, et al. 1992; Jugenburg, et al. 1995; Schechter 1972; Turner, et al. 2000b; Weidner, et al. 1991). It is not simply the benign nature of pituitary adenomas that explains their relatively low vascular density, because benign or precancerous breast or cervical lesions are more vascular than corresponding normal tissues (Brem, et al. 1978; Dobbs, et al. 1997; Turner, et al. 2003). This low vascular density or inhibition of angiogenesis may partly explain why pituitary adenomas have relatively low growing speed besides another possible explanation that these relatively slow-growing tumors have low metabolic demands that do not require increased vascularization (Turner, et al. 2003).

The neuroradiological and morphological studies suggest that pituitary adenomas receive a direct systemic arterial blood supply in contrast to the normal anterior pituitary gland, and tumors without arterial supply were described as small (Gorczyca and Hardy 1988; Powell, et al. 1974; Schechter, et al. 1988; Yuh, et al. 1994). A potential explanation for the relatively low

vascular density of pituitary adenomas is that the indeed increased angiogenesis has led to in-growth of blood vessels from the systemic circulation and the escape from the hypothalamic controlling factors found in the portal circulation (Turner, et al. 2003). In addition, it has been shown that the majority of pituitary tumors have capillaries with reduced or even absent fenestrations and complete absence or fragmentation of parenchymatous basement membrane, and the endothelial cells of the capillaries are swelling and blebbing due to the compression of the long portal veins and ischemia along with tumor growth (Farnoud, et al. 1992; Kovacs and Horvath 1973; Tuffnell, et al. 1991).

Many activators of angiogenesis, including VEGF and its receptors, FGF and its receptors, hypoxia-inducible factor-1 (HIF-1), angiogenin, angiopoietin and Tie2 tyrosine kinase receptors, matrix metalloproteinases (MMPs), pituitary tumor transforming gene (PTTG), and estrogens, have shown to be associated with pituitary tumor angiogenesis (Lloyd, et al. 2003; Turner, et al. 2003). Some studies about therapeutic application of angiogenesis inhibitors have been performed. The fumagillin analog TNP-470 and a synthetic MMPs inhibitor batimastat have been demonstrated to reduce neovascularization and lactotroph proliferation in Fischer 344 rat estrogen-induced prolactinoma model (Mucha, et al. 2007; Stepien, et al. 1996; Takechi, et al. 1994).

1.6 Sumoylation and RSUME

Sumoylation is a form of post-translational modification by SUMO (small ubiquitin-related modifier), regulating protein function (Johnson 2004). SUMO, which has four isoforms (SUMO-1, SUMO-2, SUMO-3, and SUMO-4) belongs to the ubiquitin-like protein family (Wilkinson and Henley 2010). SUMO share only ~18% sequence identity with ubiquitin, but the folded structure of SUMO is similar with ubiquitin (Bayer, et al. 1998). During the process of sumoylation, SUMO proteins are firstly activated by a thioester linkage with enzyme E1, a heterodimer of SAE1 (SUMO-activating enzyme E1) and SAE2 in mammals (Gong, et al. 1999). Then, SUMO is passed to conjugating enzyme Ubc9 (ubiquitin-conjugating 9), again via a thioester linkage (Gong, et al. 1997; Johnson and Blobel 1997; Schwarz, et al. 1998). SUMO E3 ligase acts as scaffolds bringing SUMO-loaded Ubc9 into contact with the substrate protein or holding the SUMO-Ubc9 thioester in a conformation facilitating SUMO transfer (Figure 2) (Alarcon-Vargas and Ronai 2002; Wilkinson and Henley 2010).

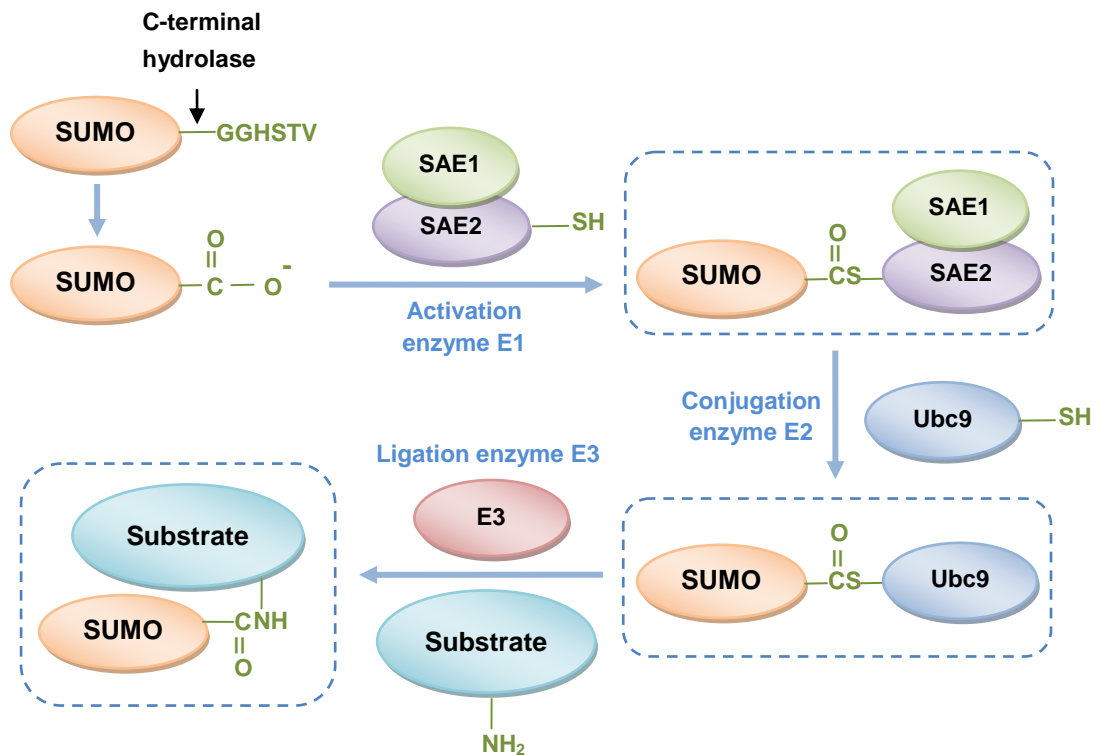


Figure 2. The SUMO conjugation pathway. SUMO is synthesized as a precursor and processed by hydrolases to make the carboxy-terminal double-glycine motif available for conjugation. It is subsequently conjugated to proteins by means of E1 activation, E2 conjugation and E3 ligation enzymes. The E3 enzymes might serve to increase the affinity between Ubc9 (E2) and the substrates by bringing them into close proximity in catalytically favorable orientations, allowing sumoylation to occur at a maximal rate. (Alarcon-Vargas and Ronai 2002)

Most sumoylation occurs in the nucleus, and has the effects on modulating activity of transcription factors negatively or positively, participates in protein nuclear transport, and also affects DNA repair and chromosome organization and function (Figure 3) (Alarcon-Vargas and Ronai 2002; Johnson 2004). In contrast to ubiquitination that leads to proteasomal degradation of proteins, the functional consequences of sumoylation vary greatly from substrate to substrate, and in many cases are not understood at molecular level (Johnson 2004). An increasing number of studies show that sumoylation positively or negatively regulates the substrate proteins which are involved in human cancers, such as PML (a nuclear body-associated phosphoprotein), I κ B α , Mdm2 and c-Jun (Verger, et al. 2003), suggesting that this process may be important in tumorigenesis and development.

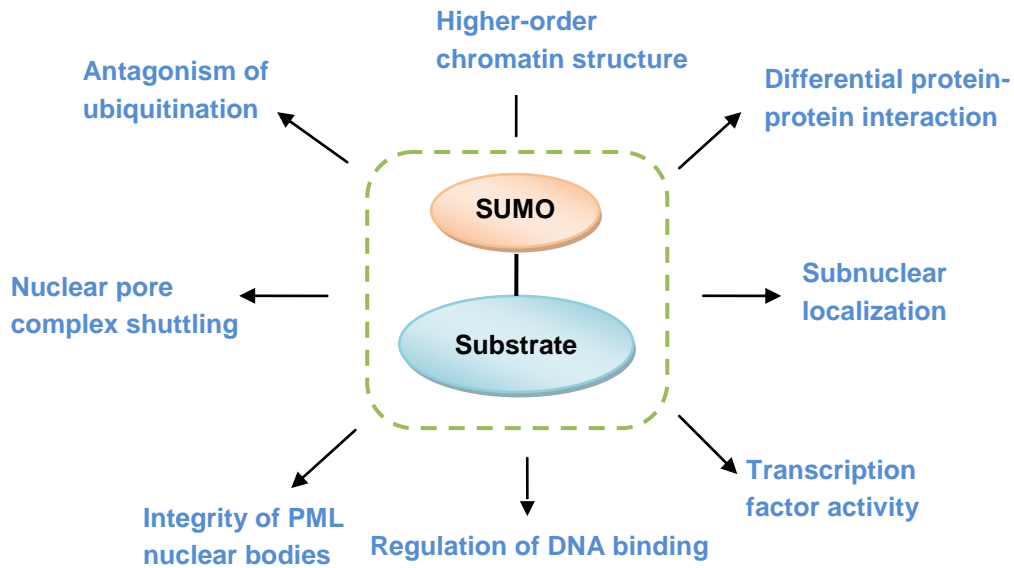


Figure 3. Functions of sumoylation. Some of the known functions of sumoylation are indicated. PML, promyelocytic leukaemia protein. (Alarcon-Vargas and Ronai 2002)

Frequently sumoylation alters protein function by influencing the interactions of substrates with other proteins or with DNA, and this may be achieved by blocking the interaction site, creating a new binding face on the substrate to recruit other binding partners, or change in conformation of the substrate protein to alter its activity or revealing previously masked binding sites (Johnson 2004; Wilkinson and Henley 2010). In addition, sumoylation can block ubiquitin binding sites by competing with ubiquitination on the same lysine residue to increase protein stabilization (Desterro, et al. 1998).

RSUME (RWD-containing sumoylation enhancer) has been recently identified in rat pituitary lactosomatotroph tumor cell line GH3 (Carbia-Nagashima, et al. 2007). As an E3 enzyme, it increases noncovalent binding of SUMO to Ubc9, enhances Ub9-SUMO thioester formation and SUMO polymerization, and therefore enhances sumoylation (Carbia-Nagashima, et al. 2007; Huang, et al. 2007). RSUME is expressed in various tissues, with higher expression in cerebellum, pituitary, heart, kidney, liver, stomach, pancreas, prostate, and spleen (Carbia-Nagashima, et al. 2007). It has been shown that RSUME is induced by hypoxia, and RSUME expression is in the necrotic inner zone rather than in the peripheral zone of two gliomas (Carbia-Nagashima, et al. 2007). By enhancing sumoylation, RSUME increases I κ B levels and stabilize HIF-1 α in monkey kidney cell line COS-7, leading to inhibition of NF- κ B transcriptional activity, and increased HIF-1 α transcriptional activity and VEGF expression (Figure 4) (Carbia-Nagashima, et al. 2007).

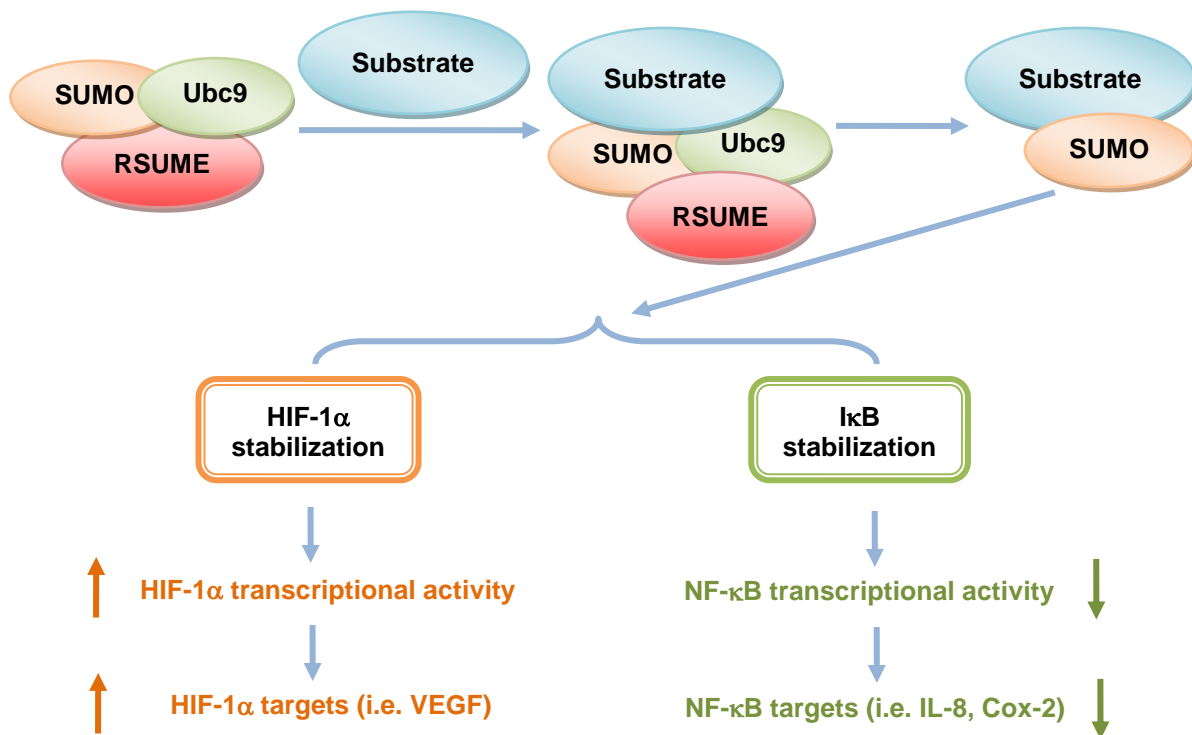


Figure 4. Actions of RSUME on the sumoylation process. RSUME enhances Ubc9-SUMO thioester formation and facilitates the progression of the SUMO transfer cascade. By enhancing sumoylation, RSUME inhibits NF- κ B activity through the stabilization of I κ B, which leads to the inhibition of its targets, and activates HIF-1 α and consequently its targets. (Carbia-Nagashima, et al. 2007)

1.7 Hypoxia-inducible factor 1 (HIF-1) α

HIF-1 plays an essential role in cellular and systemic oxygen homeostasis by adopted oxygen sensing mechanism in higher eukaryotes (Lee, et al. 2004). HIF-1 is a heterodimeric transcription factor containing the α subunit and β subunit (also known as aryl hydrocarbon receptor nuclear translocator (ARNT)), and both belong to bHLH (basic helix-loop-helix)-PAS (Per/ARNT/Sim) family (Wang, et al. 1995). The α subunit is stabilized and activated by hypoxic conditions and maintained at low levels under normoxia conditions; whereas the β subunit is constitutively expressed and its activity is not affected by hypoxia (Li, et al. 1996). HIF-1 α dimerizes with HIF-1 β through bHLH and PAS motifs and binds to the hypoxia response element (HRE) of the DNA sequence, which leads to transcription activation (Jiang, et al. 1996). Two transactivation domains (TAD), N-terminal (N-TAD) and C-terminal (C-TAD) are located in the C-terminal half of the HIF-1 α (Figure 5) (Ke and Costa 2006; Ruas, et al. 2002). The N-TAD overlaps with the oxygen-dependent degradation domain (ODDD), and it is continuous with protein stability (Cockman, et al. 2000). The C-TAD which is required for full

HIF-1 activity has been shown to interact with coactivators such as CBP/p300 to activate gene transcription independent of protein stability (Lando, et al. 2002b).

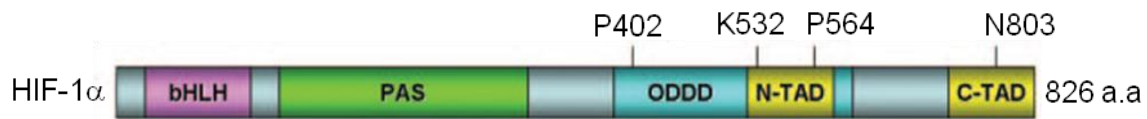


Figure 5. Domain structure of human HIF-1 α . HIF-1 α belongs to the bHLH and PAS protein family. It contains an ODDD that mediates oxygen-regulated stability through the hydroxylation of two proline (P) residues and the acetylation of a lysine (K). HIF-1 α also contains two transcription domains (C-TAD and N-TAD). The total number of amino acids of HIF-1 α is marked at the end of the domain structure. (Ke and Costa 2006)

Under normoxia, two proline residues Pro402 and Pro564 within ODD domain of HIF-1 α are hydroxylated by prolyl hydroxylase (PHD) to promote the interaction of HIF-1 α with pVHL (von Hippel-Lindau tumor suppressor) which is a part of ubiquitin ligase complex to tag HIF-1 α with ubiquitin, leading to HIF-1 α degradation by 26S proteasome (Masson and Ratcliffe 2003; Masson, et al. 2001; Srinivas, et al. 1999). The lysine residue 532 (Lys532) located in the ODDD domain of HIF-1 α is acetylated by an acetyl-transferase called arrest-defective-1 (ARD1), which facilitates the binding of HIF-1 α with pVHL, and thus destabilizes HIF-1 α (Jeong, et al. 2002). The hydroxylation of an asparagine residue N803 in the C-TAD by the factor inhibiting HIF-1 (FIH-1) prevents the association of HIF-1 α with CBP/p300 which results in transcriptional inactivity (Hewitson, et al. 2002; Lando, et al. 2002b; Sang, et al. 2002). The PHD and FIH-1, regarded as oxygen sensors, are 2-oxoglutarate (2-OG)-dependent dioxygenases requiring oxygen for hydroxylation as well as Fe²⁺ and ascorbate as cofactors. Their activity to impair HIF-1 α stabilization and transcriptional activity, respectively, is known to depend on the oxygen concentration (Epstein, et al. 2001; Jewell, et al. 2001; Lando, et al. 2002a; Lando, et al. 2002b; Schofield and Zhang 1999). The ARD1 is not influenced by oxygen, but the mRNA and protein levels of ARD1 were higher in normoxia than in hypoxia, causing more acetylated HIF-1 α in normoxia (Jeong, et al. 2002). Under hypoxia, PHD and FIH-1 lose the activity of mediating hydroxylation of HIF-1 α due to lack of oxygen, thus non-hydroxylated HIF-1 α is stabilized without pVHL binding and CBP/p300 recruitment is allowed. Then, stabilized HIF-1 α translocates into the nucleus and binds to HIF-1 β , resulting in gene transcription (Figure 6) (Ke and Costa 2006). In addition, recently sumoylation of HIF-1 α has been identified as another posttranslational modification to stabilize HIF-1 α against degradation (Bae, et al. 2004; Carbia-Nagashima, et al. 2007; Shao, et al. 2004).

Besides hypoxia, HIF-1 is also regulated by cytokines, growth factors, environmental stimuli, and other signaling molecules under normoxia (Feldser, et al. 1999; Gorlach, et al. 2001;

Haddad and Land 2001; Hellwig-Burgel, et al. 1999; Ke and Costa 2006; Li, et al. 2004; Richard, et al. 2000; Salnikow, et al. 2000; Stiehl, et al. 2002). HIF-1 α transactivation or synthesis is also shown to be induced by activation of mitogen-activated protein kinase (MAPK) or the phosphatidylinositol 3-kinase (PI3K) signaling pathways (Li, et al. 2004; Zelzer, et al. 1998).

HIF-1 α , inducing a large number of target gene transcriptions, plays a general role in multiple physiological responses to hypoxia, such as erythropoiesis and glycolysis, which quickly counteract oxygen deficiency, and angiogenesis, which provides a long-term solution (Ke and Costa 2006; Semenza 1998). Tumor growth leads to progressively hypoxic condition in the inner area as its size increases until enough blood vessels are built by tumors. Over-expression of HIF-1 α has been found in various human cancers such as breast, colon, pancreas, prostate, bladder, ovary, liver, kidney and brain, probably as a consequence of intratumoral hypoxia or genetic alteration, resulting in the subsequent induction of proangiogenic genes such as VEGF which is one the major target genes of HIF-1 (An, et al. 2000; Berra, et al. 2000; Conway, et al. 2001; Harris 2000; Josko, et al. 2000; Talks, et al. 2000; Zhong, et al. 1999). HIF-1 also induces growth factors such as insulin-like growth factor-2 (IGF-2) and transforming growth factor- α (TGF- α), leading to cell proliferation and survival in hypoxia (Feldser, et al. 1999; Krishnamachary, et al. 2003). Paradoxically, HIF-1 α has been shown to promote apoptosis induced by hypoxia (Carmeliet, et al. 1998). For example, proapoptotic protein Bcl-2/adenovirusE1B19-KDa interacting protein 3 (BNip3) and its homolog Nip3-like protein X (NIX) have shown to be up-regulated in a HIF-dependent manner (Bruick 2000).

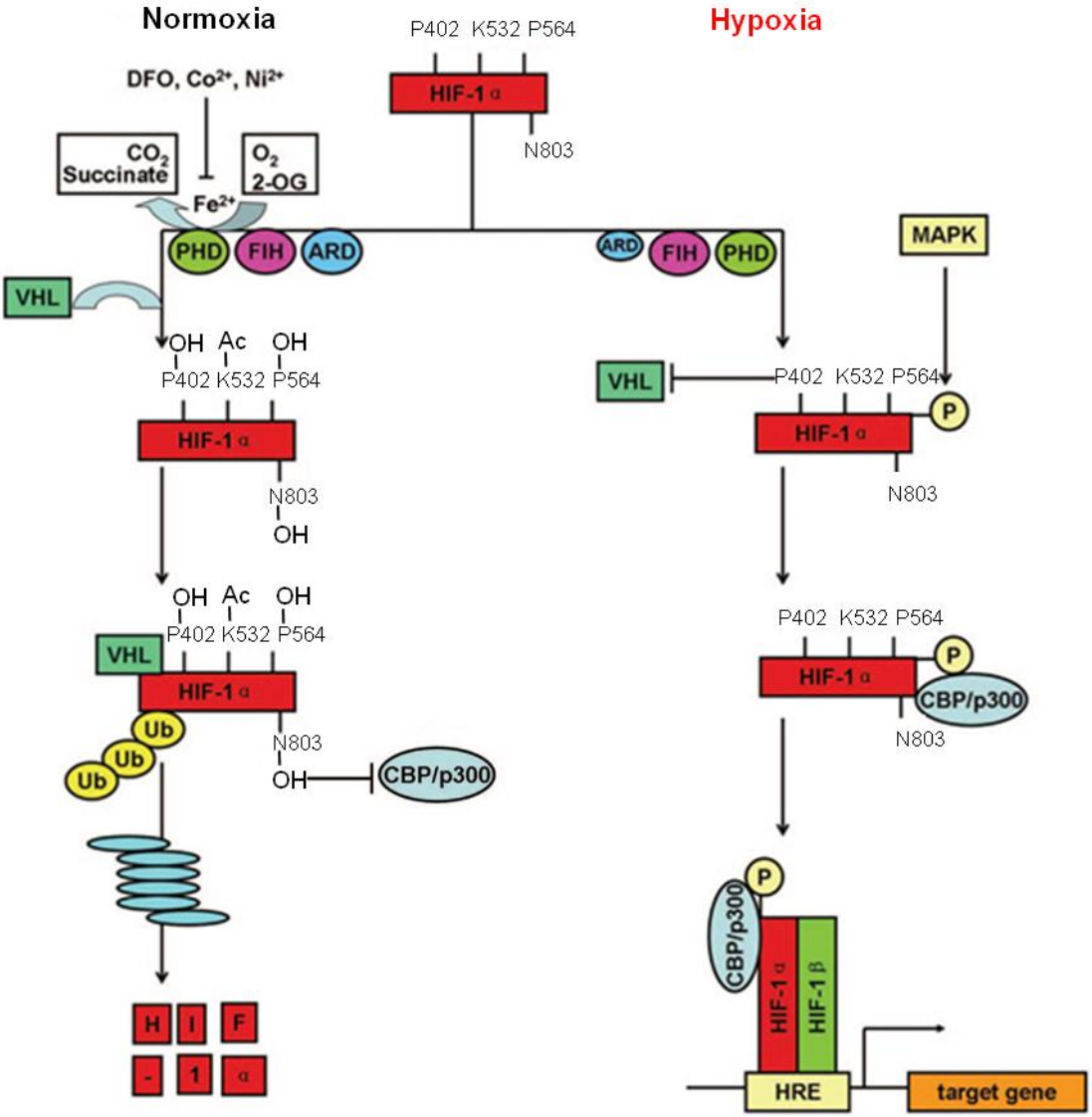


Figure 6. Oxygen-dependent regulation of HIF-1 stabilization and transactivation. In normoxia (left), two proline residues of HIF-1 α (P402 and P564) and asparagine (N803) are hydroxylated by PHDs and FIH-1, respectively, in an O₂, 2-OG, and Fe²⁺-dependent manner. Hydroxylated HIF-1 α proteins bind to the E3 ubiquitin ligase VHL complex, leading to its degradation by the proteasome. Acetylation of lysine (K532) by ARD1 favors the interaction of HIF-1 α with VHL. Hydroxylated N803 blocks the recruitment of transcriptional coactivator CBP/p300. In hypoxia (right), the activities of PHDs and FIH-1 are inhibited due to lack of O₂, resulted in no proline and asparagine hydroxylation. Therefore, there is no VHL binding and HIF-1 α is stabilized. Stabilized HIF-1 α proteins translocate to the nucleus and bind to HIF-1 β . HIF-1 β may bind preferentially to the MAPK-induced phosphorylated form of HIF-1 α . Nonhydroxylated N803 of HIF-1 α allows CBP/p300 recruitment to the target genes, resulting in gene transcription. In addition, the expression of ARD1 is decreased under hypoxia, causing less acetylated HIF-1 α . (Ke and Costa 2006)

1.8 VEGF

VEGF (also known as VEGF-A) belongs to the VEGF family which also includes VEGF-B, C, D, E, and placental growth factor (PlGF) (Achen, et al. 1998; Joukov, et al. 1996; Lee, et al. 1996; Lyttle, et al. 1994; Maglione, et al. 1991; Maglione, et al. 1993; Orlandini, et al. 1996). VEGF is a key regulator of angiogenesis, while VEGF-B is required for normal heart function in adults but is not required for cardiovascular development or for angiogenesis, and VEGF-C and VEGF-D participate in embryonic lymphangiogenesis (Ferrara 2004; Karkkainen, et al. 2004; Roskoski 2007). VEGF-E is encoded by the Orf parapoxvirus, supporting the angiogenesis associated with parapoxvirus-infected lesion (Meyer, et al. 1999). PlGF enhances VEGF signaling (Carmeliet, et al. 2001).

Alternative exon splicing of *VEGF* gene generates four different isoforms of VEGF: VEGF₁₂₁, VEGF₁₆₅, VEGF₁₈₉, and VEGF₂₀₆, having 121, 165, 189, and 206 amino acids, respectively, after signal sequence cleavage (Houck, et al. 1991; Tischer, et al. 1991). VEGF₁₆₅, which is the predominant isoform, is a heparin-binding homodimeric glycoprotein of 45 KD, and it is secreted but a significant fraction remains bound to the cell surface and extracellular matrix (Ferrara and Henzel 1989; Houck, et al. 1992; Park, et al. 1993). VEGF₁₂₁, which does not bind heparin, is a freely diffusible protein (Houck, et al. 1992; Park, et al. 1993). VEGF₁₈₃ and VEGF₂₀₆ have high affinity with heparin, and they are almost completely sequestered in the ECM (extracellular matrix), but may be released in a diffusible form by heparin or heparinase, which displaces them from their binding to heparin-like moieties, or by plasmin cleavage at the COOH terminus, which generates a bioactive fragment containing the first 110 NH₂-terminal amino acids (Houck, et al. 1992; Park, et al. 1993). VEGF interacts with two highly related receptor tyrosine kinases (RTKs), VEGFR-1 and VEGFR-2; while the co-receptor neuropilin 1 (NP1) enhances the binding of VEGF₁₆₅ to VEGFR-2 and VEGF₁₆₅-mediated chemotaxis (de Vries, et al. 1992; Soker, et al. 1998; Terman, et al. 1992).

VEGF has the ability to promote growth and survival of vascular endothelial cells (ECs) derived from arteries, veins and lymph vessels (Ferrara and Davis-Smyth 1997), and also has mitogenic effects on certain non-EC types such as retinal pigment epithelial cells, pancreatic duct cells and Schwann cells (Compornolle, et al. 2002; Guerrin, et al. 1995; Oberg-Welsh, et al. 1997; Sondell, et al. 1999). VEGF also has effects on the bone marrow-derived cells and hematopoiesis. It promotes monocyte chemotaxis and controls hematopoietic stem cell survival during hematopoietic repopulation (Clauss, et al. 1990; Gerber, et al. 2002). The potential role of VEGF as a neuronal protective factor has been demonstrated by recent studies in amyotrophic lateral sclerosis (Lambrechts, et al. 2003). Moreover, VEGF induces vascular permeability, underlining its important role in inflammation (Dvorak, et al. 1995; Senger, et al. 1983).

VEGF mRNA transcription is induced by hypoxia in various pathophysiological circumstances (Dor, et al. 2001). The *VEGF* gene has a single hypoxia response element (HRE) in the promoter, which is the HIF-1 binding site (Madan and Curtin 1993). Besides oxygen tension, several major growth factors and inflammatory cytokines, including epidermal growth factor, TGF- α , TGF- β , IGF-1, FGF, keratinocyte growth factor, IL-1 α and IL-6, also up-regulate VEGF expression, indicating that VEGF release is under regulation of the autocrine or paracrine factors together with local hypoxia in the microenvironment (Ferrara and Davis-Smyth 1997; Neufeld, et al. 1999). Oncogenic mutations or amplification of *ras* proto-oncogene over-activate the Raf-Mek-Erk MAP kinase cascade, leading to increased VEGF expression (Grugel, et al. 1995; Okada, et al. 1998).

VEGF plays an essential role in both physiological angiogenesis (such as angiogenesis during embryonic and postnatal development, skeletal growth, endochondral bone formation, and angiogenesis in endocrine glands) and pathological angiogenesis (such as angiogenesis in solid tumors, haematological malignancies, intraocular neovascular syndromes, inflammatory disorders and brain edema, and diseases of the female reproductive system) (Ferrara 2004).

As mentioned above, tumor growth has the requirement for angiogenesis, and therefore, VEGF is identified as an essential factor for tumor angiogenesis. It has been shown by *in situ* hybridization studies that VEGF mRNA is significantly up-regulated in the vast majority of human tumors, such as carcinoma of the lung, breast, gastrointestinal tract, kidney, bladder, ovary, endometrium, and several intracranial tumors including glioblastoma multiforme and sporadic, as well as VHL syndrome-associated, capillary hemangioblastomas (Ferrara 2004). VEGFR-1 and VEGFR-2 are expressed in endothelial cells, indicating that VEGF released by tumor cells may influence the endothelial cells nearby in a paracrine manner (Roskoski 2007). VEGF is also expressed in pituitary adenomas, although it has been shown to be generally less intense than in normal pituitary by immunohistochemistry (Lloyd, et al. 1999). Pituitary carcinomas show relatively increased VEGF expression compared with adenomas, suggesting an up-regulation of VEGF expression during pituitary tumor progression (Lloyd, et al. 1999). Interestingly, VEGF-A is not only acting as an angiogenic but also as a growth factor on pituitary adenomas through differently expressed VEGF receptors in tumor and vessel cells of pituitary tumors (Onofri, et al. 2006). Monoclonal anti-VEGF antibodies suppress growth of various transplanted tumor cell lines in nude mice (Kim, et al. 1993). Therapeutic trials using anti-VEGF antibodies, genetically engineered VEGF-binding proteins and VEGF receptor protein-tyrosine kinase inhibitors have been performed, and VEGF pathway inhibitors are now being explored in combination with chemotherapy for many types of solid tumor (Roskoski 2007).

2 Aim of this study

RSUME, a novel protein, was shown to enhance HIF-1 α stabilization and transcriptional activity in monkey kidney cell line COS-7, and a large number of studies have demonstrated that HIF-1 α and its target VEGF play essential roles in growth and progression of a wide variety of solid tumors by promoting tumor angiogenesis. However, only few reports focus on the role of HIF-1 α and VEGF in slowly growing and poorly vascularized pituitary adenomas, and whether RSUME is implicated in pituitary adenoma angiogenesis and development is completely unclear.

The aim of this study is to investigate the expression and regulation of HIF-1 α , VEGF and RSUME in pituitary adenomas and also to explore novel additional functions of RSUME in pathogenesis of pituitary adenomas.

In order to achieve these goals, experiments were carried out with human pituitary adenomas and mouse pituitary cell lines. HIF-1 α , VEGF and RSUME were examined at RNA level by quantitative real-time PCR in human pituitary adenoma tissues. HIF-1 α , VEGF protein expression and RSUME mRNA expression were measured by western blot, ELISA and quantitative real-time PCR respectively after hypoxia-mimicking stimulation in mouse pituitary adenoma cell lines and primary human pituitary adenoma cell cultures. HIF-1 α translocation after hypoxia mimicking treatment was demonstrated by immunofluorescence studies. RSUME knockdown was performed by siRNA technology to clarify its relationship with HIF-1 α and VEGF in pituitary cell lines and primary cell cultures. The role of RSUME in pituitary cell proliferation and survival was noticed in the experiments with RSUME knockdown and analyzed by WST-1 assay, cell number counting, cell death ELISA, and immunofluorescence studies on pro-apoptotic protein cleaved caspase-3.

3 Materials and methods

3.1 Regents

Product	Company
Acridine orange	Sigma (St. Louis. MO, USA)
Ammonium persulfate	Sigma (St. Louis. MO, USA)
Ampuwa water	Fresenius (Germany)
Alexa Fluor 594	Invitrogen (Carlsbad, CA, USA)
Beta-mercaptoethanol	MERCK (Darmstadt, Germany)
Biomax MR films	Kodak (Stuttgart, Germany)
BLOCK-iT™ Alexa Fluor® red fluorescent oligo	Invitrogen Corp. (Paisley, UK)
Bovine serum albumin (BSA)	Invitrogen Corp. (Paisley, UK)
Protein assay Dye Reagent	Biorad (Munich, Germany)
Chloroform	Sigma (St. Louis. MO, USA)
Collagenase	Worthington Biochemical Corp. (Lakewood, NJ, USA)
Culture slides	BD biosciences (California, USA)
Developer solution	Kodak (Stuttgart, Germany)
Diethyl-pyrocabonate (DEPC)	Sigma (St. Louis. MO, USA)
Dimethyl sulfoxide (DMSO)	Sigma (St. Louis. MO, USA)
Dithiothreitol (DTT)	Sigma (St. Louis. MO, USA)
DNase I	Invitrogen Corp (Paisley, UK)
dNTP Mix	MBI Fermentas (Vilnius, Lithuania)
Dulbecco's modified Eagle medium (DMEM)	Invitrogen Corp (Paisley, UK)
Ethylenediaminetetraacetic acid (EDTA)	MERCK (Darmstadt, Germany)
Ethidium bromide	Sigma (St. Louis. MO, USA)
Fetal calf serum	Gibco (Karlsruhe, Germany)
Fixer solution	Kodak (Stuttgart, Germany)
Guanidine thiocyanate	Fluka Chemie AG (Buchs, Switzerland)
Hexanucleotide Mix	Roche (Mannheim, Germany)

Hydrochloric acid	MERCK (Darmstadt, Germany)
Hyperfilm ECL	Amersham Biosciences (Uppsala, Sweden)
Isopropanol	Sigma (St. Louis, MO, USA)
KCl	MERCK (Darmstadt, Germany)
KH ₂ PO ₄	MERCK (Darmstadt, Germany)
Lipofectamine™ 2000	Invitrogen Corp (Paisley, UK)
L-Glutamine	Biochrom AG (Berlin, Germany)
Loading Buffer 4x	Roth (Karlsruhe, Germany)
Lumi-Light Western Blotting Substrate	Roche (Mannheim, Germany)
Magnesium chloride	MERCK (Darmstadt, Germany)
Marker 1kb Plus	Life Technologies (Paisley, UK)
MEM-Vitamins	Biochrom (Berlin, Germany)
Milk powder	Roth (Karlsruhe, Germany)
Nitrocellulose membrane Hybond-ECL	Amersham Biosciences (Uppsala, Sweden)
Paraformaldehyde (PFA)	MERCK (Darmstadt, Germany)
Partricin	Biochrom (Berlin, Germany)
PBS	Gibco/invitrogen (Carlsbad, CA, USA)
Penicillin+Streptavidine mix	Biochrom AG (Berlin, Germany)
Cultrex® Poly-L-Lysine	R&D Systems (Wiesbaden, Germany)
Ponceau S solution	Sigma (St. Louis, Mo, USA)
Phenol	Roth (Karlsruhe, Germany)
Phosphate based buffer PBS	Life Technologies (Paisley, UK)
Polyacrylamide	Invitrogen Corp (Paisley, UK)
ProLong gold anti-fade reagent with DAPI	Invitrogen (Carlsbad, CA, USA)
Goat serum	Sigma (St. Louis, Mo, USA)
RNAsin (RNase inhibitor)	Promega Corp. (Madison, WI, USA)
Rneasy Mini kit	QIAGEN (Hilden, Germany)
Reverse transcriptase (SuperScript II™)	Invitrogen (Carlsbad, CA, USA)
Semi-dry blotter	Invitrogen (Carlsbad, CA, USA)

siRNA against RSUME	MWG Biotech (Ebersberg, Germany)
Sodium acetate dihydrate	MERCK (Darmstadt, Germany)
Sodium acetate trihydrate	MERCK (Darmstadt, Germany)
Sodium chloride (NaCl)	Roth (Karlsruhe, Germany)
Sodium citrate dihydrate	MERCK (Darmstadt, Germany)
Sodium dihydrogen phosphate mono-hydrate ($\text{NaH}_2\text{PO}_4 \cdot \text{H}_2\text{O}$)	MERCK (Darmstadt, Germany)
Sodium hydrogen phosphate dihydrate ($\text{Na}_2\text{HPO}_4 \cdot 2\text{H}_2\text{O}$)	MERCK (Darmstadt, Germany)
Sodium peroxyde (NaOH)	MERCK (Darmstadt, Germany)
Taq DNA polymerase	MBI Fermentas
TEMED	Sigma (St. Louis, Mo, USA)
Transferrin	Sigma (St. Louis, Mo, USA)
Triiodothyronine	Henning (Berlin, Germany)
Tris-Glycine 10% gel	Anamed (Darmstadt, Germany)
Tris pure	ICN Pharmaceuticals (Aurora, OH, USA)
Triton X-100	Roth (Karlsruhe, Germany)
Trizol	Invitrogen (Carlsbad, CA, USA)
Trypsin	Sigma (St. Louis, Mo, USA)
Tween 20	Sigma (St. Louis, Mo, USA)
WST-1 reagent	Roche (Mannheim, Germany)

3.2 Solutions

Acridin orange/ ethidium bromide solution	Acridinorange: 50 μl 200 mg/l Ethidiumbromid: 50 μl 10 mg/l PBS: 900 μl
Collagenase Mix	1000 U/ml Collagenase : 4g/ 100ml solution Trypsin inhibitor : 10 mg/ 100ml solution Hyaluronidase : 100 mg/ 100ml solution BSA : 400 mg/ 100ml solution DNase : 500 μl / 100ml solution
DEPC water	200 μl DEPC/l deionized water Leave under the fume hood overnight

	Autoclave
HDB buffer	Hepes: 5,95 g/l NaCl : 8 g/l KCl: 0,37 g/l Na ₂ HPO ₄ ·H ₂ O: 0,12 g/l Glucose: 1,982 g/l Amphotericine B 25µg/ml: 10 ml Penicillin/Streptomycin 105U/l : 10 ml Adjust pH to 7,3 with NaOH Store at +4°C
4% Paraformaldehyde (PFA)	paraformaldehyde: 4 g/100 ml Sodium phosphate buffer: 20 ml/100ml Ampuwa water: 80 ml Add 1M NaOH to pH 7.4 Heat at 56°C to dissolve Filter and cool before usage Store at +4°C for maximum 2 days
Phosphate based buffer (PBS)	NaCl: 8 g/l KCl: 0.2 g/l Na ₂ HPO ₄ ·2H ₂ O: 1.44 g/l KH ₂ PO ₄ : 0.2 g/l Adjust to pH 7.4
RIPA buffer	50 mM Tris pH 8.0 150 mM NaCl 1% NP40 0.5% Sodium Deoxicholate 0.1% SDS 1% Triton X-100
10 x Running buffer for protein electrophoresis	Tris-base: 30.3 g/L Glycine: 144.2 g/L SDS: 10 g/L Adjust pH to 8.3
2M Sodium acetate	Sodium acetate trihydrate: 27.2 g/ 100ml DEPC: 20 µl Add acetic acid to pH 4.0 Leave at room temperature overnight and the next day autoclave
Solution D	4 M Guanidium thiocyanate: 250 g/337 ml 0.75 M sodium citrate pH 7.0 : 17.6 ml/337 ml 10% Sarcosyl: 26.4 ml/337 ml dissolve in 293 ml DEPC To complete the medium add: 180 µl beta-mercaptoethanol/25 ml solution just

	before use
Transfer buffer for semi-dry blotting	39 mM Glycine 48 mM Tris-Cl 0.037% SDS 10% Methanol
10x Tris borate EDTA buffer (TBE)	Boric acid (H ₃ BO ₃): 61.83 g/l EDTA: 37.2 g/l Tris pure: 30.03 g/l Adjust to pH 8.0
Tris-based buffer (TBS)	Tris pure: 2.42 g/l NaCl: 8 g/l Adjust to pH 7.6

3.3 Human pituitary and pituitary adenoma tissues

This study was performed after approval of the local ethics committee (Ethics Grant No. 141-07) and in the case of pituitary adenomas, informed written consent was received from each patient.

3.3.1 Tissues used for investigation of HIF-1 α , VEGF and RSUME mRNA expression

Normal human pituitaries (n=3) were obtained from autopsies, performed within 12 h after accidentally occurred death of 3 healthy persons: 2 males (age 67 and 47) and 1 female (age 37). The tumor tissues received after transsphenoidal surgery from 31 patients: 13 males and 18 females with 47.9 \pm 17.8 average age (range 26-80 years), classified according to clinical presentation in somatotrophinomas (n=6), corticotrophinomas (n=6), non-functioning adenomas (n=8), prolactinomas (n=7) and thyrotrophinomas (n=4) were shock frozen as soon as possible, stored at -80°C and later used for RT-PCR. All the tumors were benign and tumor grade was determined according to a modified Hardy's classification (Boggild, et al. 1994) following the medical reports after nuclear magnetic resonance and after surgery: 1 grade I, 7 grade II, 18 grade III cases were identified, and 5 cases couldn't be identified from clinical data offered by neurosurgeons (Table 4). In patients pre-treated with somatostatin analogues or dopamine agonists, medication was stopped at least 1 week prior to surgery. All the tumor tissues were received within 12~16 hours after surgery.

Table 4. The clinical characteristics of the normal and adenomatous pituitary tissues included in this study.

Tissue	Gender	Age	Grade
NP1	M	67	-
NP2	M	46	-
NP3	F	37	-
CUSH1	F	46	II
CUSH2	F	67	-
CUSH3	M	37	III
CUSH4	F	27	III
CUSH5	F	64	-
CUSH6	F	45	I
NFPA1	M	65	II
NFPA2	M	75	II
NFPA3	F	40	III
NFPA4	F	77	III
NFPA5	F	70	II
NFPA6	F	30	-
NFPA7	M	54	III
NFPA8	F	66	III
ACRO1	F	34	II
ACRO2	F	80	II
ACRO3	F	27	III
ACRO4	F	41	III
ACRO5	M	36	III
ACRO6	F	77	-
TSH1	F	29	III
TSH2	F	55	II
TSH3	F	32	III
TSH4	M	53	III
PROL1	M	40	-
PROL2	M	31	III
PROL3	M	64	III
PROL4	F	28	III
PROL5	M	30	III
PROL6	M	40	III
PROL7	M	26	III

NP, normal pituitary; CUSH, corticotrophinomas; NFPA, non-functioning adenomas; ACRO, somatotrophinomas; TSH, thyrotrophinomas; PROL, prolactinomas; “-“: no data.

3.3.2 Tissues used for primary cell culture

Human pituitary adenomas obtained from 36 patients were used for primary cell culture. For investigation of HIF-1 α expression under hypoxia-mimicking conditions, 8 human pituitary adenomas (5 non-functioning, 2 somatotroph, and 1 lactotroph) were used. For investigation

of VEGF expression under hypoxia-mimicking conditions, 17 human pituitary adenomas (11 non-functioning, 3 somatotroph, 2 lactotroph, and 1 corticotroph) were used. For investigation of RSUME mRNA expression under hypoxia-mimicking conditions, 3 human pituitary adenomas (2 non-functioning and 1 somatotroph) were used. For investigation of effect on RSUME knockdown, 8 human pituitary adenomas (6 non-functioning, 1 somatotroph, and 1 corticotroph) were used. All the tumor tissues were received within 12~16 hours after surgery and were cultivated as soon as possible. Due to the limited amount of human pituitary tumor tissue available, not all the experiments could be done in parallel in primary human pituitary tumor cells.

3.4 RNA isolation

RNA was isolated from normal human pituitaries and from human pituitary adenomas using the guanidium isothiocyanate protocol. The tissue piece was first homogenized in 800 μ l of solution D supplemented with β -mercaptoethanol, using the Ultra-TURRAX T8 (IKA Labortechnik, Germany) tissue homogenizer.

Guanidium isothiocyanate and β -mercaptoethanol inhibit the RNase action activated by cell disruption, preventing in this way RNA degradation. 80 μ l of sodium acetate 2 M pH 4.0 were added afterwards to precipitate RNA, followed by 800 μ l of saturated phenol and 160 μ l of a chloroform-isoamyl alcohol (49:1) solution. After 15 minutes incubation on ice the samples were centrifuged at 13000 rpm for 20 minutes at 4°C; this step led to the formation of two phases, the upper one containing RNA and the lower one containing DNA and proteins. The upper phase was then transferred to a new tube together with the same volume of ice-cold isopropanol. Incubation of the sample at -20°C at least for 2 hours was necessary for RNA precipitation. After centrifugation of the sample at 13000 rpm for 10 minutes at 4°C, the supernatant was discarded and the pellet was washed with ice-cold ethanol 70%. After 10 minutes centrifugation at 13000 rpm the supernatant was again discarded and the pellet left to dry at room temperature and then dissolved in an appropriate amount of DEPC-treated water. RNA extraction from pituitary adenoma cell lines (TtT/GF and AtT-20) and primary human pituitary adenoma cell cultures was performed with TRIzol[®] Reagent according to the manufacturer's instruction.

The samples absorbance was measured with a photometer. The lack of DNA contamination was assessed performing a PCR reaction for a housekeeping gene β -Actin, using the RNA sample: if no DNA contamination is present, no band is visible after loading the PCR product on an ethidium bromide gel (as described below). If DNA contamination was detected, RNA purification was performed with DNase I.

3.5 Reverse Transcriptase- Polymerase Chain Reaction

Reverse transcription was performed by incubating 1 µg of total RNA with 1 µl of dNTP mix 2 mM, 2 µl of 62.5 U/ml random primers (Hexanucleotide mix), 2 µl of dithiothreitol (DTT) 10 mM, 1 µl of 200 U reverse transcriptase (SuperScript II), 4 µl of 5x first strand buffer and DEPC-water to get a final volume of 20 µl, for 1 hour at 45°C. Reaction was stopped by boiling the samples at 95°C for 5 minutes.

For semi-quantitative RT-PCR, 1 µl of cDNA samples obtained from TtT/GF and AtT20 cells were used for PCR reaction with primers specific for mouse RSUME, mouse VEGF, mouse β -Actin, human RSUME and human β -Actin (Table 5). The cDNA samples were incubated with 1.5 µl 10x PCR buffer, 0.9 µl MgCl₂ 25 mM, 1.5 µl dNTP mix 2mM, 0.5 µl amplification primer sense 10 pmol/µl, 0.5 µl amplification primer anti-sense 10 pmol/µl, 0.15 µl *Thermus aquaticus* (Taq) DNA polymerase and 8.95 µl autoclaved distilled water. The PCR reaction consisted of 35 cycles each containing the following steps: denaturation at 94° C for 1 min, annealing at 58° C for 30 sec and finally elongation of the PCR fragment at 72° C for 1 min.

The amplified fragments were electrophoresed in ethidium bromide agarose gel 1 - 1,5% according to the size of the product (1% for 500- 1100 bp fragments, 1,5% for 200- 500 bp fragments), in 1 X TBE buffer for 15-20 minutes at 80 V and then visualized under UV light. The 1 kb Plus DNA Ladder marker was used to determine the fragments size.

Quantitative real time RT-PCR was performed with cDNA samples of TtT/GF, AtT-20 and primary human pituitary tumor cells as templates. The amplification reactions of 35 cycles were carried out with specific primers for human HIF-1 α , human VEGF, human RSUME, human β -Actin, mouse RSUME, and mouse β -Actin (Table 5). Absolute Blue QPCR SYBR Green Mix (Thermo Scientific) was used following the manufacturer's instructions. PCR amplifications were performed in a MiniOpticon Real-Time PCR Detection System (Bio-Rad, Munich, Germany), and the data were analyzed with CFX Manager Software for MiniOpticon (version 1.5, Bio-Rad). For each sample, the gene copy number was normalized by the amount of β -Actin. All experiments were carried out in triplicates.

Each sequence of the primers was checked with the NCBI BLAST program in order to exclude eventual annealing with other genes different from the ones studied. All primers were synthesized by MWG Biotech, reconstituted with sterile distilled water to a concentration of 100 µM and stored at -20 ° C.

Table 5. Primers used for RT-PCR

Target	Sequence (5'-3')	T _m (° C)	Fragment (bp)
Human HIF-1α	Sense: CAT AGA ACA GAC AGA AAA ATC TCA TCC Anti-sense: TTA ACT TGA TCC AAA GCT CTG AGT AAT	58	450
Human VEGF	Sense: CAG ATT ATG CGG ATC AAA CCT Anti-sense: CAA ATG CTT TCT CCG CTC TGA	58	148
Human RSUME	Sense: TAC CTG GTA TCT CGA TTA ACT CTG AAC Anti-sense: TCA GTA TTA TTT TAC CCA TGA ACA TCA	58	300
Human β-Actin	Sense: ACG GGG TCA CCC ACA CTG TGC Anti-sense: CTA GAA GCA TTT GCG GTG GAC GAT G	58	660
Mouse VEGF	Sense: TCT ACC AGC GAA GCT ACT GCC Anti-sense: TTA CAC GTC TGC GGA TCT TG	58	349
Mouse RSUME	Sense: GAC TCA AGT GGA AAG AAA TGC AA Anti-sense: GGA AAT CAA AAC CAG GCT GT	58	199
Mouse β-Actin	Sense: AGT ATC CAT GAA ATA AGT GGT TAC AGG Anti-sense: CAC TTT TAT TGG TCT CAA GTC AVT GTA	58	300

3.6 Cell culture and stimulation experiments

Folliculostellate TtT/GF and corticotroph AtT20 mouse pituitary tumor cells were grown in DMEM supplemented with 10% FCS, 2 nmol/l glutamine, 0.5 mg/l partricin, and 10⁵ U/l penicillin-streptomycin at 37°C and 5% CO₂.

For primary human pituitary tumor cell culture, adenoma tissue was cultivated as below. The tissue was washed with HDB buffer. Sliced fragments were enzymatically dispersed in a buffer containing 4 g/l collagenase, 10 mg/l DNase II, 0.1 g/l soybean trypsin inhibitor, and 1 g/l hyaluronidase (37°C, approximately 45 minutes). Dispersed cells were centrifuged and resuspended in tumor medium (DMEM supplemented with 2 mM essential vitamins, 40U/l insulin, 20 ng/l natrium selenate, 5 mg/l transferrin, 30 pM triiodothyronine (T₃), 10% fetal calf serum, 2 mmol/l L-glutamine, 0.5 mg/l partricin and 10⁵ U/ml penicillin-streptomycin). Cell viability was determined by fluorescence microscopy after staining with acridin orange and ethidium bromide. Acridin orange enters the membranes of normal cells, yielding green fluorescence in viable cells. Ethidium bromide does not pass the healthy cell membrane and enters only in dead cells with damaged membranes, yielding a red fluorescence. Cell viability of pituitary cells was determined as the percentage of green cells in the total number of cells (counted in a Neubauer chamber). Cells were distributed in 48-well plates or 24-well plates and incubated at 37°C under 5 % CO₂. The human adenoma cells attached to the plastic wells within 24 h and were then used for stimulation experiments.

CoCl₂ was dissolved in distilled water as a stock solution of 200 mM, and was diluted in cell culture medium to stimulate pituitary tumor cells for various time periods and at different concentrations as indicated.

3.7 Cell counting

In this study, cell number was counted with the Neubauer chamber before seeding plates or petri dishes. After trypsinizing and washing the cells, the cells were resuspended according to the size of pellet in 5ml, 10ml or 20 ml Medium. 50 µl cell suspension and 50 µl color solution (mixture of 50 µl 200mg/l Acridinorange, 50 µl 10 mg/l Ethidiumbromid and 900 µl PBS) were mixed. The coverslip was placed over the counting chambers and the diluted cell suspension was loaded into the counting chambers. Approximately 10 µl was required. The entire volume of the chamber was filled, but not overfilled. The cells were viewed under a microscope at 100x magnification. The cells were visible above the grid of the counting chamber (Figure 7). The number of viable cells (cells with green color under UV light) was determined overlying 4 x 1 mm² areas of the counting chamber (labeled A-D in Figure 7). The cell concentration was calculated: firstly, the total cells counted in 4 mm² was divided by 4; secondly, the average of cell number in 1 mm² area was divided by the dilution factor 1/2; thirdly, the cell number of 1 mm² area was divided by 10⁻⁴ ml, the volume of 1 mm² area; finally, the cell number of 1 ml medium was obtained.

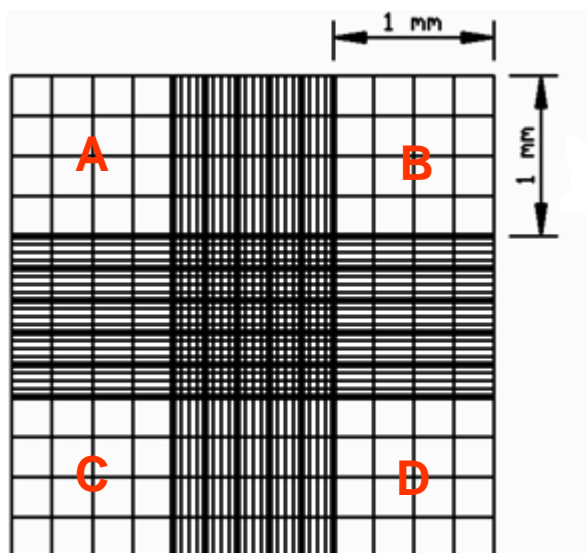


Figure 7. The Neubauer chamber for cell counting.

3.8 Transfection of siRNA against RSUME

RNA interference (RNAi) is a gene silencing system in eukaryotic cells, by which double-stranded RNA (dsRNA) triggers the destruction of mRNA with sequence complementarity.

RNAi is initiated by the conversion of dsRNA into 21~23 nt fragments known as small interfering RNAs (siRNAs) by the multidomain RNase III enzyme (Dicer). These siRNAs are then incorporated into a second enzyme complex, the RNA-induced silencing complex (RISC), in an ATP-dependent step or series of steps during which the siRNA duplex is unwound into single strands. The resulting single stranded siRNA guides the RISC to recognize and cleave the target RNA complementary to the siRNA sequence (Figure 8) (Schwarz, et al. 2002).

Nowadays, siRNA is applied in biology research. Designed siRNA is transfected into mammalian cells to suppress expression of specific genes, which has become a useful tool to explore the function of target genes.

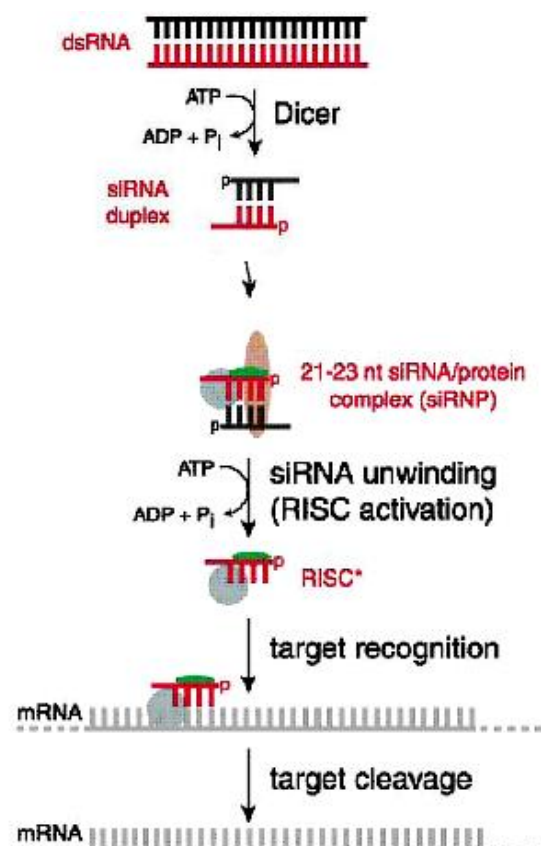


Figure 8. The siRNA pathway. Long double-stranded RNA (dsRNA) is digested by Dicer in an ATP-dependant way. Then siRNAs are uptaken by RISC. ATPs are hydrolysed to help unwind of siRNA but the incorporation is ATP independent. The single-stranded antisense strand help RISC to find the target mRNA, and the mRNA is cleaved. (Schwarz, et al. 2002)

3.8.1 Transfection of siRNA against mouse RSUME in pituitary cell lines

TtT/GF and AtT20 cells were seeded in plates with antibiotics-free culture medium. After overnight growing, 100 nM siRNA against mouse RSUME (5'- GGA CTT GTG GGT GAG GAT G-3', supplied by Prof. Arzt, FCEN-Universidad de Buenos Aires, Argentina) was transfected

into cells with lipofectamineTM 2000 (Invitrogen, Karlsruhe, Germany) to suppress endogenous RSUME expression. 100 nM scrambled siRNA (Scramble II, MWG Biotech, Ebersberg, Germany) was used as a control. The time periods of transfection are described in results.

3.8.2 Transfection of siRNA against human RSUME in primary human pituitary adenoma cells

Transfection of siRNA in primary human pituitary adenoma cells was established in 6 primary cell cultures of human non-functioning pituitary adenomas in this study. BLOCK-iTTM Alexa Fluor[®] red fluorescent oligo (Invitrogen Corp, Paisley, UK) was used for determination of transfection efficiency. The BLOCK-iTTM Alexa Fluor[®] red fluorescent oligo is Alexa Fluor 555-labeled, double-stranded RNA (dsRNA) oligomer. It is designed for use in RNAi analysis to facilitate assessment and optimization of dsRNA oligonucleotides delivery into mammalian cells using cationic lipids (such as lipofectamineTM 2000). In this study, 10 nM, 20 nM, 50 nM or 100 nM fluorescent oligo was transfected with lipofectamineTM 2000 into primary human pituitary cells. 24 hours after transfection, primary cells were observed under fluorescence microscope with standard filter set for detection of Texas red (Carl Zeiss MicroImaging, Munich, Germany). Transfection efficiency was determined by counting the number of cells with red color in 100 cells.

The optimized transfection conditions are described as follows. After dispersion of human pituitary adenomas, 200,000~250,000 adenoma cells/well were cultivated in poly-L-Lysine coated 24-well plates with 500 µl antibiotics-free tumor medium. After overnight incubation, for each well, 100 µl Opti-MEM I reduced serum medium containing 20 nM or 50 nM siRNA against human RSUME (5'- GGA TTT ATG GAT GCG GAT A-3', supplied by Prof. Arzt, FCEN-Universidad de Buenos Aires, Argentina) and 1 µl lipofectamineTM 2000 was added to the cells to suppress endogenous RSUME expression. 100 nM scrambled siRNA (Scramble II, MWG Biotech, Ebersberg, Germany) was used as a control. The time periods of transfection are described in the results.

3.9 Western blot analysis

The western blot is a kind of immunoblot technique for detection of specific proteins in various samples, such as tissue homogenate or extract of cell cultures. The native or denatured proteins are firstly separated by molecular weight or 3D-structure, respectively, using gel electrophoresis, and then the proteins are transferred onto nitrocellulose or polyvinylidene fluoride membranes. For the two-step method, the primary antibody is applied to probe the target protein after blocking the membrane typically with bovine serum albumin (BSA) or non-fat milk solution to avoid unspecific binding. Afterwards, the membrane is incubated with the

secondary antibody which binds to a species-specific binding site of the primary antibody. The secondary antibody is usually conjugated with a reporter enzyme such as horseradish peroxidase (HRP), which produces luminescence visualized on the film in proportion to the amount of target protein after reaction with chemiluminescent agent.

In this study, after CoCl_2 stimulation, the cells were washed with cold PBS, removed from the dish with a plastic scraper and the proteins were extracted breaking the cell membranes by pipetting up and down through a very small (insulin) syringe, in proteases inhibitor cocktail diluted 1:100 in RIPA buffer, working always on ice.

The protein samples concentration was determined with Bradford dye assay (Bradford 1976). In the acidic environment of the reagent, protein binds to the coomassie dye. This results in a spectral shift from the reddish/brown form of the dye (absorbance maximum at 465 nm) to the blue form of the dye (absorbance maximum at 610 nm). The difference between the two forms of the dye is greatest at 595 nm, which therefore is the optimal wavelength to measure the blue color from the coomassie dye-protein complex. The linear standard curve was established by a serial concentration (0, 1, 2, 4, 6, 10, 15 $\mu\text{g/ml}$) of BSA/coomassie dye solution. The absorbance was measured by a spectrophotometer (Bio-rad, SmartSpecTMPlus). This standard curve is valid when the square of coefficient of determination value $R^2 \geq 0.991$; otherwise, the assay should be repeated. To determine the protein concentration of a test sample from absorbance, the standard curve was used to find the concentration of standard that would have the same absorbance as the sample.

30 μg of each sample was separated by a pre-cast Tris-glycine gel (Anamed, Darmstadt, Germany) in an electrophoresis apparatus (Invitrogen). Then, the separated proteins were transferred on a nitrocellulose membrane (Hybond ECL) with Novex[®] Semi-Dry Blotter (Invitrogen) through a electrophoresis procedure, in which the gel was on the negative side of the apparatus and the nitrocellulose membrane on the positive side, in this way the negative-charged proteins are driven from the gel to the positive-charged membrane, in the same position. The membrane was then blocked in 5% non-fat milk solution (dissolved in TBS/0.1% tween) for 2 h. The blocked membrane was incubated with mouse monoclonal antibody against HIF-1 α (diluted in 2.5% non-fat milk solution, 1:500, R&D Systems, Germany) or β -Actin (dilute in 2.5% non-fat milk solution, 1:10000, Milipore, USA) overnight at 4 °C. After washing three times with TBS/0.1% tween, the membrane was incubated with HRP-conjugated anti-mouse antibody (diluted in 2.5% non-fat milk solution, 1:2000, Cell Signaling, USA) for 1 h. ECL system and hyperfilm (GE Health, Germany) were used for membrane visualization.

3.10 Immunofluorescence assay

Immunocytochemistry was applied in cultured cells in this study. It is a common technique to assess the localization, distribution and expression level of target protein in situ, using a specific antibody, and this antibody-antigen interaction can be visualized by many methods under the conventional microscope, fluorescence microscope or confocal microscope. Immunofluorescence is a method widely used in immunocytochemistry to visualize the target proteins with fluorescent dye. As for the indirect immunofluorescence assay, the secondary antibody labeled with fluorescent dye is used to bind with the primary antibody which is against the antigen being probed for (Figure 9). The Alexa Fluor fluorescent dyes conjugated secondary antibodies are typically used, because the Alexa Fluor family has more robust fluorophores which are less prone to photobleaching.

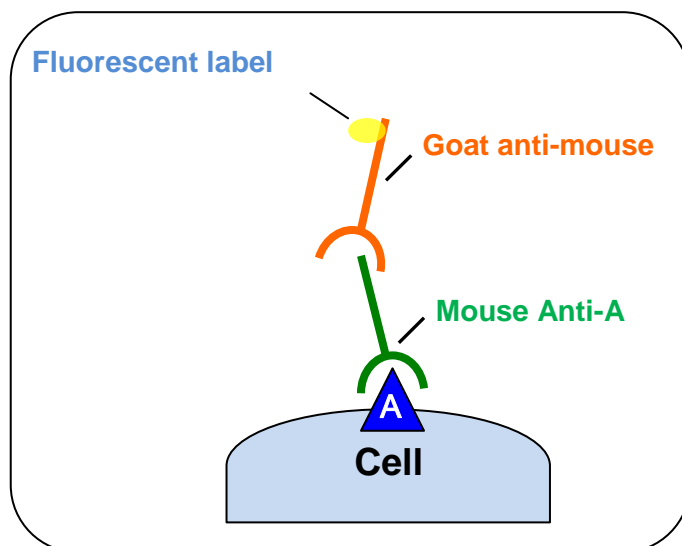


Figure 9. The principle of indirect fluorescence assay. The target antigen is recognized by the specific primary antibody which is recognized by the fluorescent labeled secondary antibody. The fluorescence is observed under fluorescence microscope or confocal microscope.

The confocal microscope is popularly applied in life sciences, and it uses a kind of optical imaging technique which can increase micrograph contrast and reconstruct three dimensional images. With conventional microscopes, the fluorescence of the entire of specimen excited in the optical path is detected as background signal. In contrast, the confocal microscope uses point illumination and an aperture in front of fluorescence detector to eliminate out-of-focus signal, so only fluorescence very closed to the focal plane and in the sample depth direction can be detected, which results in higher image resolution than that of conventional fluorescence microscopes. However, scanning over a regular raster (i.e. a rectangular pattern

of parallel scanning lines) in the specimen is required in 2D or 3D imaging, because only one point in the sample is illuminated at a time (Figure 10).

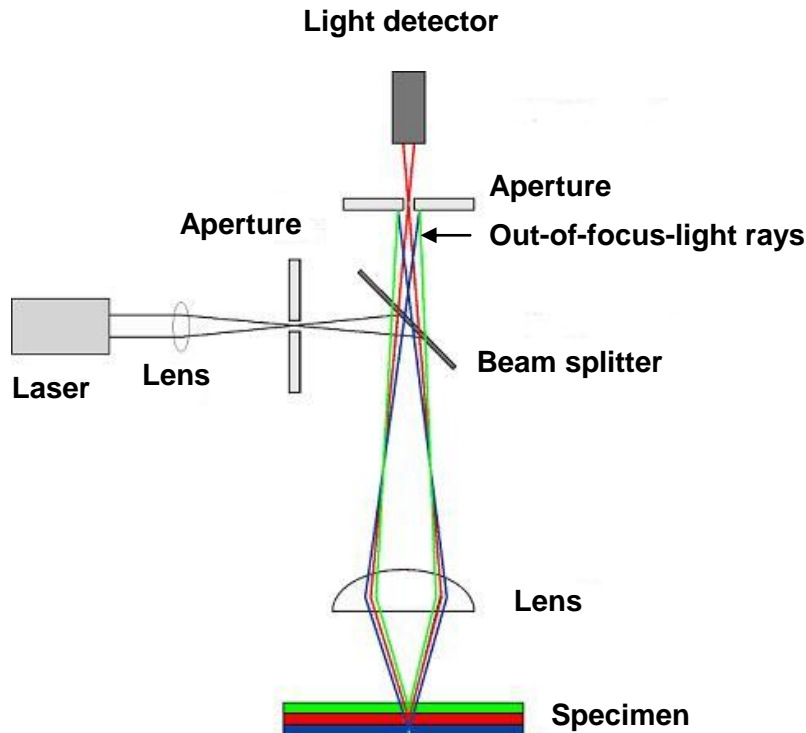


Figure 10. The principal light pathways in confocal microscope. A laser provides the excitation light, and the laser light reflects off a beam splitter to get across the specimen. Afterwards, the fluorescence dyes in the specimen is emitted, then the emitted light passes through the beam splitter and is focused onto the aperture. The light passing through the aperture is measured by the fluorescence detector.

In this study, 24 hours after transfection with siRNA against RSUME and scramble siRNA in 6-well plates, cells were split onto Falcon culture slides (BD biosciences), and stimulated with 250 μM CoCl_2 for 3 hours the next day. After treatment, cells were fixed in 4% paraformaldehyde for 5 minutes on ice, and then blocked in 5% goat serum with 0.1% (v/v) triton X-100 for 30 minutes at room temperature. Slides were incubated with mouse monoclonal anti-HIF-1 α (1: 100, Novus Biologicals, USA), rabbit polyclonal anti-cleaved-caspase-3 (1:200, Cell Signaling, USA) or rabbit polyclonal anti-VEGF (1:100, Abcam, USA) overnight at 4 $^{\circ}\text{C}$, and then washed and incubated with Alexa Fluor[®] 594 goat anti-mouse antibody ((Invitrogen, Paisley, UK) or Alexa Fluor[®] 594 goat anti-rabbit antibody (Invitrogen, Paisley, UK) for 45 minutes at room temperature. ProLong[®] Gold antifade reagent with DAPI (Invitrogen, Paisley, UK) was used for visualization of the cell nucleus. Images were obtained using a confocal microscope (FluoView[™] FV1000, Olympus, Munich, Germany). The proportion of cells immunopositive for cleaved caspase-3 was determined by counting the

number of positive cells out of 100 cells in five different areas of each slice. Images were obtained using 10x, 20x or 60x objectives.

3.11 Enzyme-Linked Immunosorbent Assay (ELISA)

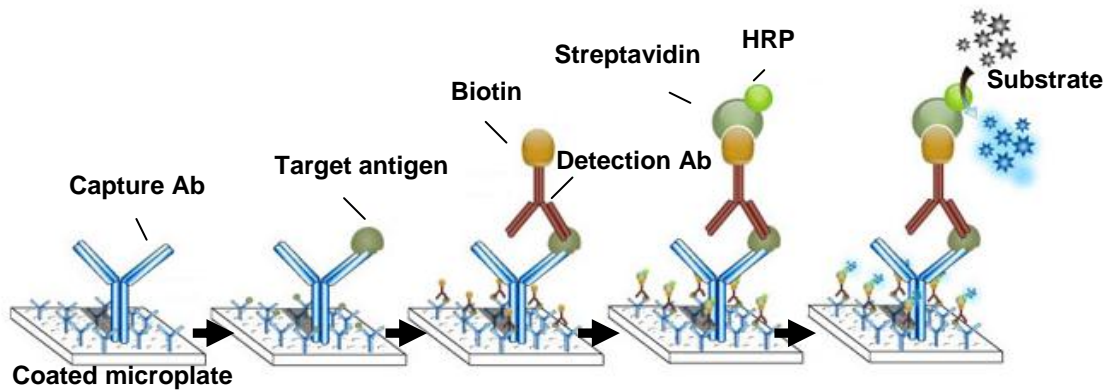


Figure 11. The procedure of sandwich ELISA.

ELISA is a biochemical technique to detect and quantify target antigen from ng/ml to pg/ml in samples, such as blood, urine and cell culture supernatant. The sandwich ELISA which measures the amount of antigen between two layers of antibodies (i.e. capture and detection antibody) is more sensitive and specific compared with other ELISA methods.

The general steps are as follows (Figure 11): 1) a known quantity of capture antibody is coated in a 96-well polystyrene plate; 2) non specific binding sites of the coated plate are blocked with blocking buffer (i.e. 5% BSA solution); 3) the appropriately diluted sample is applied and incubated for 2 hours at room temperature; 4) unbound antigen is washed away from the plate; 5) the biotinylated detection antibody that binds specifically to the antigen is applied and incubated for 2 hours at room temperature; 6) unbound biotinylated detection antibody is washed away from the plate; 7) the horseradish-peroxidase (HRP)-conjugated streptavidin which binds to the detection antibody is applied and incubate the plate for 30 minutes; 8) unbound streptavidin conjugates are washed away from the plate; 9) the substrate (1:1 mixture of H_2O_2 and tetramethylbenzidine), which is converted by HRP into a color, is applied and incubated for 15~30 minutes; 10) the absorbance of each well is measured using a multiwell spectrophotometer set to 450 nm to determine the presence and quantity of antigen.

In this study, cells were seeded in 48-well plates. After stimulation, the supernatant of cell culture was collected. The measurement of VEGF secreted into the cell culture supernatant

was carried out with VEGF ELISA kit (R&D Systems, Wiesbaden, Germany) following the manufacturer's instruction. All experiments were carried out in quadruplicates.

3.12 Proliferation assay

Cell proliferation was assessed using the non-radioactive colorimetric WST-1 assay. The Cell Proliferation Reagent WST-1 is a clear, slightly red ready-to-use solution, containing tetrazolium salt WST-1 and an electron coupling reagent, diluted in sterile phosphate buffered saline. This assay is based on the cleavage of WST-1 into formazan dye by mitochondrial dehydrogenases in viable cells, and provides a non-radioactive alternative to the [³H]-thymidine incorporation assay. An expansion in the number of viable cells results in an increase in the overall activity of mitochondrial dehydrogenases in the sample. This augmentation in enzyme activity leads to an increase in the amount of formazan dye formed, which directly correlates to the number of metabolically active cells in the culture. The absorbance of the dye solution is measured by a multiwell spectrophotometer (DYNATECH, MR5000) at 420-480 nm.

In this study, 6×10^3 cells/well TtT/GF cells or 15×10^3 cells/well AtT20 cells were seeded into 96-well plates, and 24 hours after transfection of siRNA against RSUME, the cell culture medium was changed to DMEM containing 2% FCS and incubated the cells for indicated time periods. Then, 10 μ l of WST-1 solution was added into the cell culture medium of each well and the plate was incubated at 37°C and 5% CO₂ for 30 minutes. The absorbance of samples was measured by a multiwell spectrophotometer set to 450 nm. All experiments were carried out in quadruplicates.

The effect of RSUME knockdown on cell growth was confirmed by direct cell counting using a cell size-adapted coulter counter (Beckman, Z1™ Series COULTER COUNTER®). The cell counting was carried out in triplicates.

3.13 Apoptosis detection

Apoptosis is characterized by membrane blebbing (zeiosis), condensation of cytoplasm, and the activation of an endogenous endonuclease. This nuclease cleaves double-stranded DNA at the most accessible internucleosomal linker region, generating mono- and oligonucleosomes. In contrast, the DNA of the nucleosomes is tightly complexed with the core histones H2A, H2B, H3, and H4, and is thus protected from cleavage by the endonuclease. The yielded DNA fragments are discrete multiples of a 180-bp subunit, detected as a "DNA ladder" on agarose gels after extraction and separation of the fragmented DNA. The enrichment of mono- and oligonucleosomes in the cytoplasm of the apoptotic cell is due to the fact that DNA degradation occurs several hours before plasma membrane breakdown.

DNA fragmentation as an indicator of apoptosis was measured by a cell death ELISA kit (Roche Molecular Biochemicals, Germany) according to the manufacturer's instruction. All experiments were carried out in triplicates. This assay is based on the quantitative "sandwich enzyme immunoassay" principle using mouse monoclonal antibodies directed against DNA and histones. This allows the specific determination of mono- and oligonucleosomes in the cytoplasmic fraction of cell lysates. The samples are placed into a streptavidin-coated microplate and incubated with a mixture of anti-histone-biotin and anti-DNA-peroxidase. During the incubation interval, nucleosomes will be captured via their histone component by the anti-histone-biotin antibody, while binding to the streptavidin-coated microplate. Simultaneously, anti-DNA-peroxidase binds to the DNA part of the nucleosomes. After removal of the unbound antibodies, the amount of peroxidase retained in the immunocomplex is photometrically determined with ABTS as the substrate (Figure 12, Roche Applied science).

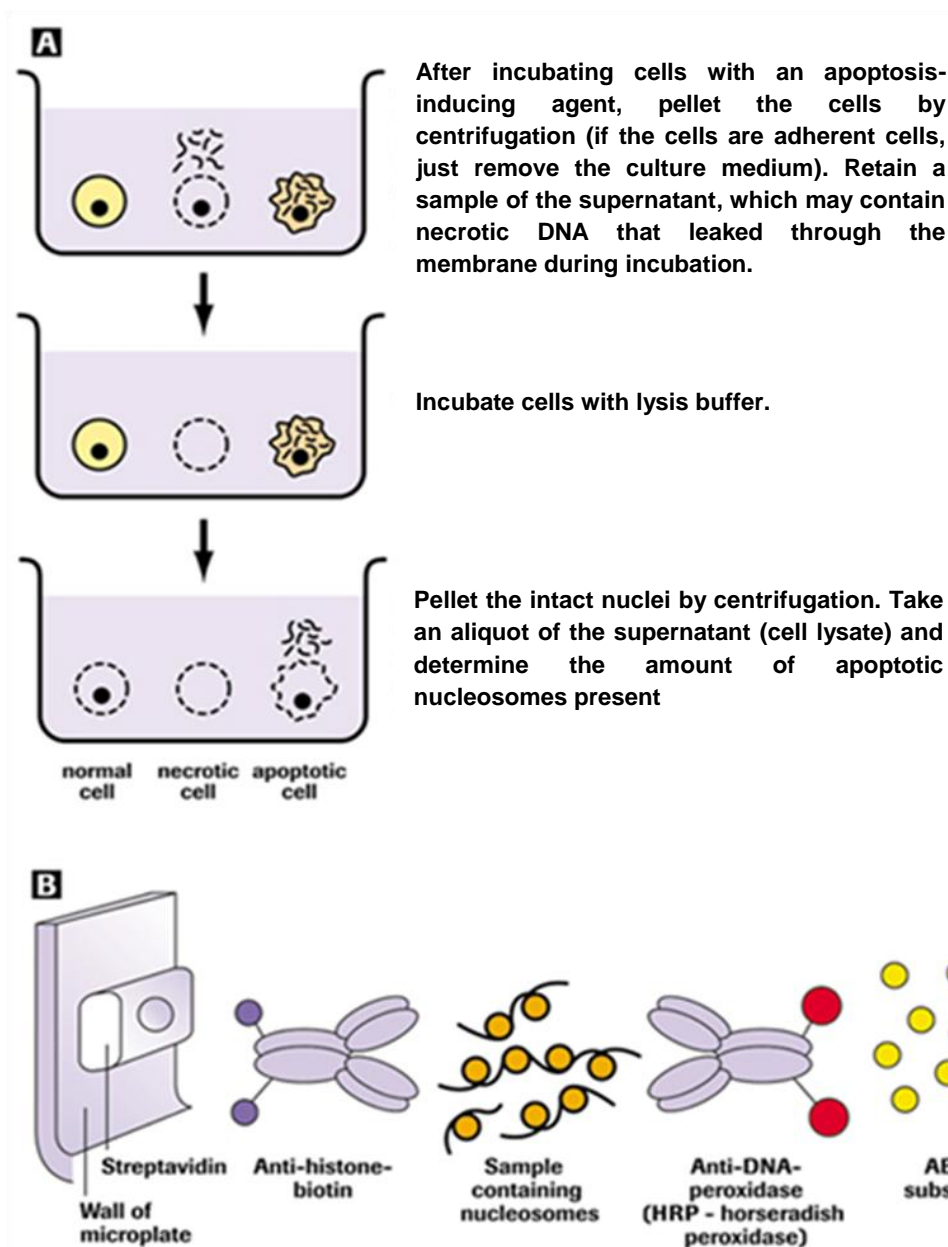


Figure 12. The principle of the Cell Death Detection ELISA^{PLUS}. Panel A: sample preparation; Panel B: ELISA. (Roche Applied Science).

3.14 Statistics

Results are expressed as mean \pm SD. The correlation analysis of HIF-1 α , VEGF and RSUME mRNA expression with the tumor grade, age and gender of patients was performed with the Fisher exact test, and statistical significance was considered at $P < 0.05$. The simple linear regression analysis was used to examine the correlation of HIF-1 α , VEGF and RSUME mRNA expression between each other, and a contribution ratio (square of coefficient of determination value R^2) >0.6 were considered significant. One-way ANOVA was used to compare variables in stimulation experiments and HIF-1 α , VEGF and RSUME mRNA expression in different

tumor types and normal pituitary glands, and $P < 0.05$ was considered as significant. The statistic analyses were performed with SigmaStat 2.0 (SPSS Inc).

4 Results

4.1 HIF-1 α , VEGF and RSUME mRNA expression in human normal pituitaries and pituitary adenomas

RNA were extracted from 3 human normal pituitaries and 31 pituitary adenomas, and then quantitative real time RT-PCR was performed to evaluate HIF-1 α , VEGF and RSUME mRNA levels with normalization to the amount of house keeping gene β -Actin (Figure 13 A-C).

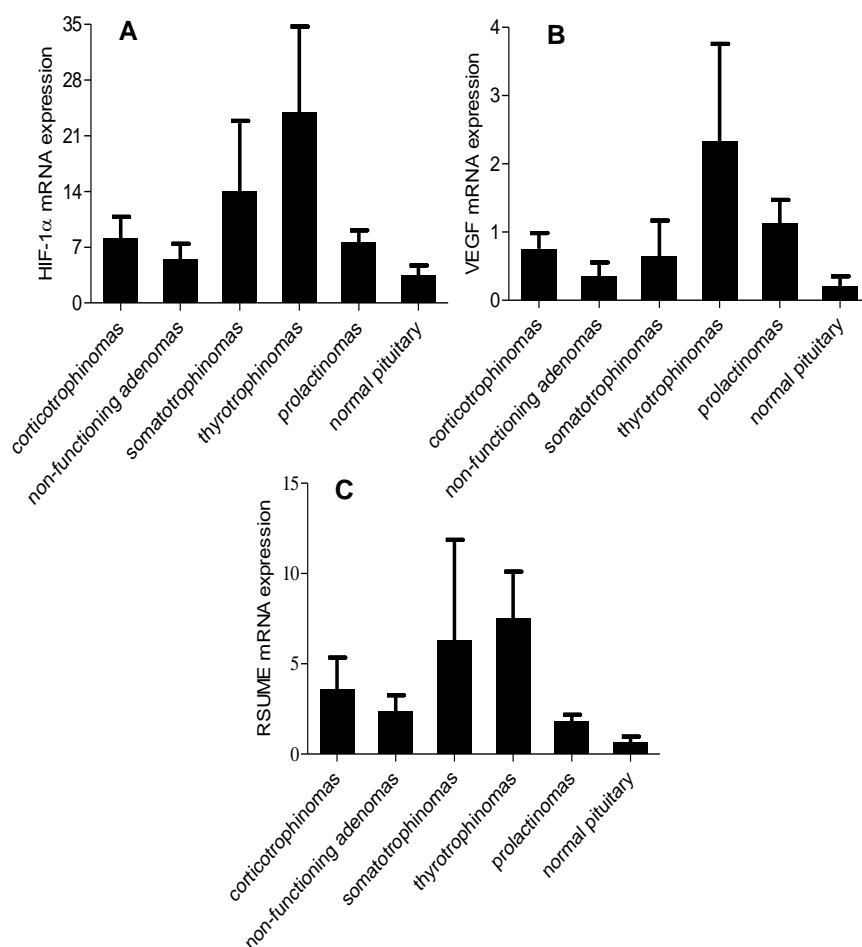


Figure 13. mRNA expression levels of HIF-1 α , RSUME and VEGF in human normal pituitaries and pituitary adenomas. Quantitative real time PCR was performed with 31 human pituitary adenomas and 3 normal pituitaries to detect the mRNA levels of HIF-1 α (A), VEGF (B) and RSUME (C). Values are given as mean \pm SD (standard deviation) after normalization to the amount of β -Actin. While the mRNA expression levels of HIF-1 α , RSUME and VEGF in human pituitary adenomas tended to be higher compared with normal pituitaries, the difference was not statistically significant, and the difference among the various types of adenomas examined was not statistically significant as well.

One-way ANOVA statistical analysis showed that the mRNA expression levels of HIF-1 α , RSUME and VEGF in human pituitary adenomas tended to be higher compared with normal pituitaries, the difference was not statistically significant, and the difference among the various types of adenomas examined was not statistically significant as well, although thyrotroph adenomas appeared to produce highest HIF-1 α , VEGF and RSUME levels. Lowest level of HIF-1 α and VEGF mRNA were found in non-functioning adenomas and lowest level of RSUME was found in prolactinomas.

Simple linear regression analyses showed that in the pituitary adenomas studied, VEGF and RSUME mRNA levels were significantly correlated with HIF-1 α mRNA levels ($R^2=0.6610$ or $R^2=0.7296$, respectively) (Figure 14 A, B). No significant correlation was found between HIF-1 α , VEGF, RSUME mRNA expression and patient age, gender, or tumor grade.

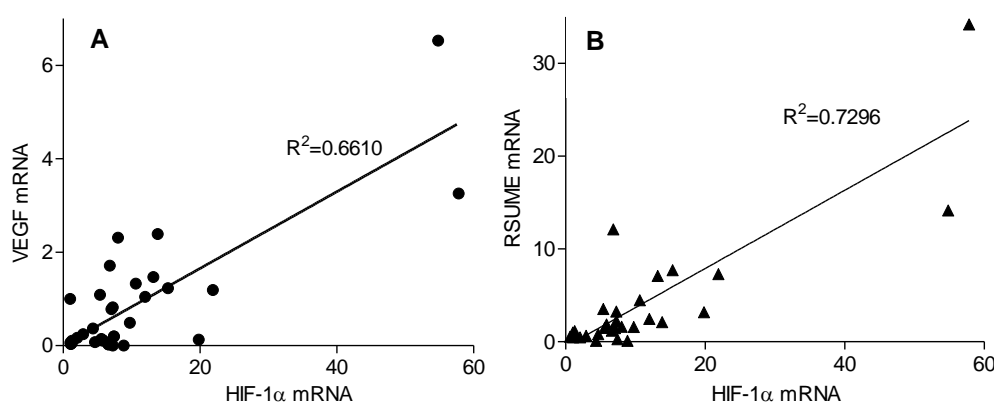


Figure 14. Correlations of mRNA expression levels among HIF-1 α , RSUME and VEGF in human normal pituitaries and pituitary adenomas. Values are given as mean \pm SD (standard deviation) after normalization to the amount of β -Actin. A, B: Simple linear regression analyses showed that VEGF and RSUME mRNA levels were significantly correlated with HIF-1 α mRNA levels in the tested pituitary adenomas ($R^2=0.6610$ or $R^2=0.7296$, respectively).

4.2 Effect of hypoxia mimicking conditions on RSUME mRNA expression

In order to test whether RSUME responds to hypoxia in pituitary tumor cells, RSUME mRNA expression under hypoxia mimicking conditions was investigated.

Before stimulation with hypoxia-mimicking agent CoCl₂, AtT20 and TtT/GF cells were exposed to medium containing only 1% FCS overnight, and then stimulated with 250 μ M CoCl₂ in the same medium. After CoCl₂ treatment, RSUME mRNA expression was measured with quantitative real time PCR. RSUME mRNA levels in AtT20 and TtT/GF cells were significantly increased shortly after CoCl₂ treatment and reached the peak at 30 minutes. Maximal

stimulations of 3.22 ± 0.58 and 2.65 ± 0.69 fold versus untreated cells were achieved in AtT20 and TtT/GF cells, respectively (Figure 15).

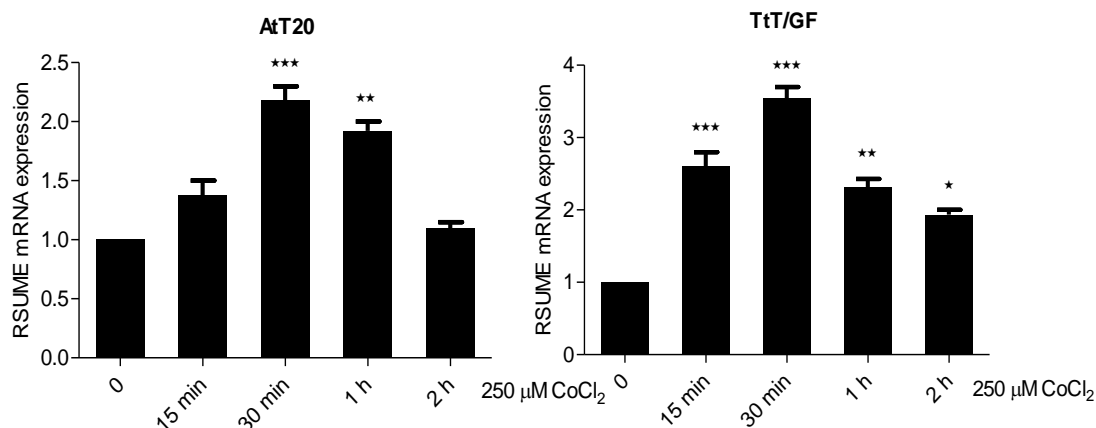


Figure 15. RSUME mRNA expression were increased under CoCl_2 stimulation in AtT20 and TtT/GF cells. AtT20 and TtT/GF cells were stimulated with $250 \mu\text{M}$ CoCl_2 . RSUME mRNA level was analyzed by quantitative real time PCR in triplicates, and the values are given as mean \pm SD after normalization to β -Actin. *, $P < 0.05$; **, $P < 0.01$; ***, $P < 0.001$ vs. untreated cells.

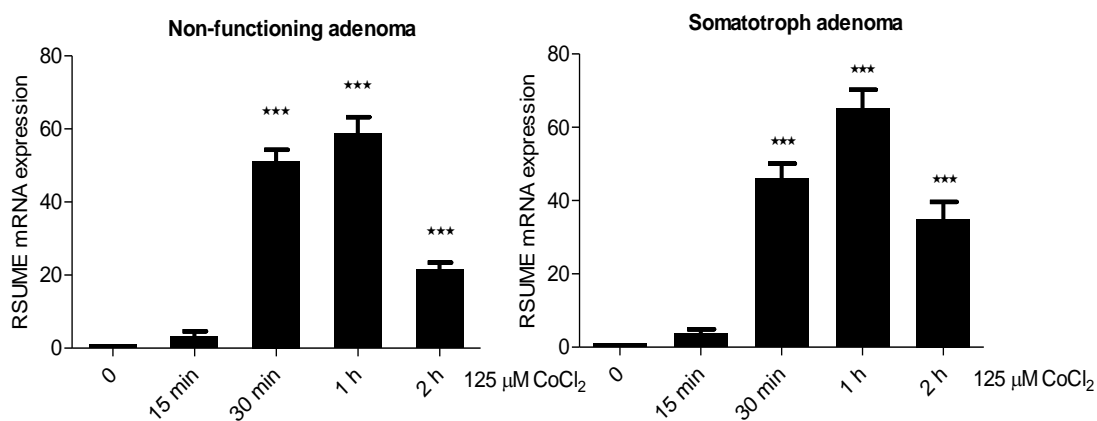


Figure 16. RSUME mRNA expression were increased under CoCl_2 stimulation in primary human pituitary tumor cells. Primary human pituitary tumor cells were stimulated with $125 \mu\text{M}$ CoCl_2 . RSUME mRNA level was analyzed by quantitative real time PCR in triplicates, and the values are given as mean \pm SD after normalization to β -Actin. ***, $P < 0.001$ vs. untreated cells. The similar effect was found in another primary non-functioning adenoma cells (data not shown).

The primary cell cultures of 2 non-functioning adenomas and 1 somatotroph adenoma were also tested. Before stimulation, primary human pituitary tumor cells were exposed to tumor

medium containing 2% FCS over night, and stimulated with 125 μM CoCl_2 in the same medium. After CoCl_2 treatment, RSUME mRNA expression was measured with quantitative real time PCR. RSUME mRNA levels were also significantly increased under CoCl_2 treatment in all the tested tumor cells (Figure 16 shows the results of 1 non-functioning adenoma and 1 somatotroph adenoma). Maximal stimulations of 58.80 ± 7.64 and 65.10 ± 8.84 fold versus untreated cells were achieved in the non-functioning adenoma and somatotroph adenoma shown above, respectively. RSUME mRNA expression reached the peak at 1 hour after stimulation. The similar result was found in another non-functioning adenoma (data not shown).

4.3 Effect of hypoxia mimicking conditions on HIF-1 α protein expression

In order to investigate whether HIF-1 α can be activated after hypoxia in pituitary tumor cells, HIF-1 α protein levels under hypoxia mimicking conditions were determined by western blot. Before stimulation, TtT/GF and AtT20 cells were exposed to medium containing only 1% FCS overnight, and then stimulated in the same medium with CoCl_2 of different doses and for different time periods. After stimulation, HIF-1 α was determined in cell lysates by western blot. CoCl_2 dose-dependently increased HIF-1 α protein levels in both cell lines (Figure 17). With stimulation of 5 hours, the maximal HIF-1 α expression was achieved at 500 μM CoCl_2 . The stimulatory effect was time-dependent and with the stimulation of 250 μM CoCl_2 the maximum HIF-1 α protein levels were reached after 2 h and 3 h in AtT20 and TtT/GF cell lines, respectively (Figure 17). During CoCl_2 stimulation, compared with untreated cells, the toxic effects of CoCl_2 and the changes in cell viability were not observed.

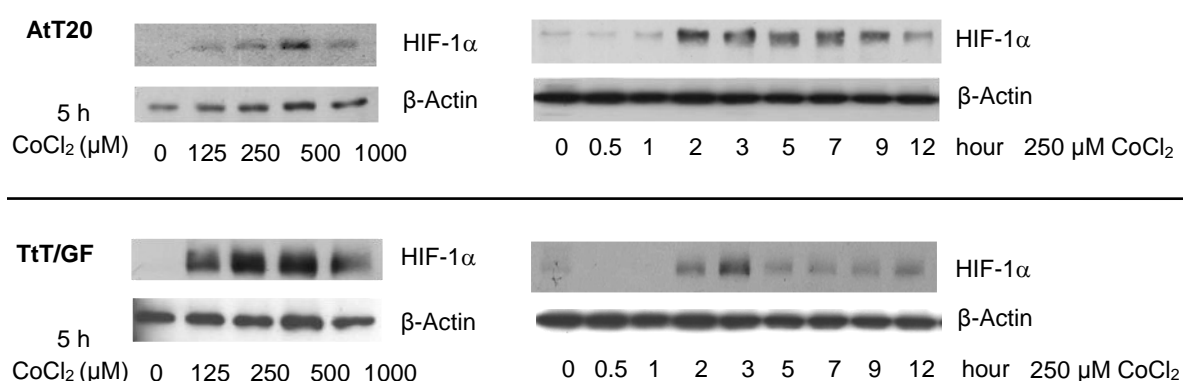


Figure 17. HIF-1 α protein level was increased under CoCl_2 stimulation in a concentration- and time-dependent manner in AtT20 and TtT/GF cells. AtT20 and TtT/GF cells were stimulated with indicated concentrations of CoCl_2 and time periods. Each image is representative of 3 experiments with similar results.

For immunofluorescence studies, after stimulation of 250 μM CoCl_2 for 3 hours, AtT20 and TtT/GF cells were fixed and immunofluorescence assay for HIF-1 α was performed. By confocal immunofluorescence microscopy, CoCl_2 did not only stimulate expression of HIF-1 α but also its translocation into the nucleus as shown in both cell lines (Figure 18).

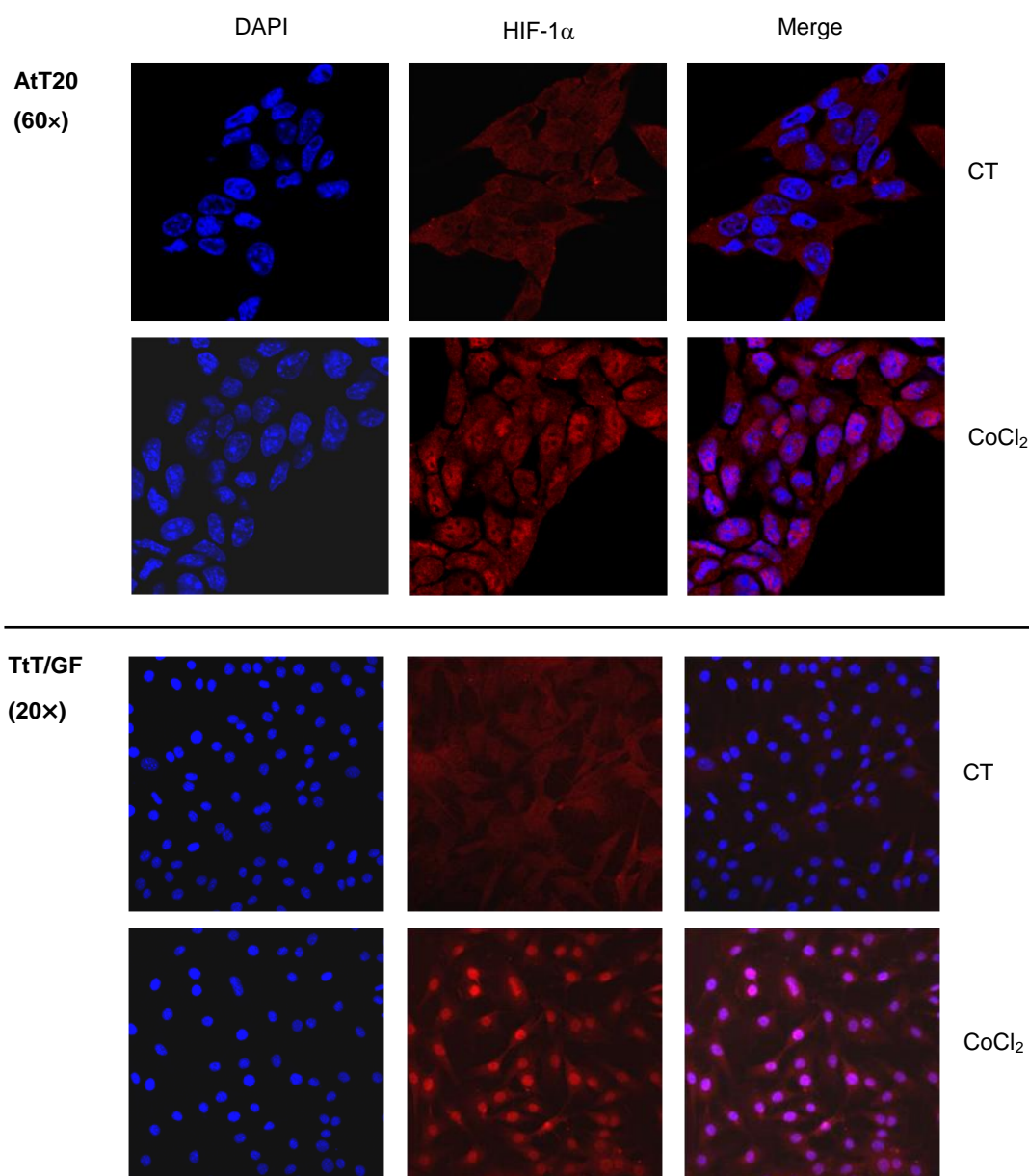


Figure 18. HIF-1 α is translocated and accumulated in nucleus after CoCl_2 treatment in AtT20 and TtT/GF cells. AtT20 and TtT/GF cells were stimulated with 250 μM CoCl_2 for 3 hours. Red color corresponds to HIF-1 α , and blue color corresponds to nucleus. The immunofluorescence images were taken from confocal microscope using 60x and 20x objectives for AtT20 and TtT/GF cells, respectively. The parameters were fixed when taking images by confocal microscopy, and one representative image of 5 observations from two independent experiments with similar results is shown.

Primary cell cultures of 8 human pituitary adenomas (5 non-functioning, 2 somatotroph adenomas, 1 lactotroph adenomas) were also treated with CoCl_2 in order to find out whether HIF-1 α can be activated as in mouse pituitary tumor cell lines. Before stimulation, primary tumor cells were exposed to tumor medium containing only 2% FCS overnight, and then stimulated in the same medium with CoCl_2 of different doses and for different time periods. After stimulation, HIF-1 α was determined in cell lysates by western blot. HIF-1 α protein expression was time- and dose-dependently increased after CoCl_2 treatment in all the tested primary cell cultures (Figure 19 shows the representative findings from two tumor cell cultures). Due to limited amount of primary tumor cells, not all the stimulation experiments of different doses and time periods could be done in parallel.

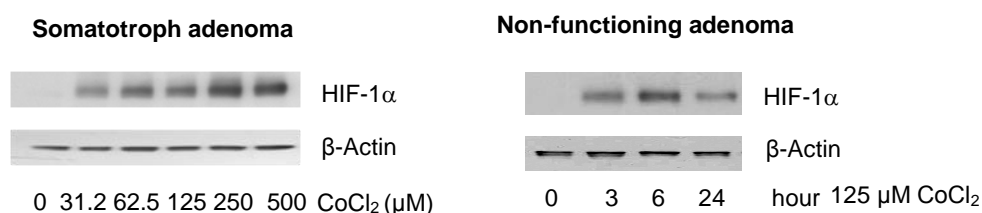


Figure 19. HIF-1 α expression was increased under CoCl_2 stimulation in a concentration- and time-dependent manner in primary human pituitary tumor cells.

Primary somatotroph adenoma cells were stimulated with different concentrations of CoCl_2 for 3 h, and primary non-functioning adenoma cells were stimulated with 125 μM CoCl_2 for different time periods. Each image is representative of 3 experiments with similar results. HIF-1 α was increased in all the tested primary human pituitary tumor cell cultures after CoCl_2 treatment, following a time- and concentration-dependent manner. Western blots from primary human somatotroph adenoma cells and non-functioning adenoma cells were shown as representatives.

4.4 Effect of hypoxia mimicking conditions on VEGF expression

VEGF is a well-characterized HIF-1 α target and a key factor in angiogenesis. In order to find out whether CoCl_2 not only induces HIF-1 α protein expression but also stimulates VEGF secretion, VEGF secretion after CoCl_2 stimulation was investigated by VEGF ELISA.

Before stimulation, TtT/GF and AtT20 cells were exposed to medium containing only 1% FCS overnight, and then stimulated in the same medium with CoCl_2 of different doses and for different time periods. After stimulation, the supernatant of the cell culture was collected and VEGF secretion was determined by ELISA. VEGF was significantly increased under CoCl_2 treatment, following a time- and concentration-dependent manner, in TtT/GF cells (Figure 20). However, CoCl_2 treatment did not significantly stimulate the increase of VEGF secretion in

AtT20 cells. From the previous study, it is shown that AtT20 cells have a very high basal VEGF production rate (Lohrer, et al. 2001). It may be that the VEGF output by AtT20 cells is already saturated and can not be further enhanced under hypoxia mimicking conditions.

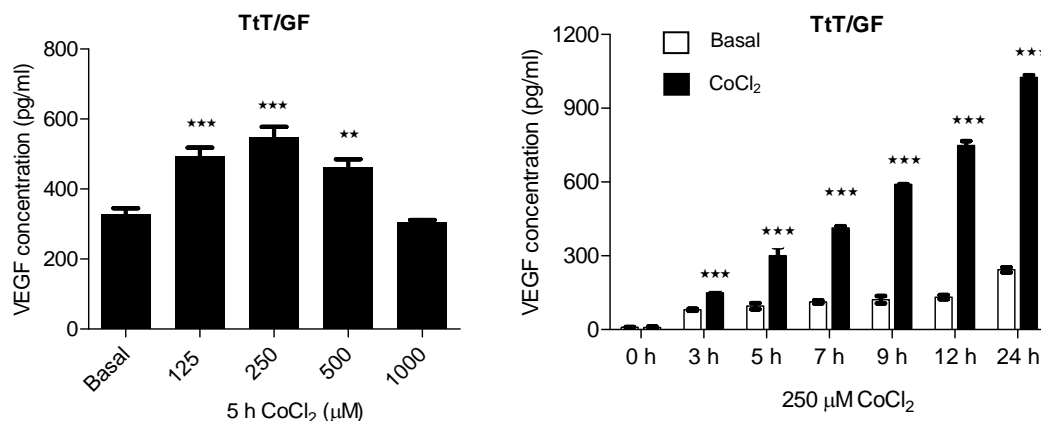


Figure 20. VEGF expression was increased under CoCl₂ stimulation in a concentration- and time-dependent manner in TtT/GF. TtT/GF cells were stimulated with indicated concentrations of CoCl₂ and time periods. Values were from ELISA assays, and given as mean±SD. **, *P* < 0.01; ***, *P* < 0.001 vs. untreated cells. All experiments were carried out in quadruplicates.

VEGF secretion under CoCl₂ stimulation in primary cell cultures of 17 human pituitary adenomas (11 non-functioning, 3 somatotroph, 2 lactotroph, 1 corticotroph) was also tested. Before stimulation, primary tumor cells were exposed to tumor medium containing only 2% FCS overnight, and then stimulated in the same medium with different doses of CoCl₂ and for different time periods. After stimulation, VEGF secretion in the supernatant of culture medium was determined by ELISA. CoCl₂ dose-dependently increased VEGF secretion in all the tested primary tumor cells (Figure 21 A-D show the representative findings). Due to limited amount of primary tumor cells, not all the stimulation experiments of different doses and time periods could be done in parallel.

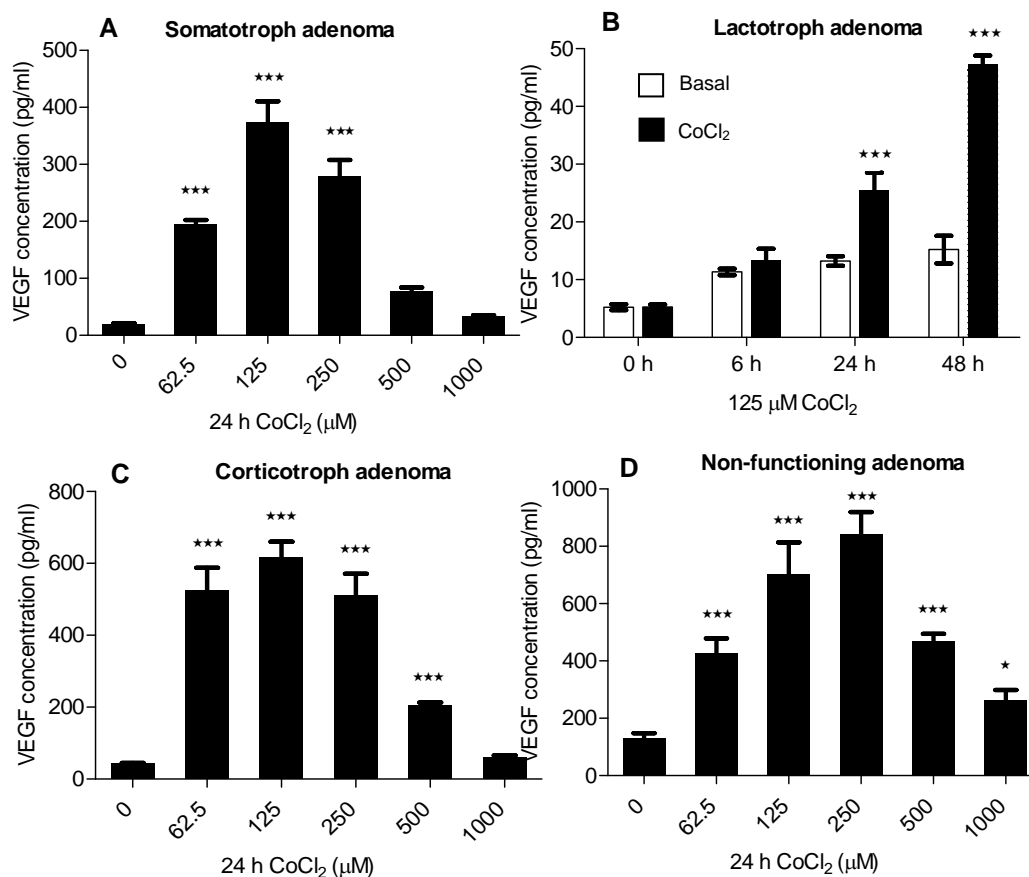


Figure 21. VEGF expression was increased under CoCl₂ stimulation in a concentration- and time-dependent manner in primary human pituitary tumor cells. Primary human tumor cells were stimulated with indicated concentrations of CoCl₂ and time periods. Values were from ELISA assays, and given as mean±SD. **, $P < 0.01$; ***, $P < 0.001$ vs. untreated cells. All experiments were carried out in quadruplicates.

4.5 Effect of RSUME knockdown on HIF-1 α and VEGF production

4.5.1 In mouse pituitary cell lines

In order to investigate whether RSUME plays a role in HIF-1 α increase after hypoxia in pituitary tumor cells, siRNA against mouse RSUME and scrambled siRNA were transfected into AtT20 and TtT/GF cells. 24 hours after transfection, the total RNA was extracted and RT-PCR for mouse RSUME was performed. RSUME mRNA was obviously decreased in both cell lines 24 hours after RSUME siRNA transfection compared with un-transfected and scrambled siRNA transfected control (Figure 22). 48 hours after transfection of RUSME siRNA and scrambled siRNA, AtT20 and TtT/GF cells were stimulated with 250 μ M CoCl₂ in medium containing 1% FCS for 3 hours. After stimulation, HIF-1 α was determined in cell lysates by western blot. CoCl₂-stimulated HIF-1 α expression was significantly suppressed in RSUME

siRNA transfected AtT20 cells and TtT/GF compared with un-transfected and scrambled siRNA transfected control (Figure 23).

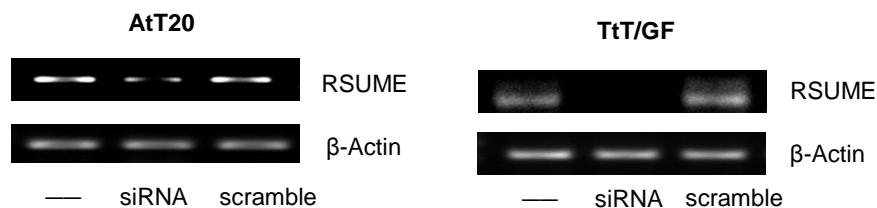


Figure 22. RSUME mRNA expression was suppressed by transfection of siRNA against mouse RSUME in AtT20 and TtT/GF cells. AtT20 and TtT/GF cells were transfected with siRNA against mouse RSUME, and RT-PCR was performed 24 hours after transfection.

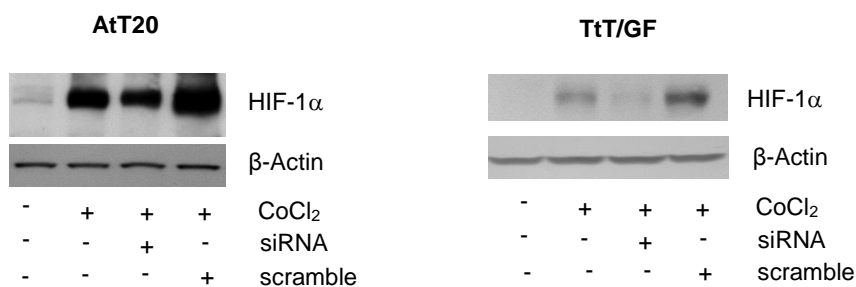


Figure 23. RSUME knockdown suppressed HIF-1 α in both TtT/GF and AtT20 cells. AtT20 and TtT/GF cells were transfected with mouse RSUME siRNA for 48 h, and then treated with 250 μ M CoCl₂ for 3 h. Each image is representative of 3 experiments with similar results.

For immunofluorescence studies, 48 hours after transfection of RSUME siRNA and scrambled siRNA, AtT20 and TtT/GF cells were stimulated with 250 μ M CoCl₂ in medium containing 1% FCS for 3 hours. After stimulation, AtT20 and TtT/GF cells were fixed and immunofluorescence assay for HIF-1 α was performed. Confocal immunofluorescence microscopy showed that the translocation of HIF-1 α in response to CoCl₂ treatment was impaired in AtT20 and TtT/GF cells in which RSUME had been knocked down (Figure 24 and Figure 25).

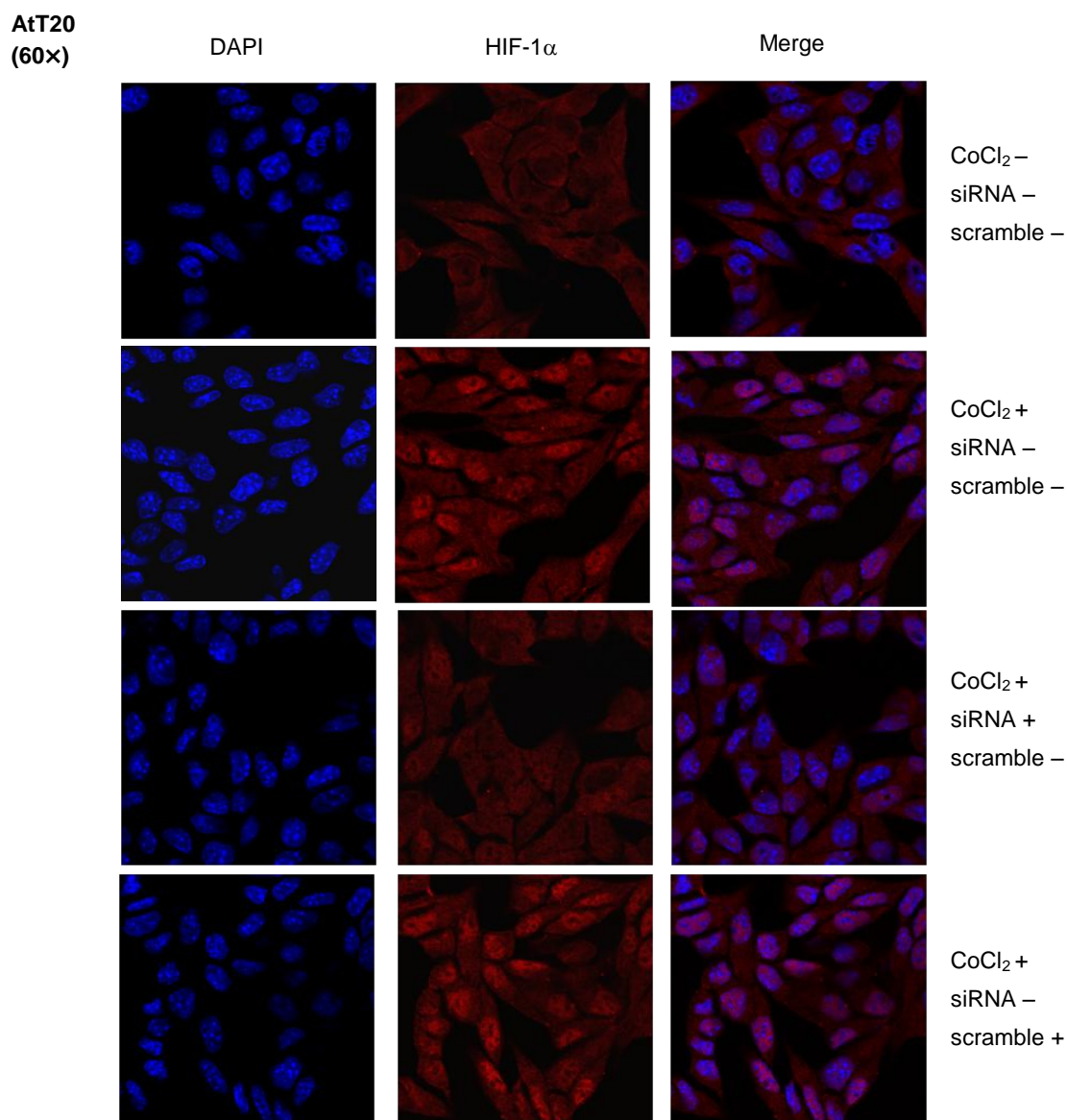


Figure 24. HIF-1 α was suppressed by RSUME knockdown in AtT20 cells as shown by immunofluorescence assay. 48 hours after transfection of RUSME siRNA and scrambled siRNA, AtT20 cells were stimulated with 250 μ M CoCl₂ for 3 hours. Red color corresponds to HIF-1 α , and blue color corresponds to nucleus. The immunofluorescence images were taken from confocal microscope using 60x objectives. The parameters were fixed when taking images by confocal microscopy, and one representative image of 5 observations from two independent experiments with similar results is shown.

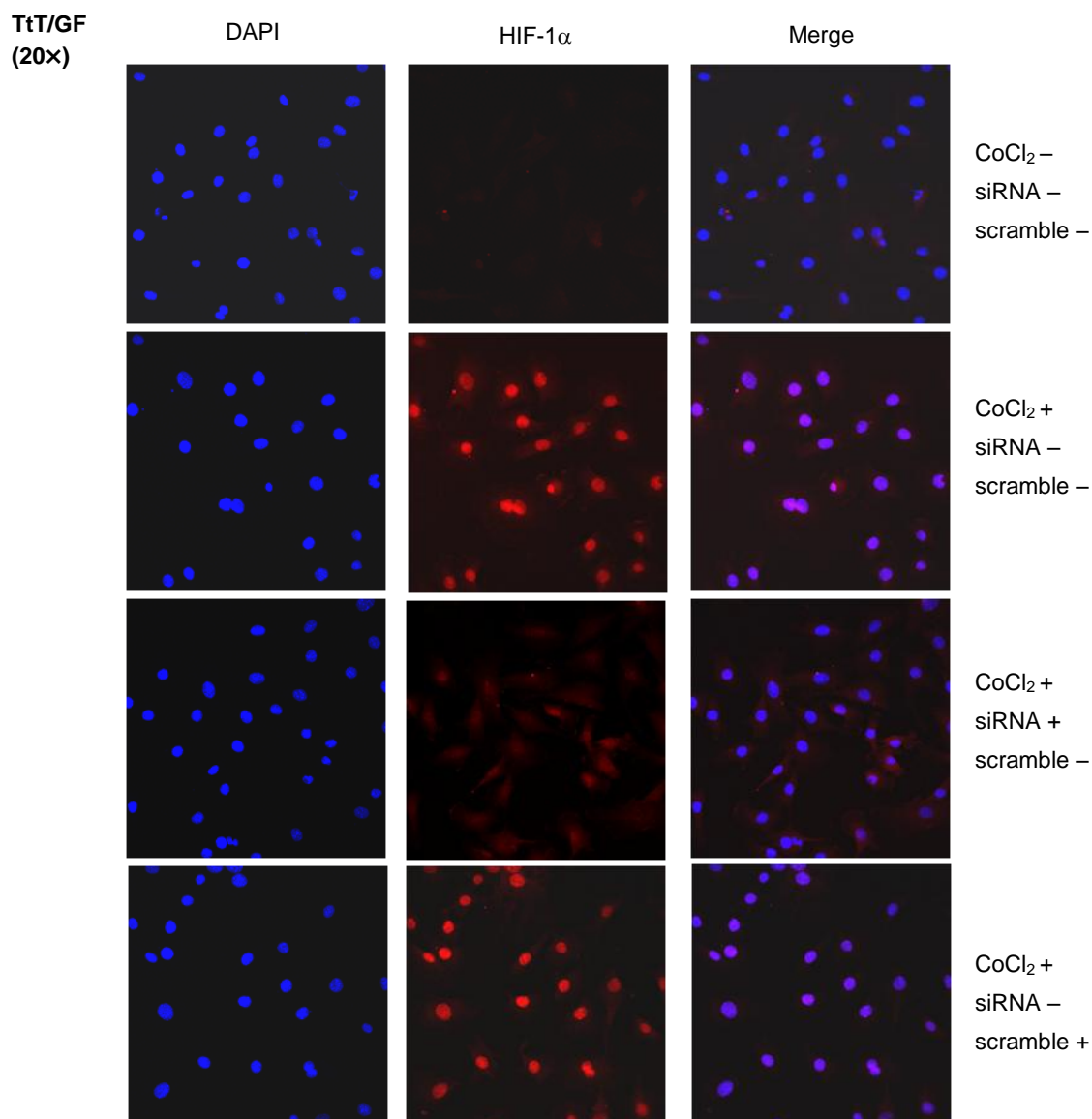


Figure 25. HIF-1 α was suppressed by RSUME knockdown in TtT/GF cells as shown by immunofluorescence assay. 48 hours after transfection of RUSME siRNA and scrambled siRNA, TtT/GF cells were stimulated with 250 μ M CoCl₂ for 3 hours. Red color corresponds to HIF-1 α , and blue color corresponds to nucleus. The immunofluorescence images were taken from confocal microscope using 20 \times objectives. The parameters were fixed when taking images by confocal microscopy, and one representative image of 5 observations from two independent experiments with similar results is shown.

In order to find out whether RSUME knockdown not only suppresses HIF-1 α protein expression but also reduces VEGF secretion, VEGF ELISA was performed to determine VEGF secretion in AtT20 and TtT/GF cells after transfection of siRNA against RSUME.

For TtT/GF cells, 48 hours after transfection of RSUME siRNA, cells were treated with 250 μ M CoCl₂ for 24 h, and then the culture supernatant was collected for VEGF ELISA and RNA was extracted for RT-PCR. From VEGF ELISA, it was found that RSUME knockdown did not significantly reduce the basal VEGF secretion, but significantly decreased CoCl₂-stimulated VEGF expression. From RT-PCR, VEGF mRNA expression was obviously increased by CoCl₂ stimulation, and was significantly suppressed by RSUME knockdown compared with un-transfected and scrambled siRNA transfected control (Figure 26)

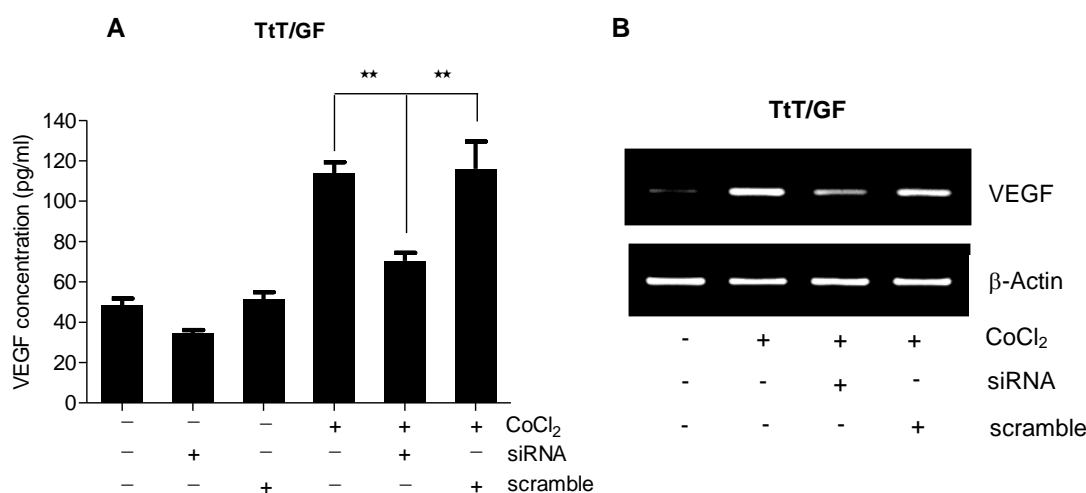


Figure 26. CoCl₂-stimulated VEGF expression was suppressed by RSUME knockdown at both protein and mRNA levels in TtT/GF cells. After 48 h transfection of RSUME siRNA, TtT/GF cells were treated with 250 μ M CoCl₂ for 24 h, and then VEGF ELISA (A) and RT-PCR (B) were performed to determine VEGF protein and mRNA expression. ELISA assay was carried out in quadruplicates and values were given as mean \pm SD. **, $P < 0.01$. Images of ethidium bromide agarose gel are representatives of 3 experiments with similar results.

For AtT20 cells, the effect of RSUME silencing was only tested at basal conditions, as it was shown that CoCl₂ treatment did not significantly enhance VEGF secretion in this cell line. To this end, 48 hours after transfection of RSUME siRNA, the culture supernatant of AtT20 cells was collected for VEGF ELISA, RNA from a part of cells was extracted for RT-PCR, and cells were also fixed to perform immunofluorescence studies. From VEGF ELISA and RT-PCR, it was found that basal VEGF expression was suppressed at both protein and mRNA levels by RSUME knockdown compared with un-transfected and scrambled siRNA transfected control

(Figure 27). From Immunofluorescence studies, VEGF staining was obviously weaker in cells with RSUME knockdown compared with un-transfected and scrambled siRNA transfected control, confirming that RSUME knockdown resulted in a significant reduction of basal VEGF expression in AtT20 cells (Figure 28).

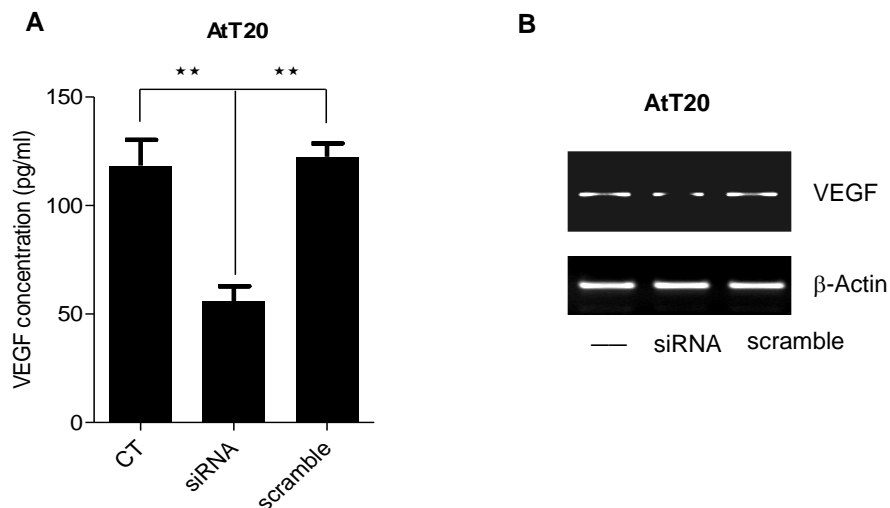


Figure 27. Basal VEGF expression was suppressed by RSUME knockdown at both protein and mRNA levels in AtT20 cells. After 48 h transfection of RSUME siRNA, VEGF ELISA (A) and RT-PCR (B) were performed to determine VEGF protein and mRNA expression. ELISA assay was carried out in quadruplicates and values were given as mean \pm SD. **, $P < 0.01$. Images of ethidium bromide agarose gel are representatives of 3 experiments with similar results.

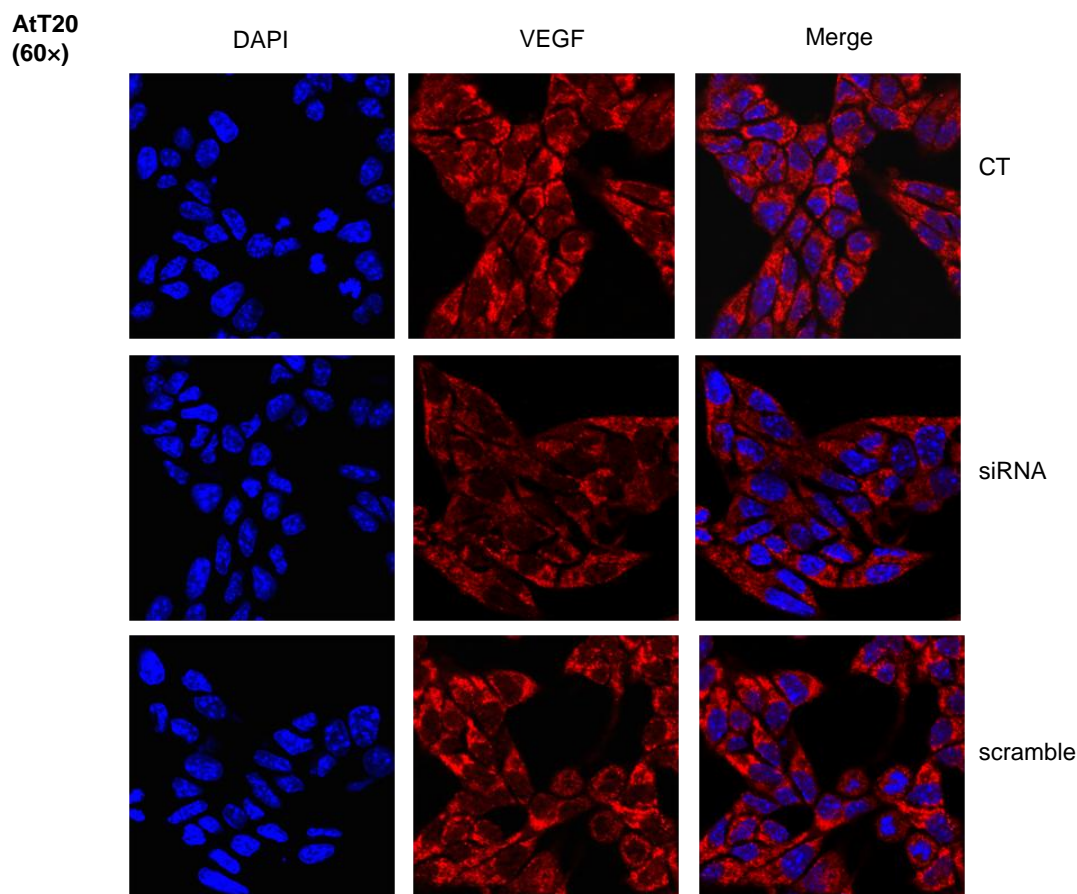


Figure 28. Basal VEGF production was suppressed by RSUME knockdown in AtT20 cells as shown by immunofluorescence assay. After 48 h transfection of RSUME siRNA, immunofluorescence was performed to stain VEGF. Red color corresponds to VEGF, and blue color corresponds to nucleus. The parameters were fixed when taking images by confocal microscopy using 60x objectives, and one representative image of 5 observations from two independent experiments with similar results is shown.

4.5.2 In primary human pituitary tumor cell cultures

RSUME knockdown was applied in primary human pituitary tumor cell cultures to find out whether RSUME is implicated in HIF-1 α activation as in mouse pituitary cell lines. Due to limited amount of primary tumor cells, the experiments on HIF-1 α and VEGF expression after RSUME knockdown could not be done in parallel.

Transfection of siRNA in primary human pituitary tumor cells was established for the first time in 6 primary cell cultures of human pituitary non-functioning adenomas, and BLOCK-iT™ Alexa Fluor® red fluorescent oligo was used to estimate transfection efficiency. With optimized transfection conditions, transfection efficiency was determined to be about 50% by counting red fluorescence stained cells in 100 cells 24 hours after transfection of fluorescent oligo (Figure 29). RNA was extracted for RT-PCR 24 hours after transfection of RSUME siRNA.

From RT-PCR, it was confirmed that 50 nM siRNA against human RSUME obviously suppressed RSUME mRNA in primary tumor cells (Figure 30).

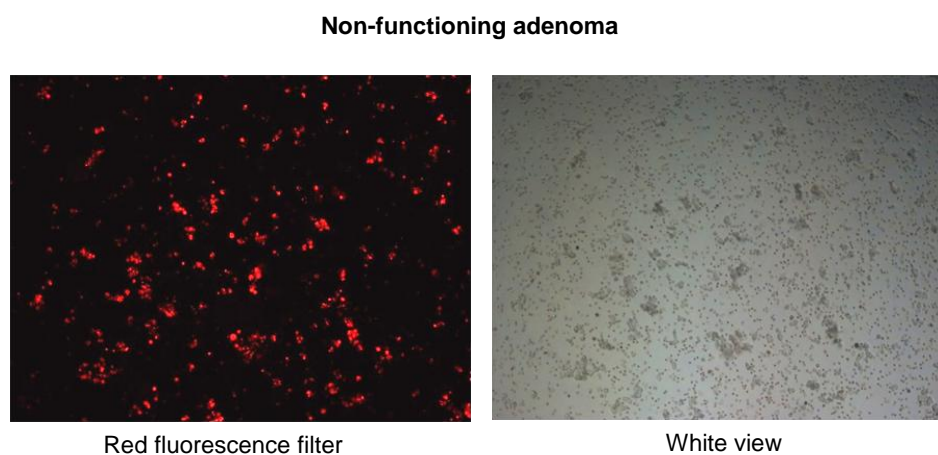


Figure 29. Evaluation of siRNA transfection efficiency in primary human pituitary tumor cells. The red fluorescent oligo was transfected into primary cells. 24 hours after transfection, the cells were observed under fluorescence microscope, and the number of cells with red color was counted in 100 cells to determine the transfection efficiency. The images were taken from fluorescence microscope using 10× objectives.

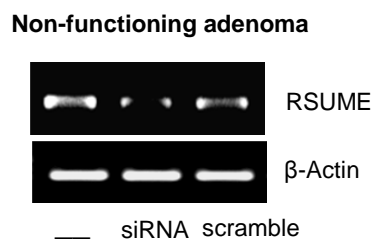


Figure 30. RSUME mRNA expression was suppressed by transfection of siRNA against human RSUME in primary human pituitary tumor cells. The primary human non-functioning tumor cells were transfected with siRNA against human RSUME, and RT-PCR was performed 24 hours after transfection.

With optimized transfection conditions, RSUME knockdown was also performed in the primary human cell cultures of 1 corticotroph adenoma and 1 somatotroph adenoma. 5 days after transfection of 20 nM or 50 nM RSUME siRNA, the corticotroph tumor cells were stimulated with 125 μ M CoCl₂ for 3 hours, and then HIF-1 α expression in cell lysates was determined by western blot. For the primary somatotroph tumor cells, 4 days after transfection of RSUME siRNA, cells were stimulated with 125 μ M CoCl₂ for 24 hours, and then the supernatant of cell culture was collected for VEGF ELISA. CoCl₂-stimulated HIF-1 α protein expression and VEGF secretion was significantly suppressed in that corticotroph adenoma and somatotroph

adenoma, respectively, compared with scrambled siRNA transfected controls (Figure 31 A, B). The suppression of HIF-1 α and VEGF expression by RSUME knockdown was not found until 5 days after transfection of siRNA.

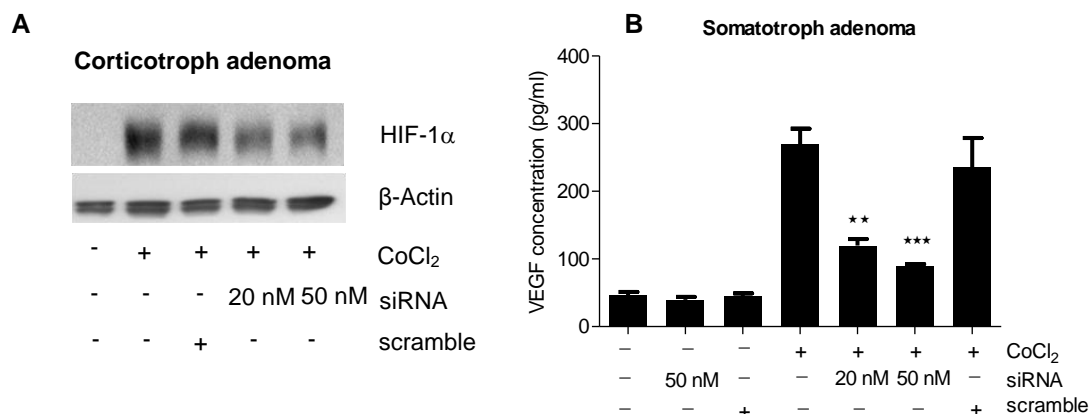


Figure 31. CoCl₂-stimulated HIF-1 α and VEGF secretion were suppressed by RSUME knockdown in primary human pituitary adenoma cells. The primary human corticotroph and somatotroph tumor cells were stimulated with CoCl₂ 5 days and 4 days after transfection of RSUME siRNA, respectively. HIF-1 α and VEGF expression were determined by western blot in corticotroph tumor cells (A) and by VEGF ELISA in somatotroph tumor cells (B), respectively. **, $P < 0.01$; ***, $P < 0.001$.

4.6 Effect of RSUME knockdown on proliferation and apoptosis in mouse pituitary cell lines

During the application of RSUME silencing, it was noticed that a part of cells appeared dead. Therefore, the effect of RSUME knockdown on proliferation and apoptosis in pituitary tumor cells was studied in AtT20 and TtT/GF cells.

AtT20 and TtT/GF cells were transfected with RSUME siRNA in 6-well plates. 24 hours after transfection, the cells were split into 96-well plates and cultured in medium containing 2% FCS for 48 hours. Afterwards, WST-1 assays were performed and the absorbance of samples was measured by a multiwell spectrophotometer set to 450 nm. Meanwhile, the cell number was also counted using a cell size-adapted coulter counter. By decreased absorbance values from WST-1 assay and the decreased cell number, RSUME knockdown significantly suppressed cell proliferation in both AtT20 and TtT/GF cells compared with un-transfected and scrambled siRNA transfected control (Figure 32 A, B).

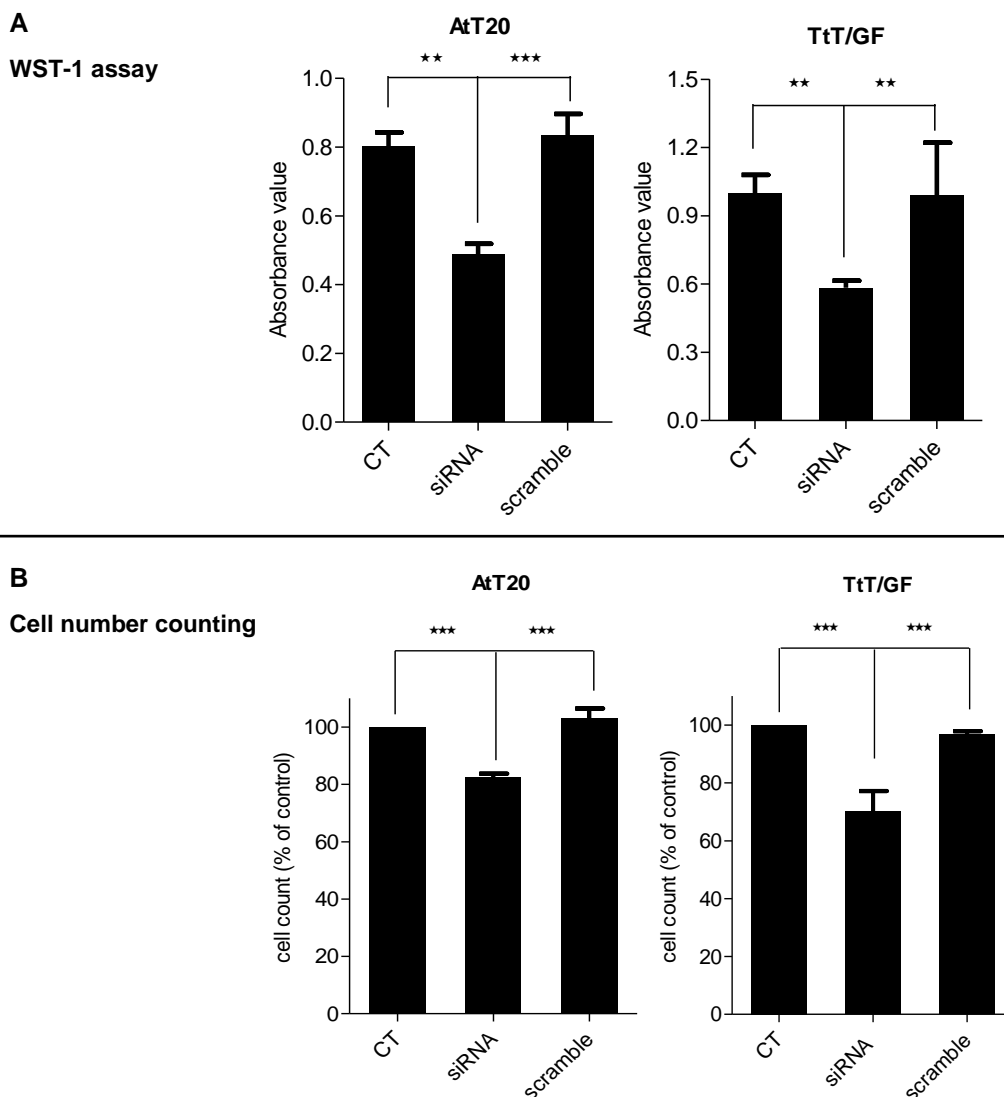


Figure 32. RSUME knockdown suppressed proliferation in both AtT20 and TtT/GF cells. AtT20 and TtT/GF cells were transfected with RSUME siRNA for 72 h, and then cell proliferation was determined by WST-1 assay (A) and cell number counting (B). **, $P < 0.01$; ***, $P < 0.001$. The WST-1 assay was carried out in quadruplicates and cell number counting was carried out in triplicates.

RSUME knockdown could be involved in induction of apoptosis besides in the suppression of cell proliferation in pituitary tumor cells. Therefore, studies on apoptosis in AtT20 and TtT/GF cells were carried out. AtT20 and TtT/GF cells were transfected with RSUME siRNA in 6-well plates. 24 hours after transfection, the cells were split into 96-well plates or slides and cultured in medium containing 2% FCS for 48 hours. Afterwards, apoptosis-associated DNA fragmentation was measured with a specific ELISA in 96-well plates, and the cells on slides were fixed to perform immunofluorescence studies on cleaved caspase-3. From cell death ELISA, a significant increase of apoptosis-associated DNA fragmentation by RSUME knockdown was observed in both AtT20 and TtT/GF cells compared with un-transfected and

scrambled siRNA transfected control (Figure 33). From immunofluorescence studies on cleaved caspase-3, the active fragment of a well-known pro-apoptotic protein caspase-3, it was found that the number of cells with immunoreaction of cleaved caspase-3 strongly increased by RSUME knockdown compared with un-transfected and scrambled siRNA transfected control in both AtT20 cells (Figure 34) and TtT/GF cells (data not shown). This finding indicates that the RSUME knockdown induces pro-apoptotic caspase-3, and thus confirms the involvement of RSUME in apoptosis of pituitary tumor cells.

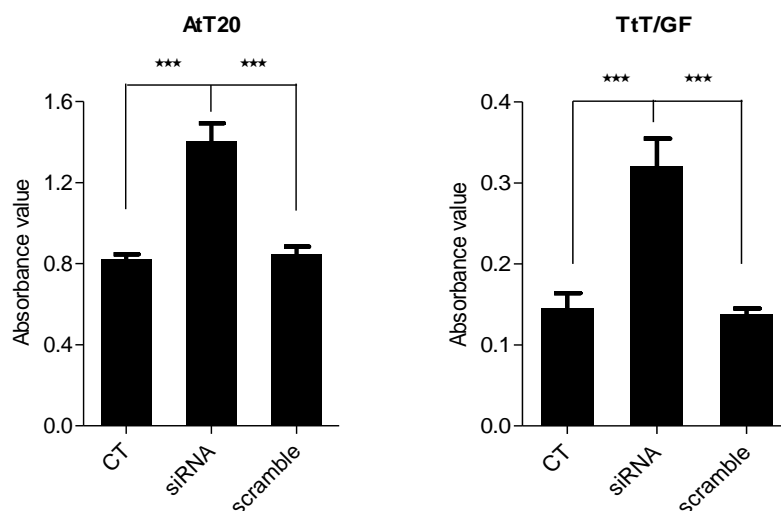


Figure 33. RSUME knockdown induced apoptosis in AtT20 and TtT/GF cells by cell death ELISA. AtT20 and TtT/GF cells were transfected with RSUME siRNA for 72 h, and then cell death ELISA was performed to detect apoptosis-associated DNA fragmentation. ***, $P < 0.001$. All the experiments were carried out in triplicates.

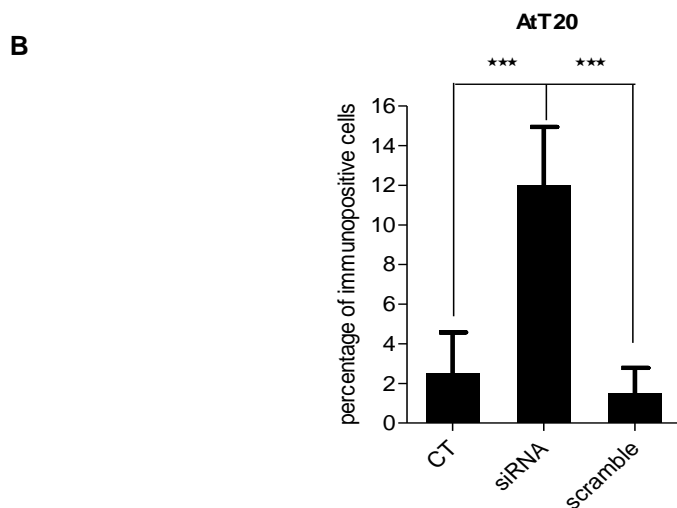
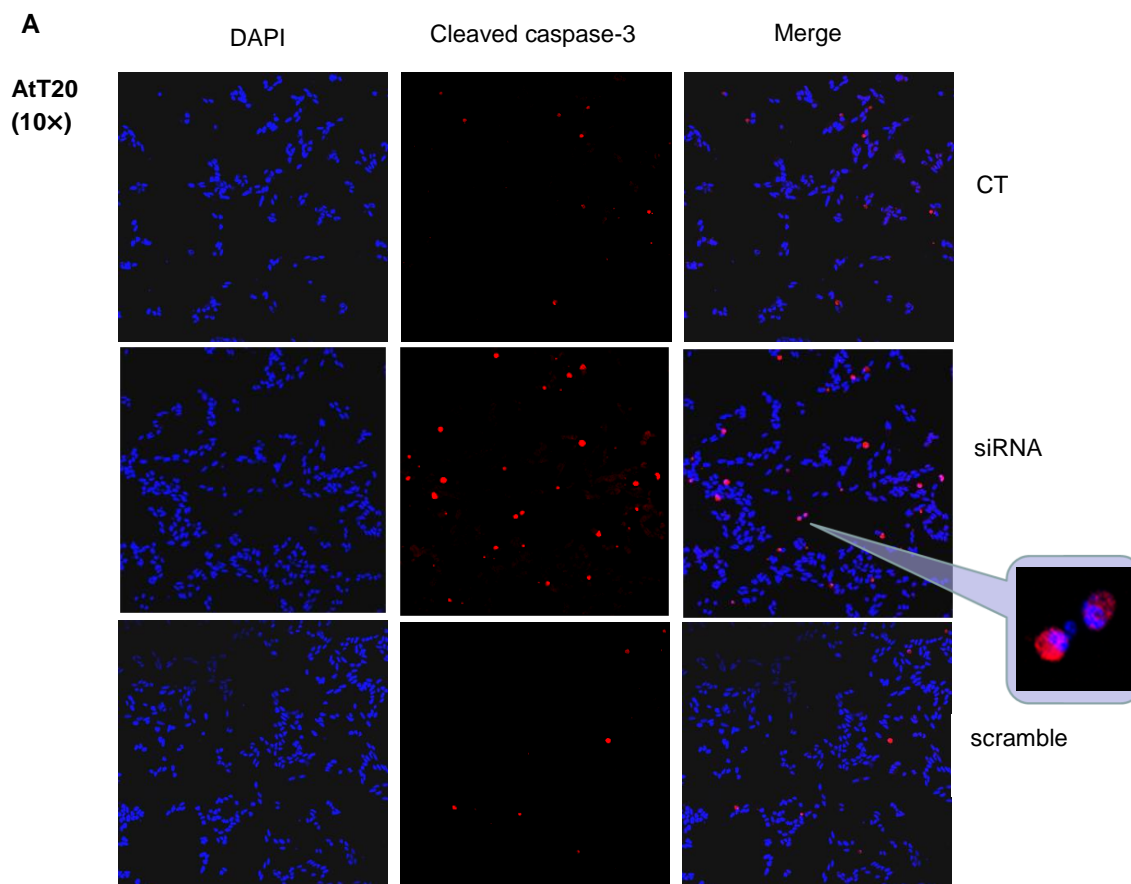


Figure 34. RSUME knockdown increased cleaved caspase-3 in AtT20 cells. AtT20 cells were transfected with RSUME siRNA for 72 h, and then immunofluorescence was performed to detect cleaved caspase-3. Red color corresponds to cleaved caspase-3, and blue color corresponds to nucleus. The images were taken by confocal microscopy using 10x objectives, and one representative image of 5 observations from two independent experiments with similar results is shown (A). The proportion of cells immunopositive for cleaved caspase-3 was determined by counting the number of positive cells out of 100 cells in five different areas of each slice (B). ***, $P < 0.001$.

5 Discussion

In the present study, the role of the novel sumoylation enhancer RSUME in pituitary tumorigenesis was comprehensively studied for the first time. In particular, its co-expression with HIF-1 α and VEGF in pituitary adenomas as well as its implication in the regulation of these two potent angiogenesis regulating factors in pituitary tumor cells was investigated. It could be demonstrated that RSUME critically regulates HIF-1 α and VEGF production and thus might play an important role in pituitary tumor neovascularization. Moreover, novel functions of RSUME on proliferation and survival of pituitary tumor cells have been identified suggesting that RSUME is of considerable importance for pituitary tumor development and progression and therefore, represents an interesting candidate for development of novel targeted therapies for the treatment of pituitary tumors.

An essential step in the development of any kind of solid tumor is the neovascularization of the expanding tumor mass by angiogenesis to supply the tumor cell with enough nutrients and oxygen (Carmeliet 2003). The expansion of the tumor mass causes intratumoral cellular hypoxia (Harris 2002), which induces the formation of the dimeric transcription factor HIF-1 by stabilizing its regulated subunit HIF-1 α . Activated HIF-1 triggers the expression of VEGF protein, which is a key mediator of angiogenesis (Carmeliet 2005). A large number of studies have demonstrated that vascularization is more advanced and HIF-1 α and VEGF are over-expressed in the majority of human cancers in comparison to their corresponding normal tissues (Ferrara 2004; Zhong, et al. 1999). However, so far little is known about HIF-1 α and VEGF regulation in pituitary adenomas due to limited and controversial information from few immunohistochemistry studies.

Herein the mRNA expression of RSUME as well as HIF-1 α and VEGF was studied in parallel in a series of 31 pituitary adenomas by quantitative RT-PCR and the results were compared with the findings from 3 normal human pituitaries. Expression analysis at mRNA level had been chosen since for comparative analysis at protein level, still no appropriate RSUME antibodies are available for immunohistochemistry. RSUME, HIF-1 α and VEGF mRNA levels were all slightly but not significantly enhanced in pituitary tumors in comparison to normal pituitaries.

This is the first time to show RSUME expression in pituitary adenomas, indicating its involvement in pituitary adenoma pathogenesis. Inspired by its function of enhancing HIF-1 α stabilization (Carbia-Nagashima, et al. 2007), if the appropriated RSUME antibodies are available, it would be interesting to explore RSUME protein expression in pituitary adenomas and its relationship with tumor microvessel density by immunohistochemistry, which could offer more evidences about the role of RSUME in angiogenesis of pituitary adenomas.

The present study showed HIF-1 α mRNA expression in both normal and adenomatous pituitaries, whereas one immunohistochemistry study showed no HIF-1 α staining in normal pituitary gland but distributed HIF-1 α staining in pituitary adenomas (Vidal, et al. 2003a). This could be explained by previous conclusions that the transcription and synthesis of HIF-1 α is constitutive but this protein is degraded rapidly in normoxia and stabilized in hypoxia (Ke and Costa 2006). The slight increase of HIF-1 α mRNA expression in pituitary adenomas compared with normal pituitaries shown here underlines that activated HIF-1 up-regulates target genes such as PDGF and triggers MAPK and PI3K pathways that contribute to up-regulating transcription of HIF-1 α (Semenza 2003; Zhang, et al. 2003). Such autocrine-signaling pathways are crucial for tumor progression.

Previous studies from ISH and immunohistochemistry have shown higher VEGF expression in the non-tumorous pituitary which is adjacent to tumor tissue compared with pituitary adenomas (Lloyd, et al. 1999). In contrast, a RT-PCR study using autopsy-derived pituitary as a normal control like in the present study showed the same result as obtained here that VEGF expression is higher in pituitary adenomas compared with normal pituitaries (McCabe, et al. 2002). The differing results between these studies may be caused by different controls. The non-tumorous pituitary tissue surrounding the tumor may theoretically be subject to subtle changes due to the presence of a tumor, whereas degradation and time to fixation may lead to loss of detectable antigens in autopsy tissue (Turner, et al. 2003).

In contrast to studies in other types of solid tumors, it has been shown that pituitary adenomas appear less vascularized than non-tumorous anterior pituitary tissues (Jugenburg, et al. 1995; Schechter 1972; Turner, et al. 2000b). However, higher HIF-1 α and VEGF expression is shown here in adenomatous tissues compared with normal pituitary gland. One of the explanations could be that HIF-1 α can induce growth factors such as IGF-1 and TGF- α to activate signal transduction pathways that lead to cell proliferation and survival under hypoxia (Feldser, et al. 1999; Krishnamachary, et al. 2003). Moreover, VEGF may not only play a role in angiogenesis but may also participate in proliferation and survival of pituitary tumor cells through VEGFR-1 as shown in our previous study (Onofri, et al. 2006). Additionally, non-tumorous pituitary tissue which is adjacent to tumor tissue may differ in its characteristics of vascularization from normal pituitary gland. Therefore, using normal tissue besides the tumor to address vascularization of normal pituitary is not convincing.

In this study, RSUME, HIF-1 α and VEGF mRNA expression is not significantly different among the various types of pituitary adenomas examined, which is consistent with previous studies. Despite this, there was a tendency that all of them appeared highest level in thyrotroph adenomas, and lowest level of HIF-1 α and VEGF were found in non-functioning adenomas and lowest level of RSUME was found in prolactinomas. One

immunohistochemistry study showed strongest staining of HIF-1 α in prolactinomas and weak staining in corticotroph adenomas (Yoshida, et al. 2005), whereas another immunohistochemistry study showed strongest HIF-1 α staining in GH-producing adenomas and lowest in corticotroph as well (Vidal, et al. 2003a). Additionally, previous immunohistochemistry study with a large cohorts of human pituitary adenomas showed strongest VEGF staining in GH, corticotroph, silent corticotroph, silent subtype3, and non-oncocytic null cell adenomas and relatively weak staining in PRL, gonadotroph and thyrotroph adenomas (Lloyd, et al. 1999), whereas another study by RT-PCR showed strongest VEGF staining in thyrotroph adenomas and lowest in GH-producing adenomas (Kim, et al. 2005). The present study could not confirm the results from the study mentioned above, and this is probably due to different investigating technology and limited sample number, and different classification of non-functioning adenomas. These controversial previous reports together with present study indicate that HIF-1 α and VEGF expression are not associated with pituitary adenoma histotypes. Whether RSUME expression has significant relationship with types of pituitary adenomas need to be clarified with more samples.

An immunohistochemistry study on angiogenesis by measurement of microvessel density (MVD) in pituitary adenomas showed highest and lowest MVD in thyrotroph adenomas and prolactinomas, respectively (Niveiro, et al. 2005). In the present study, RSUME mRNA expression level is highest in thyrotroph adenomas and lowest in prolactinomas, which is probably correlated with the MVD reported in the study mentioned above; however, relatively low level of RSUME mRNA expression did not correlate with relatively high MVD in non-functioning adenomas (Niveiro, et al. 2005). Although in the present study HIF-1 α and VEGF mRNA expression were highest in thyrotroph adenomas as well, they showed lowest level in non-functioning adenomas which have high MVD reported in some studies (Niveiro, et al. 2005; Turner, et al. 2000b). It was concluded that the present study could not correlate the HIF-1 α , VEGF mRNA expression with the microvessel density of pituitary adenomas described in previous study. This conclusion is consistent with other studies. One study using RT-PCR showed higher levels of HIF-1 α expression in pituitary carcinomas and GH-producing adenomas (Vidal, et al. 2003a), the most and least vascularized pituitary tumors, respectively, which was shown by another study (Vidal, et al. 2001). And a high rate of HIF-1 α has been shown in cases of non-small cell lung cancer with both high and low MVD (Giatromanolaki, et al. 2001). This could be explained by the hypothesis that HIF-1 α is required not for vessel formation but for the regular distribution of the vascular network, and disordered vasculature causes microenvironmental hypoxia which induces HIF-1 α activity (Vidal, et al. 2003a; Yu, et al. 2001). A study based on microvessel structural entropy has shown that rather than microvessel density, regular and less chaotic microvascular geometry contributes to increased

cell proliferation activity in PRL-producing tumors. This conclusion indicates that the interactions between vascular supply and pituitary tumor cell behavior may not be fully explained only by microvessel density (Vidal, et al. 2003a; Vidal, et al. 2003b). On the other hand, most of patients with prolactinomas or somatotroph adenomas have the history of dopamine agonist or somatostatin treatment that show anti-angiogenic effects (Gomez, et al. 2006; Novella-Maestre, et al. 2009), which probably leads to alteration in HIF-1 α , VEGF and RSUME expression. Therefore, it is necessary to perform separate studies for treated and untreated adenomas, and otherwise a comparison may not be valid.

Consistent with previous study, no correlation was found in the present study between HIF-1 α , VEGF expression and tumor grade, age and gender of patients (Viacava, et al. 2003; Vidal, et al. 2003a), and RSUME mRNA expression also did not correlate with these parameters. A relationship between tumor size and MVD in prolactinomas has been shown, and microprolactinomas were less vascular than macroprolactinomas; in contrast, there was no such a difference between vascular densities of microadenomas and macroadenomas producing GH (Turner, et al. 2000b). No significant difference was found in MVD between invasive and non-invasive pituitary adenomas (Jugenburg, et al. 1995; Vallar, et al. 1987), whereas another study showed significant higher MVD in invasive than non-invasive PRL-producing adenomas but not in GH and ACTH-producing adenomas (Vallar, et al. 1987). Therefore, it seems that HIF-1 α , VEGF and RSUME expression and even MVD are not significantly implicated in pituitary adenoma behavior. However, HIF-1 α , VEGF and MVD are significantly higher in pituitary carcinoma than adenomas (Jugenburg, et al. 1995; Lloyd, et al. 1999; Turner, et al. 2000a; Vidal, et al. 2003a), indicating the up-regulation of HIF-1 α and VEGF during pituitary tumor progression and also a relationship between aggressive pituitary behavior and angiogenesis.

Based on previous observations that RSUME acts through enhancing sumoylation on HIF-1 α expression (Carbia-Nagashima, et al. 2007) and thus probably on angiogenesis-regulating VEGF, correlation analyses among RSUME, HIF-1 α and VEGF mRNA expression were performed in pituitary tumors. HIF-1 α mRNA significantly and positively correlated with RSUME and VEGF mRNA expression in pituitary tumors indicating an interrelationship among these factors in pituitary adenomas.

Regulation of VEGF expression has been studied previously in pituitary adenomas, and it has been shown that several stimuli such as IL-6, estradiol and pituitary adenylate cyclase activating peptide (PACAP) up-regulate VEGF expression (Banerjee, et al. 1997; Gloddek, et al. 1999), whereas glucocorticoids inhibit VEGF (Lohrer, et al. 2001). However, whether VEGF can be induced in pituitary adenomas by hypoxia through HIF-1 signaling pathway involving RSUME has not yet been studied.

In the present study, CoCl_2 was chosen to simulate hypoxia condition. CoCl_2 is a well established hypoxia mimicking substance (Ebert and Bunn 1999; Webb, et al. 2009). Co^{2+} are thought to mimic the hypoxia by binding instead of Fe^{2+} to the heme molecules which are regarded as oxygen sensors in both mammalian and bacteria, causing decreased oxygen affinity due to a conformational change (Ebert and Bunn 1999; Goldberg, et al. 1988). Additionally, It has been shown that sharing similar mechanism in hypoxia Co^{2+} are able to stabilize HIF-1 α in normoxia by substituting Fe^{2+} from the Fe^{2+} -binding site of PHDs, leading to inhibition of PHDs activity (Masson and Ratcliffe 2003), and Co^{2+} inhibits the Interaction between HIF-1 α and VHL Protein by direct binding to HIF-1 α (Yuan, et al. 2003). Moreover, like in hypoxia, Co^{2+} activates mRNA transcription of hypoxia response genes such as erythropoietin, glycolytic enzymes and VEGF by stimulating reactive oxygen species (ROS) generation, although mitochondrial-dependent ROS generation was found in hypoxia but not found after Co^{2+} exposure (Chandel, et al. 1998).

In order to test whether RSUME responds to hypoxia in pituitary tumor cells, stimulation with CoCl_2 was performed. RSUME mRNA expression was shown to increase within 30 minutes after CoCl_2 stimulation and to go down within 2 hours in mouse pituitary cell lines and primary human pituitary adenoma cell cultures. This is not paradoxical in view of the results obtained for HIF-1 α which reached its accumulation peak 2 hours after the onset of CoCl_2 stimulation. As shown in the previous study, RUSME enhances HIF-1 α stabilization by facilitating SUMO transfer (Carbia-Nagashima, et al. 2007), therefore RSUME mRNA expression is probably down-regulated after SUMO chain formation. Due to lack of proper antibody of RSUME, determination of RSUME at protein level could not be performed.

It was next tested whether CoCl_2 induces HIF-1 α and VEGF in mouse pituitary cell lines and as well as in primary cell cultures of human pituitary adenomas. As shown in other cell types (Liu, et al. 1999; Okada, et al. 1998; Shima, et al. 1995; Steinbrech, et al. 2000; Webb, et al. 2009), CoCl_2 treatment time- and dose-dependently stimulated HIF-1 α protein expression in AtT-20, TtT/GF cell lines and all the tested human pituitary adenoma cultures, and HIF-1 α accumulation in nucleus was shown in both AtT20 and TtT/GF cells. A significant rise in VEGF release by CoCl_2 stimulation following a time- and dose- dependent manner was found in TtT/GF cells and all the human pituitary adenoma cell cultures, indicating that HIF-1 α can be induced and activated in hypoxia-mimicking conditions in pituitary adenoma cells.

Since neither RSUME inhibitors nor neutralizing antibodies are actually available, RSUME was down regulated by siRNA technology to further clarify the involvement of RSUME in regulation of HIF-1 α and VEGF in pituitary adenomas. Transfection of siRNA in primary human pituitary tumor cells was established for the first time. siRNA against RSUME strongly down-regulated RSUME expression examined by RT-PCR and significantly reduced the HIF-

1 α expression in both mouse pituitary cell lines and primary human pituitary tumor cells. Additionally, it was shown that the RSUME knockdown abolished nucleus accumulation of HIF-1 α in both AtT20 and TtT/GF cell lines, and also decreased CoCl₂-stimulated VEGF secretion in TtT/GF cells and primary human pituitary tumor cells. These findings suggest that RSUME is required in HIF-1 activation in pituitary tumor cells under hypoxia-mimicking conditions. Although all these experiments with CoCl₂ need to be confirmed under real hypoxic conditions at 1% oxygen, the results shown here already point to an essential role of RSUME in the induction of angiogenic processes in pituitary adenomas, and probably other types of solid tumors.

In the present study, a significant rise in VEGF release by CoCl₂ stimulation was not found in AtT20 cells, but RSUME knockdown significantly decreased basal secretion of VEGF in AtT20 cells. It is known that AtT20 cells basally secrete the highest level of VEGF compared with other pituitary tumor cell lines such as TtT/GF, GH3 and α T3-1 (Lohrer, et al. 2001). From previous studies, VEGF is also regulated by other mechanisms besides hypoxia. It has been demonstrated that the gene promoter of VEGF contains consensus binding sites for transcription factor β -catenin/TCF complex, and VEGF is up-regulated by transfection of normal colon epithelial cells with activated β -catenin (Easwaran, et al. 2003). The transcriptional activity of β -catenin/TCF complex is reduced when TCF-4 lacks SUMO attachment sites, suggesting that sumoylation activates β -catenin/TCF (Yamamoto, et al. 2003). Activated β -catenin/TCF signaling may be responsible for the constitutively high secretion of VEGF by AtT20 cells, and CoCl₂ induced HIF-1 accumulation may not be able further stimulate already saturated VEGF production. Additionally, RSUME knockdown in AtT20 cells probably leads to lack of sumoylation of TCF-4, and thus abolishes the activity of β -catenin/TCF, which results in decreased VEGF expression.

Since RSUME has been detected only recently, little is known about other functions beyond its action on HIF-1 α stabilization and thus, angiogenesis. Interestingly, it was found that a part of cells were floating after RSUME knockdown, whereas the control cells without RSUME silencing had no changes. Therefore, the putative role of RSUME is implicated in the regulation of proliferation and survival was investigated in the present study for the first time. RSUME knockdown by siRNA in pituitary tumor cell lines led to a significant suppression of proliferation as shown by WST-1 assay and direct cell number counting. Cell death ELISA and detection of cleaved caspase-3 proved that apoptosis was induced by RSUME knockdown. This would mean that in pituitary adenomas in which RSUME is present and probably over-expressed, this factor would stimulate pituitary adenoma cell proliferation and would prevent intratumoral apoptosis and thus in total would support pituitary adenoma progression.

Some apoptosis key regulators involved in human cancers which have been shown to be regulated by sumoylation may be affected also in pituitary tumor cells by the sumoylation enhancer RSUME (Alarcon-Vargas and Ronai 2002; Kim and Baek 2006). For instance, it has already been demonstrated, that RSUME can block the transcriptional activity of nuclear factor- κ B (NF- κ B) by enhancing the sumoylation of I κ B (Carbia-Nagashima *et al.* 2007). Sumoylated I κ B escapes from ubiquitin-mediated degradation and acts as the inhibitor of NF- κ B. NF- κ B generally acts as a tumor promoter through up-regulating anti-apoptotic proteins; however it is sometimes pro-apoptotic depending on cell types, stimuli as well as the subunit involved (Radhakrishnan and Kamalakaran 2006). It has been shown that inhibition of NF- κ B activity combined with expression of oncogenic Ras in epidermal keratinocytes leads to invasive neoplasia with features similar to those of squamous cell carcinoma (Dajee, et al. 2003; Dutta, et al. 2006; Kim and Baek 2006). From our previous study, NF- κ B is expressed in normal anterior pituitary and in pituitary adenomas and facilitates the inhibitory effect of interferon- γ on *POMC* gene transcription in AtT20 cells (Labeur, et al. 2008). It is speculated that NF- κ B activation by RSUME knockdown could be responsible for the here observed apoptosis induction in pituitary tumor cells.

The sumoylation of the important tumor suppressor p53 is well studied. It has been demonstrated that PIAS1 (protein inhibitor of activated STAT-1), which is an E3-like ligase, promotes sumoylation of p53 and in this way represses its transcriptional activity, suggesting that sumoylation of p53 restricts its ability to control cell death and/or growth (Alarcon-Vargas and Ronai 2002; Schmidt and Muller 2002). Furthermore, Mdm2 which mediates ubiquitination and degradation of p53 is also SUMO-modified (Alarcon-Vargas and Ronai 2002; Buschmann, et al. 2000). Sumoylation of Mdm2 enhances its stabilization and increases its activity of mediating degradation of p53 through ubiquitination (Buschmann, et al. 2000). Therefore, it was speculated that the activation of p53 by RSUME silencing through abolished sumoylation of p53 and Mdm2 contributes to apoptosis induction in pituitary tumor cells.

Alternatively, the pro-apoptotic effects of RSUME knockdown on pituitary adenoma cell proliferation may be explained by the down-regulation of HIF-1 α and VEGF, since HIF-1 α and VEGF not only promote angiogenesis but also facilitate cell proliferation and survival (Feldser, et al. 1999; Krishnamachary, et al. 2003; Lee, et al. 2004; Onofri, et al. 2006). Through supporting pituitary tumor neovascularization and growth in parallel, RSUME might enhance pituitary adenoma progression and therefore represents a putative therapeutic target for the development of novel concepts for the treatment of human pituitary tumors (Figure 35).

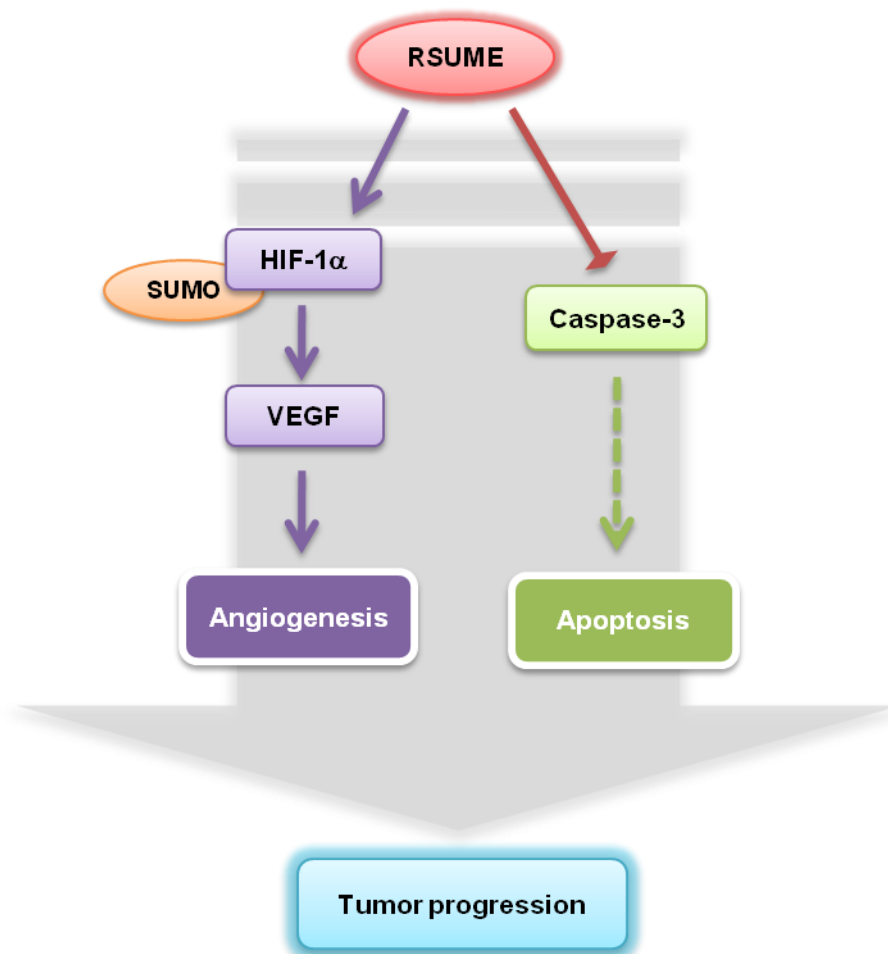


Figure 35. Schematic model for the role of RSUME on pituitary tumor pathogenesis.

It is proposed that RSUME enhances pituitary tumor progression through supporting tumor angiogenesis and growth as well as inhibiting tumor cell apoptosis.

Sumoylation consequences are variable with different substrates and different cell types, and therefore sumoylation may promote or inhibit tumor progression. In Wnt signaling pathway, sumoylation of TCF-4 enhances its transcriptional activity, thus enhances its target gene expression, including some proto-oncogenes such as c-Myc, c-jun and cyclin-D1 (He, et al. 1998; Mann, et al. 1999; Tetsu and McCormick 1999; Yamamoto, et al. 2003). SUMO-

conjugating enzyme Ubc9 is over-expressed in several human tumors such as lung adenocarcinoma, ovarian carcinoma and melanoma, and several approaches to target Ubc9 functions are in experimental phases to explore the therapeutic application (Hoeller and Dikic 2009). However, sumoylation may reversely suppress tumor progression. It has been shown that sumoylation negatively regulates c-jun activity, thereby limits its oncogenic capacity (Muller, et al. 2000). Additionally, arsenic trioxide, which stimulates degradation of oncogenic fusion protein PML-RAR- α by enhancing its sumoylation, is currently used in clinics as an efficient therapeutic agent for the treatment of patients with APL (acute promyelocytic leukemia) (Hoeller and Dikic 2009). As a sumoylation enhancer, RSUME could adopt both tumor-promoting and tumor-suppressing roles, and it would be meaningful to perform more extensive studies on the exploration of RSUME actions and putative therapeutic strategies not only in human pituitary tumors but also in other types of human cancers.

6 Summary

Despite considerable progress, neither the processes involved in the genesis nor the mechanisms triggering the progression of pituitary adenomas are well understood. A large number of studies have shown that HIF-1 α and VEGF play essential roles in growth and progression of a wide variety of solid tumors by promoting tumor neovascularization. However, so far only few reports focus on the role of these two most powerful, hypoxia-induced angiogenic factors in slowly growing and poorly vascularized pituitary adenomas. RSUME was recently isolated from experimentally induced pituitary tumors in nude mice, and was shown to increase stability and transcriptional activity of HIF-1 α in monkey kidney cell line COS-7 by acting as a sumoylation enhancer. These findings suggest a putative role of RSUME in pituitary tumor formation and progression.

In the present study, the pathological role of RSUME in angiogenesis and progression of pituitary adenomas was studied for the first time in mouse pituitary cell lines AtT20 and TtT/GF as well as in human pituitary adenoma cells.

By real-time quantitative PCR, it was demonstrated that RSUME, HIF-1 α and VEGF mRNA expression tended to be over-expressed in human pituitary adenomas compared with the expression levels in normal pituitaries. However, no significant differences among adenoma types, tumor grade, age or gender of patients were observed. Nevertheless, correlation analyses showed that HIF-1 α mRNA level was significantly correlated with VEGF and RSUME mRNA levels in the examined pituitary adenomas, giving the first evidence for the interference of RSUME with the two major angiogenic factors and thus, with pituitary adenoma neovascularization.

To further explore the angiogenic role of RSUME, the hypoxia-mimicking substance CoCl₂ was applied in mouse pituitary cell lines and primary human pituitary tumor cell cultures to investigate the regulatory role of RSUME on HIF-1 α and VEGF. Under CoCl₂ treatment, RSUME mRNA expression was significantly enhanced and HIF-1 α with translocation into nucleus was remarkably increased at protein level. The increased transcriptional activity of HIF-1 α was demonstrated by a significant elevation of the VEGF production in pituitary tumor cells. In order to test whether RSUME was implicated in up-regulation of HIF-1 α and VEGF under hypoxia-mimicking conditions, the corresponding experiments were performed after RSUME knockdown using the siRNA technology. This approach was not only performed in easily transfectable pituitary tumor cell lines but also for the first time in primary cell cultures of human pituitary adenomas. RSUME knockdown significantly suppressed HIF-1 α and VEGF expression in mouse pituitary tumor cell lines and primary cell cultures of human pituitary adenomas, indicating that RSUME is critically involved in pituitary tumor angiogenesis through regulating HIF-1 α and VEGF production.

As changes in pituitary tumor cell viability were noticed after RSUME silencing, this factor may have additional functions in pituitary tumors. Indeed, RSUME knockdown was shown to inhibit pituitary tumor cell proliferation and to enhance the apoptosis in these cells. Therefore, in addition to its pro-angiogenic action, RSUME has proliferative and anti-apoptotic activities in pituitary tumor cells.

In conclusion, the findings of the present study suggest that, the novel protein RSUME is an important player in pituitary tumor pathogenesis by supporting intratumoral angiogenesis, stimulating pituitary tumor cell proliferation and inhibiting tumor cell apoptosis. Therefore, this factor could represent a novel future target for the development of new concepts for the treatment of pituitary tumors.

7 References

Achen MG, Jeltsch M, Kukk E, Makinen T, Vitali A, Wilks AF, Alitalo K & Stacker SA 1998 Vascular endothelial growth factor D (VEGF-D) is a ligand for the tyrosine kinases VEGF receptor 2 (Flk1) and VEGF receptor 3 (Flt4). *Proc Natl Acad Sci U S A* **95** 548-553.

Acosta M, Filippa V & Mohamed F 2010 Folliculostellate cells in pituitary pars distalis of male viscacha: immunohistochemical, morphometric and ultrastructural study. *Eur J Histochem* **54** e1.

Alarcon-Vargas D & Ronai Z 2002 SUMO in cancer--wrestlers wanted. *Cancer Biol Ther* **1** 237-242.

Alexander JM, Biller BM, Bikkal H, Zervas NT, Arnold A & Klibanski A 1990 Clinically nonfunctioning pituitary tumors are monoclonal in origin. *J Clin Invest* **86** 336-340.

Allaerts W & Vankelecom H 2005 History and perspectives of pituitary folliculo-stellate cell research. *Eur J Endocrinol* **153** 1-12.

An FQ, Matsuda M, Fujii H & Matsumoto Y 2000 Expression of vascular endothelial growth factor in surgical specimens of hepatocellular carcinoma. *J Cancer Res Clin Oncol* **126** 153-160.

Ando S, Sarlis NJ, Oldfield EH & Yen PM 2001 Somatic mutation of TRbeta can cause a defect in negative regulation of TSH in a TSH-secreting pituitary tumor. *J Clin Endocrinol Metab* **86** 5572-5576.

Asa SL & Ezzat S 2009 The pathogenesis of pituitary tumors. *Annu Rev Pathol* **4** 97-126.

Asa SL, Kelly MA, Grandy DK & Low MJ 1999 Pituitary lactotroph adenomas develop after prolonged lactotroph hyperplasia in dopamine D2 receptor-deficient mice. *Endocrinology* **140** 5348-5355.

Bae SH, Jeong JW, Park JA, Kim SH, Bae MK, Choi SJ & Kim KW 2004 Sumoylation increases HIF-1alpha stability and its transcriptional activity. *Biochem Biophys Res Commun* **324** 394-400.

Bahar A, Simpson DJ, Cutty SJ, Bicknell JE, Hoban PR, Holley S, Mourtada-Maarabouni M, Williams GT, Clayton RN & Farrell WE 2004 Isolation and characterization of a novel pituitary tumor apoptosis gene. *Mol Endocrinol* **18** 1827-1839.

Banerjee SK, Sarkar DK, Weston AP, De A & Campbell DR 1997 Over expression of vascular endothelial growth factor and its receptor during the development of estrogen-induced rat pituitary tumors may mediate estrogen-initiated tumor angiogenesis. *Carcinogenesis* **18** 1155-1161.

Bayer P, Arndt A, Metzger S, Mahajan R, Melchior F, Jaenicke R & Becker J 1998 Structure determination of the small ubiquitin-related modifier SUMO-1. *J Mol Biol* **280** 275-286.

Bergland RM & Page RB 1978 Can the pituitary secrete directly to the brain? (Affirmative anatomical evidence). *Endocrinology* **102** 1325-1338.

- Berra E, Pages G & Pouyssegur J 2000 MAP kinases and hypoxia in the control of VEGF expression. *Cancer Metastasis Rev* **19** 139-145.
- Bicknell AB 2008 The tissue-specific processing of pro-opiomelanocortin. *J Neuroendocrinol* **20** 692-699.
- Boggild MD, Jenkinson S, Pistorello M, Boscaro M, Scanarini M, McTernan P, Perrett CW, Thakker RV & Clayton RN 1994 Molecular genetic studies of sporadic pituitary tumors. *J Clin Endocrinol Metab* **78** 387-392.
- Bradford MM 1976 A rapid and sensitive method for the quantitation of microgram quantities of protein utilizing the principle of protein-dye binding. *Anal Biochem* **72** 248-254.
- Brem SS, Jensen HM & Gullino PM 1978 Angiogenesis as a marker of preneoplastic lesions of the human breast. *Cancer* **41** 239-244.
- Bruick RK 2000 Expression of the gene encoding the proapoptotic Nip3 protein is induced by hypoxia. *Proc Natl Acad Sci U S A* **97** 9082-9087.
- Buschmann T, Fuchs SY, Lee CG, Pan ZQ & Ronai Z 2000 SUMO-1 modification of Mdm2 prevents its self-ubiquitination and increases Mdm2 ability to ubiquitinate p53. *Cell* **101** 753-762.
- Caccavelli L, Feron F, Morange I, Rouer E, Benarous R, Dewailly D, Jaquet P, Kordon C & Enjalbert A 1994 Decreased expression of the two D2 dopamine receptor isoforms in bromocriptine-resistant prolactinomas. *Neuroendocrinology* **60** 314-322.
- Cao R, Brakenhielm E, Wahlestedt C, Thyberg J & Cao Y 2001 Leptin induces vascular permeability and synergistically stimulates angiogenesis with FGF-2 and VEGF. *Proc Natl Acad Sci U S A* **98** 6390-6395.
- Carbia-Nagashima A, Gerez J, Perez-Castro C, Paez-Pereda M, Silberstein S, Stalla GK, Holsboer F & Arzt E 2007 RSUME, a small RWD-containing protein, enhances SUMO conjugation and stabilizes HIF-1alpha during hypoxia. *Cell* **131** 309-323.
- Carmeliet P 2003 Angiogenesis in health and disease. *Nat Med* **9** 653-660.
- Carmeliet P 2005 VEGF as a key mediator of angiogenesis in cancer. *Oncology* **69 Suppl 3** 4-10.
- Carmeliet P, Dor Y, Herbert JM, Fukumura D, Brusselmans K, Dewerchin M, Neeman M, Bono F, Abramovitch R, Maxwell P, et al. 1998 Role of HIF-1alpha in hypoxia-mediated apoptosis, cell proliferation and tumour angiogenesis. *Nature* **394** 485-490.
- Carmeliet P, Moons L, Luttun A, Vincenti V, Compernelle V, De Mol M, Wu Y, Bono F, Devy L, Beck H, et al. 2001 Synergism between vascular endothelial growth factor and placental growth factor contributes to angiogenesis and plasma extravasation in pathological conditions. *Nat Med* **7** 575-583.
- Chandel NS, Maltepe E, Goldwasser E, Mathieu CE, Simon MC & Schumacker PT 1998 Mitochondrial reactive oxygen species trigger hypoxia-induced transcription. *Proc Natl Acad Sci U S A* **95** 11715-11720.

Chandrasekharappa SC, Guru SC, Manickam P, Olufemi SE, Collins FS, Emmert-Buck MR, Debelenko LV, Zhuang Z, Lubensky IA, Liotta LA, et al. 1997 Positional cloning of the gene for multiple endocrine neoplasia-type 1. *Science* **276** 404-407.

Ciccarelli A, Daly AF & Beckers A 2005 The epidemiology of prolactinomas. *Pituitary* **8** 3-6.

Clauss M, Gerlach M, Gerlach H, Brett J, Wang F, Familletti PC, Pan YC, Olander JV, Connolly DT & Stern D 1990 Vascular permeability factor: a tumor-derived polypeptide that induces endothelial cell and monocyte procoagulant activity, and promotes monocyte migration. *J Exp Med* **172** 1535-1545.

Cockman ME, Masson N, Mole DR, Jaakkola P, Chang GW, Clifford SC, Maher ER, Pugh CW, Ratcliffe PJ & Maxwell PH 2000 Hypoxia inducible factor- α binding and ubiquitylation by the von Hippel-Lindau tumor suppressor protein. *J Biol Chem* **275** 25733-25741.

Colville-Nash PR & Scott DL 1992 Angiogenesis and rheumatoid arthritis: pathogenic and therapeutic implications. *Ann Rheum Dis* **51** 919-925.

Compernelle V, Brusselmans K, Acker T, Hoet P, Tjwa M, Beck H, Plaisance S, Dor Y, Keshet E, Lupu F, et al. 2002 Loss of HIF-2 α and inhibition of VEGF impair fetal lung maturation, whereas treatment with VEGF prevents fatal respiratory distress in premature mice. *Nat Med* **8** 702-710.

Conway EM, Collen D & Carmeliet P 2001 Molecular mechanisms of blood vessel growth. *Cardiovasc Res* **49** 507-521.

Dajee M, Lazarov M, Zhang JY, Cai T, Green CL, Russell AJ, Marinkovich MP, Tao S, Lin Q, Kubo Y, et al. 2003 NF- κ B blockade and oncogenic Ras trigger invasive human epidermal neoplasia. *Nature* **421** 639-643.

Dameron KM, Volpert OV, Tainsky MA & Bouck N 1994 Control of angiogenesis in fibroblasts by p53 regulation of thrombospondin-1. *Science* **265** 1582-1584.

de Keyzer Y, Rene P, Beldjord C, Lenne F & Bertagna X 1998 Overexpression of vasopressin (V3) and corticotrophin-releasing hormone receptor genes in corticotroph tumours. *Clin Endocrinol (Oxf)* **49** 475-482.

de Vries C, Escobedo JA, Ueno H, Houck K, Ferrara N & Williams LT 1992 The fms-like tyrosine kinase, a receptor for vascular endothelial growth factor. *Science* **255** 989-991.

Desterro JM, Rodriguez MS & Hay RT 1998 SUMO-1 modification of I κ B α inhibits NF- κ B activation. *Mol Cell* **2** 233-239.

di Iorgi N, Secco A, Napoli F, Calandra E, Rossi A & Maghnie M 2009 Developmental abnormalities of the posterior pituitary gland. *Endocr Dev* **14** 83-94.

DiGiovanni R, Serra S, Ezzat S & Asa SL 2007 AIP Mutations are not identified in patients with sporadic pituitary adenomas. *Endocr Pathol* **18** 76-78.

Dobbs SP, Hewett PW, Johnson IR, Carmichael J & Murray JC 1997 Angiogenesis is associated with vascular endothelial growth factor expression in cervical intraepithelial neoplasia. *Br J Cancer* **76** 1410-1415.

- Dor Y, Porat R & Keshet E 2001 Vascular endothelial growth factor and vascular adjustments to perturbations in oxygen homeostasis. *Am J Physiol Cell Physiol* **280** C1367-1374.
- Dutta J, Fan Y, Gupta N, Fan G & Gelinas C 2006 Current insights into the regulation of programmed cell death by NF-kappaB. *Oncogene* **25** 6800-6816.
- Dvorak HF, Brown LF, Detmar M & Dvorak AM 1995 Vascular permeability factor/vascular endothelial growth factor, microvascular hyperpermeability, and angiogenesis. *Am J Pathol* **146** 1029-1039.
- Dworakowska D & Grossman AB 2009 The pathophysiology of pituitary adenomas. *Best Pract Res Clin Endocrinol Metab* **23** 525-541.
- Easwaran V, Lee SH, Inge L, Guo L, Goldbeck C, Garrett E, Wiesmann M, Garcia PD, Fuller JH, Chan V, et al. 2003 beta-Catenin regulates vascular endothelial growth factor expression in colon cancer. *Cancer Res* **63** 3145-3153.
- Ebert BL & Bunn HF 1999 Regulation of the erythropoietin gene. *Blood* **94** 1864-1877.
- Epstein AC, Gleadle JM, McNeill LA, Hewitson KS, O'Rourke J, Mole DR, Mukherji M, Metzen E, Wilson MI, Dhanda A, et al. 2001 C. elegans EGL-9 and mammalian homologs define a family of dioxygenases that regulate HIF by prolyl hydroxylation. *Cell* **107** 43-54.
- Ezzat S, Asa SL, Couldwell WT, Barr CE, Dodge WE, Vance ML & McCutcheon IE 2004 The prevalence of pituitary adenomas: a systematic review. *Cancer* **101** 613-619.
- Ezzat S, Smyth HS, Ramyar L & Asa SL 1995 Heterogenous in vivo and in vitro expression of basic fibroblast growth factor by human pituitary adenomas. *J Clin Endocrinol Metab* **80** 878-884.
- Ezzat S, Zheng L, Zhu XF, Wu GE & Asa SL 2002 Targeted expression of a human pituitary tumor-derived isoform of FGF receptor-4 recapitulates pituitary tumorigenesis. *J Clin Invest* **109** 69-78.
- Farnoud MR, Lissak B, Kujas M, Peillon F, Racadot J & Li JY 1992 Specific alterations of the basement membrane and stroma antigens in human pituitary tumours in comparison with the normal anterior pituitary. An immunocytochemical study. *Virchows Arch A Pathol Anat Histopathol* **421** 449-455.
- Fauquier T, Guerineau NC, McKinney RA, Bauer K & Mollard P 2001 Folliculostellate cell network: a route for long-distance communication in the anterior pituitary. *Proc Natl Acad Sci U S A* **98** 8891-8896.
- Feldser D, Agani F, Iyer NV, Pak B, Ferreira G & Semenza GL 1999 Reciprocal positive regulation of hypoxia-inducible factor 1alpha and insulin-like growth factor 2. *Cancer Res* **59** 3915-3918.
- Ferrara N 2004 Vascular endothelial growth factor: basic science and clinical progress. *Endocr Rev* **25** 581-611.
- Ferrara N & Davis-Smyth T 1997 The biology of vascular endothelial growth factor. *Endocr Rev* **18** 4-25.

Ferrara N & Henzel WJ 1989 Pituitary follicular cells secrete a novel heparin-binding growth factor specific for vascular endothelial cells. *Biochem Biophys Res Commun* **161** 851-858.

Fiorentini C, Guerra N, Facchetti M, Finardi A, Tiberio L, Schiaffonati L, Spano P & Missale C 2002 Nerve growth factor regulates dopamine D(2) receptor expression in prolactinoma cell lines via p75(NGFR)-mediated activation of nuclear factor-kappaB. *Mol Endocrinol* **16** 353-366.

Folkman J 1972 Anti-angiogenesis: new concept for therapy of solid tumors. *Ann Surg* **175** 409-416.

Folkman J 1990 What is the evidence that tumors are angiogenesis dependent? *J Natl Cancer Inst* **82** 4-6.

Friedman E, Adams EF, Hoog A, Gejman PV, Carson E, Larsson C, De Marco L, Werner S, Fahlbusch R & Nordenskjold M 1994 Normal structural dopamine type 2 receptor gene in prolactin-secreting and other pituitary tumors. *J Clin Endocrinol Metab* **78** 568-574.

Gasparini G & Harris AL 1995 Clinical importance of the determination of tumor angiogenesis in breast carcinoma: much more than a new prognostic tool. *J Clin Oncol* **13** 765-782.

Gerber HP, Malik AK, Solar GP, Sherman D, Liang XH, Meng G, Hong K, Marsters JC & Ferrara N 2002 VEGF regulates haematopoietic stem cell survival by an internal autocrine loop mechanism. *Nature* **417** 954-958.

Giatromanolaki A, Koukourakis MI, Sivridis E, Turley H, Talks K, Pezzella F, Gatter KC & Harris AL 2001 Relation of hypoxia inducible factor 1 alpha and 2 alpha in operable non-small cell lung cancer to angiogenic/molecular profile of tumours and survival. *Br J Cancer* **85** 881-890.

Gicquel C, Le Bouc Y, Luton JP, Girard F & Bertagna X 1992 Monoclonality of corticotroph macroadenomas in Cushing's disease. *J Clin Endocrinol Metab* **75** 472-475.

Gillam MP, Molitch ME, Lombardi G & Colao A 2006 Advances in the treatment of prolactinomas. *Endocr Rev* **27** 485-534.

Gloddek J, Pagotto U, Paez Pereda M, Arzt E, Stalla GK & Renner U 1999 Pituitary adenylate cyclase-activating polypeptide, interleukin-6 and glucocorticoids regulate the release of vascular endothelial growth factor in pituitary folliculostellate cells. *J Endocrinol* **160** 483-490.

Goldberg MA, Dunning SP & Bunn HF 1988 Regulation of the erythropoietin gene: evidence that the oxygen sensor is a heme protein. *Science* **242** 1412-1415.

Gomez R, Gonzalez-Izquierdo M, Zimmermann RC, Novella-Maestre E, Alonso-Muriel I, Sanchez-Criado J, Remohi J, Simon C & Pellicer A 2006 Low-dose dopamine agonist administration blocks vascular endothelial growth factor (VEGF)-mediated vascular hyperpermeability without altering VEGF receptor 2-dependent luteal angiogenesis in a rat ovarian hyperstimulation model. *Endocrinology* **147** 5400-5411.

Gong L, Kamitani T, Fujise K, Caskey LS & Yeh ET 1997 Preferential interaction of sentrin with a ubiquitin-conjugating enzyme, Ubc9. *J Biol Chem* **272** 28198-28201.

- Gong L, Li B, Millas S & Yeh ET 1999 Molecular cloning and characterization of human AOS1 and UBA2, components of the sentrin-activating enzyme complex. *FEBS Lett* **448** 185-189.
- Gorczyca W & Hardy J 1988 Microadenomas of the human pituitary and their vascularization. *Neurosurgery* **22** 1-6.
- Gorlach A, Diebold I, Schini-Kerth VB, Berchner-Pfannschmidt U, Roth U, Brandes RP, Kietzmann T & Busse R 2001 Thrombin activates the hypoxia-inducible factor-1 signaling pathway in vascular smooth muscle cells: Role of the p22(phox)-containing NADPH oxidase. *Circ Res* **89** 47-54.
- Greenman Y & Stern N 2009 Non-functioning pituitary adenomas. *Best Pract Res Clin Endocrinol Metab* **23** 625-638.
- Gross PM, Joneja MG, Pang JJ, Polischuk TM, Shaver SW & Wainman DS 1993 Topography of short portal vessels in the rat pituitary gland: a scanning electron-microscopic and morphometric study of corrosion cast replicas. *Cell Tissue Res* **272** 79-88.
- Grugel S, Finkenzeller G, Weindel K, Barleon B & Marme D 1995 Both v-Ha-Ras and v-Raf stimulate expression of the vascular endothelial growth factor in NIH 3T3 cells. *J Biol Chem* **270** 25915-25919.
- Guerrin M, Moukadiri H, Chollet P, Moro F, Dutt K, Malecaze F & Plouet J 1995 Vasculotropin/vascular endothelial growth factor is an autocrine growth factor for human retinal pigment epithelial cells cultured in vitro. *J Cell Physiol* **164** 385-394.
- Haddad JJ & Land SC 2001 A non-hypoxic, ROS-sensitive pathway mediates TNF-alpha-dependent regulation of HIF-1alpha. *FEBS Lett* **505** 269-274.
- Hanahan D & Folkman J 1996 Patterns and emerging mechanisms of the angiogenic switch during tumorigenesis. *Cell* **86** 353-364.
- Harris AL 2000 von Hippel-Lindau syndrome: target for anti-vascular endothelial growth factor (VEGF) receptor therapy. *Oncologist* **5 Suppl 1** 32-36.
- Harris AL 2002 Hypoxia--a key regulatory factor in tumour growth. *Nat Rev Cancer* **2** 38-47.
- He TC, Sparks AB, Rago C, Hermeking H, Zawel L, da Costa LT, Morin PJ, Vogelstein B & Kinzler KW 1998 Identification of c-MYC as a target of the APC pathway. *Science* **281** 1509-1512.
- Heinrichs M, von Dawans B & Domes G 2009 Oxytocin, vasopressin, and human social behavior. *Front Neuroendocrinol* **30** 548-557.
- Hellstrom A, Svensson E, Carlsson B, Niklasson A & Albertsson-Wikland K 1999 Reduced retinal vascularization in children with growth hormone deficiency. *J Clin Endocrinol Metab* **84** 795-798.
- Hellwig-Burgel T, Rutkowski K, Metzen E, Fandrey J & Jelkmann W 1999 Interleukin-1beta and tumor necrosis factor-alpha stimulate DNA binding of hypoxia-inducible factor-1. *Blood* **94** 1561-1567.

- Herman V, Fagin J, Gonsky R, Kovacs K & Melmed S 1990 Clonal origin of pituitary adenomas. *J Clin Endocrinol Metab* **71** 1427-1433.
- Hewitson KS, McNeill LA, Riordan MV, Tian YM, Bullock AN, Welford RW, Elkins JM, Oldham NJ, Bhattacharya S, Gleadle JM, et al. 2002 Hypoxia-inducible factor (HIF) asparagine hydroxylase is identical to factor inhibiting HIF (FIH) and is related to the cupin structural family. *J Biol Chem* **277** 26351-26355.
- Hibberts NA, Simpson DJ, Bicknell JE, Broome JC, Hoban PR, Clayton RN & Farrell WE 1999 Analysis of cyclin D1 (CCND1) allelic imbalance and overexpression in sporadic human pituitary tumors. *Clin Cancer Res* **5** 2133-2139.
- Hoeller D & Dikic I 2009 Targeting the ubiquitin system in cancer therapy. *Nature* **458** 438-444.
- Horak ER, Leek R, Klenk N, LeJeune S, Smith K, Stuart N, Greenall M, Stepniowska K & Harris AL 1992 Angiogenesis, assessed by platelet/endothelial cell adhesion molecule antibodies, as indicator of node metastases and survival in breast cancer. *Lancet* **340** 1120-1124.
- Houck KA, Ferrara N, Winer J, Cachianes G, Li B & Leung DW 1991 The vascular endothelial growth factor family: identification of a fourth molecular species and characterization of alternative splicing of RNA. *Mol Endocrinol* **5** 1806-1814.
- Houck KA, Leung DW, Rowland AM, Winer J & Ferrara N 1992 Dual regulation of vascular endothelial growth factor bioavailability by genetic and proteolytic mechanisms. *J Biol Chem* **267** 26031-26037.
- Huang DT, Hunt HW, Zhuang M, Ohi MD, Holton JM & Schulman BA 2007 Basis for a ubiquitin-like protein thioester switch toggling E1-E2 affinity. *Nature* **445** 394-398.
- Hyder SM, Nawaz Z, Chiappetta C & Stancel GM 2000 Identification of functional estrogen response elements in the gene coding for the potent angiogenic factor vascular endothelial growth factor. *Cancer Res* **60** 3183-3190.
- Inoue K, Couch EF, Takano K & Ogawa S 1999 The structure and function of folliculo-stellate cells in the anterior pituitary gland. *Arch Histol Cytol* **62** 205-218.
- Jeong JW, Bae MK, Ahn MY, Kim SH, Sohn TK, Bae MH, Yoo MA, Song EJ, Lee KJ & Kim KW 2002 Regulation and destabilization of HIF-1 α by ARD1-mediated acetylation. *Cell* **111** 709-720.
- Jewell UR, Kvietikova I, Scheid A, Bauer C, Wenger RH & Gassmann M 2001 Induction of HIF-1 α in response to hypoxia is instantaneous. *FASEB J* **15** 1312-1314.
- Jiang BH, Rue E, Wang GL, Roe R & Semenza GL 1996 Dimerization, DNA binding, and transactivation properties of hypoxia-inducible factor 1. *J Biol Chem* **271** 17771-17778.
- Jin L, Tsumanuma I, Ruebel KH, Bayliss JM & Lloyd RV 2001 Analysis of homogeneous populations of anterior pituitary folliculostellate cells by laser capture microdissection and reverse transcription-polymerase chain reaction. *Endocrinology* **142** 1703-1709.
- Johnson ES 2004 Protein modification by SUMO. *Annu Rev Biochem* **73** 355-382.

- Johnson ES & Blobel G 1997 Ubc9p is the conjugating enzyme for the ubiquitin-like protein Smt3p. *J Biol Chem* **272** 26799-26802.
- Jordan S, Lidhar K, Korbonits M, Lowe DG & Grossman AB 2000 Cyclin D and cyclin E expression in normal and adenomatous pituitary. *Eur J Endocrinol* **143** R1-6.
- Josko J, Gwozdz B, Jedrzejowska-Szypulka H & Hendryk S 2000 Vascular endothelial growth factor (VEGF) and its effect on angiogenesis. *Med Sci Monit* **6** 1047-1052.
- Joukov V, Pajusola K, Kaipainen A, Chilov D, Lahtinen I, Kukk E, Saksela O, Kalkkinen N & Alitalo K 1996 A novel vascular endothelial growth factor, VEGF-C, is a ligand for the Flt4 (VEGFR-3) and KDR (VEGFR-2) receptor tyrosine kinases. *EMBO J* **15** 1751.
- Jugenburg M, Kovacs K, Jugenburg I & Scheithauer BW 1997 Angiogenesis in endocrine neoplasms. *Endocr Pathol* **8** 259-272.
- Jugenburg M, Kovacs K, Stefanescu L & Scheithauer BW 1995 Vasculature in nontumorous hypophyses, pituitary adenomas, and carcinomas: a quantitative morphologic study. *Endocr Pathol* **6** 115-124.
- Kagayama M 1965 The follicular cell in the pars distalis of the dog pituitary gland: an electron microscope study. *Endocrinology* **77** 1053-1060.
- Kaltsas GA, Kola B, Borboli N, Morris DG, Gueorguiev M, Swords FM, Czirjak S, Kirschner LS, Stratakis CA, Korbonits M, et al. 2002 Sequence analysis of the PRKAR1A gene in sporadic somatotroph and other pituitary tumours. *Clin Endocrinol (Oxf)* **57** 443-448.
- Karkkainen MJ, Haiko P, Sainio K, Partanen J, Taipale J, Petrova TV, Jeltsch M, Jackson DG, Talikka M, Rauvala H, et al. 2004 Vascular endothelial growth factor C is required for sprouting of the first lymphatic vessels from embryonic veins. *Nat Immunol* **5** 74-80.
- Karl M, Lamberts SW, Koper JW, Katz DA, Huizenga NE, Kino T, Haddad BR, Hughes MR & Chrousos GP 1996a Cushing's disease preceded by generalized glucocorticoid resistance: clinical consequences of a novel, dominant-negative glucocorticoid receptor mutation. *Proc Assoc Am Physicians* **108** 296-307.
- Karl M, Von Wichert G, Kempter E, Katz DA, Reincke M, Monig H, Ali IU, Stratakis CA, Oldfield EH, Chrousos GP, et al. 1996b Nelson's syndrome associated with a somatic frame shift mutation in the glucocorticoid receptor gene. *J Clin Endocrinol Metab* **81** 124-129.
- Ke Q & Costa M 2006 Hypoxia-inducible factor-1 (HIF-1). *Mol Pharmacol* **70** 1469-1480.
- Kelberman D & Dattani MT 2007 Hypothalamic and pituitary development: novel insights into the aetiology. *Eur J Endocrinol* **157** Suppl 1 S3-14.
- Kelberman D, Rizzoti K, Lovell-Badge R, Robinson IC & Dattani MT 2009 Genetic regulation of pituitary gland development in human and mouse. *Endocr Rev* **30** 790-829.
- Kim K, Yoshida D & Teramoto A 2005 Expression of hypoxia-inducible factor 1alpha and vascular endothelial growth factor in pituitary adenomas. *Endocr Pathol* **16** 115-121.

Kim KI & Baek SH 2006 SUMOylation code in cancer development and metastasis. *Mol Cells* **22** 247-253.

Kim KJ, Li B, Winer J, Armanini M, Gillett N, Phillips HS & Ferrara N 1993 Inhibition of vascular endothelial growth factor-induced angiogenesis suppresses tumour growth in vivo. *Nature* **362** 841-844.

Kirschner LS, Carney JA, Pack SD, Taymans SE, Giatzakis C, Cho YS, Cho-Chung YS & Stratakis CA 2000a Mutations of the gene encoding the protein kinase A type I-alpha regulatory subunit in patients with the Carney complex. *Nat Genet* **26** 89-92.

Kirschner LS, Sandrini F, Monbo J, Lin JP, Carney JA & Stratakis CA 2000b Genetic heterogeneity and spectrum of mutations of the PRKAR1A gene in patients with the carney complex. *Hum Mol Genet* **9** 3037-3046.

Kola B, Korbonits M, Diaz-Cano S, Kaltsas G, Morris DG, Jordan S, Metherell L, Powell M, Czirjak S, Arnaldi G, et al. 2003 Reduced expression of the growth hormone and type 1 insulin-like growth factor receptors in human somatotroph tumours and an analysis of possible mutations of the growth hormone receptor. *Clin Endocrinol (Oxf)* **59** 328-338.

Kovacs K & Horvath E 1973 Vascular alterations in adenomas of human pituitary glands. An electron microscopic study. *Angiologica* **10** 299-309.

Kovacs K & Horvath E 1986 Tumors of pituitary gland. *Washington DC: Armed Force Institute of Pathology*.

Kovacs K, Horvath E & Vidal S 2001 Classification of pituitary adenomas. *J Neurooncol* **54** 121-127.

Kowarik M, Onofri C, Colaco T, Stalla GK & Renner U 2010 Platelet-derived growth factor (PDGF) and PDGF receptor expression and function in folliculostellate pituitary cells. *Exp Clin Endocrinol Diabetes* **118** 113-120.

Krishnamachary B, Berg-Dixon S, Kelly B, Agani F, Feldser D, Ferreira G, Iyer N, LaRusch J, Pak B, Taghavi P, et al. 2003 Regulation of colon carcinoma cell invasion by hypoxia-inducible factor 1. *Cancer Res* **63** 1138-1143.

Labeur M, Refojo D, Wölfel B, Stalla J, Vargas V, Theodoropoulou M, Buchfelder M, Paez-Pereda M, Arzt E & Stalla GK 2008 Interferon-gamma inhibits cellular proliferation and ACTH production in corticotroph tumor cells through a novel janus kinases-signal transducer and activator of transcription 1/nuclear factor-kappa B inhibitory signaling pathway. *J Endocrinol* **199** 177-189.

Lambrechts D, Storkebaum E, Morimoto M, Del-Favero J, Desmet F, Marklund SL, Wyns S, Thijs V, Andersson J, van Marion I, et al. 2003 VEGF is a modifier of amyotrophic lateral sclerosis in mice and humans and protects motoneurons against ischemic death. *Nat Genet* **34** 383-394.

Landis CA, Masters SB, Spada A, Pace AM, Bourne HR & Vallar L 1989 GTPase inhibiting mutations activate the alpha chain of Gs and stimulate adenylyl cyclase in human pituitary tumours. *Nature* **340** 692-696.

Lando D, Peet DJ, Gorman JJ, Whelan DA, Whitelaw ML & Bruick RK 2002a FIH-1 is an asparaginyl hydroxylase enzyme that regulates the transcriptional activity of hypoxia-inducible factor. *Genes Dev* **16** 1466-1471.

Lando D, Peet DJ, Whelan DA, Gorman JJ & Whitelaw ML 2002b Asparagine hydroxylation of the HIF transactivation domain a hypoxic switch. *Science* **295** 858-861.

Landolt AM, Vance ML & Reilly PL Eds 2006 *Pituitary adenomas*. New York: Churchill livingstone.

Lania AG, Mantovani G, Ferrero S, Pellegrini C, Bondioni S, Peverelli E, Braidotti P, Locatelli M, Zavanone ML, Ferrante E, et al. 2004 Proliferation of transformed somatotroph cells related to low or absent expression of protein kinase a regulatory subunit 1A protein. *Cancer Res* **64** 9193-9198.

Leclercq TA & Grisoli F 1983 Arterial blood supply of the normal human pituitary gland. An anatomical study. *J Neurosurg* **58** 678-681.

Lee HJ, Macbeth AH, Pagani JH & Young WS, 3rd 2009 Oxytocin: the great facilitator of life. *Prog Neurobiol* **88** 127-151.

Lee J, Gray A, Yuan J, Luoh SM, Avraham H & Wood WI 1996 Vascular endothelial growth factor-related protein: a ligand and specific activator of the tyrosine kinase receptor Flt4. *Proc Natl Acad Sci U S A* **93** 1988-1992.

Lee JW, Bae SH, Jeong JW, Kim SH & Kim KW 2004 Hypoxia-inducible factor (HIF-1)alpha: its protein stability and biological functions. *Exp Mol Med* **36** 1-12.

Levine AJ 1997 p53, the cellular gatekeeper for growth and division. *Cell* **88** 323-331.

Li A, Dubey S, Varney ML, Dave BJ & Singh RK 2003 IL-8 directly enhanced endothelial cell survival, proliferation, and matrix metalloproteinases production and regulated angiogenesis. *J Immunol* **170** 3369-3376.

Li H, Ko HP & Whitlock JP 1996 Induction of phosphoglycerate kinase 1 gene expression by hypoxia. Roles of Arnt and HIF1alpha. *J Biol Chem* **271** 21262-21267.

Li J, Davidson G, Huang Y, Jiang BH, Shi X, Costa M & Huang C 2004 Nickel compounds act through phosphatidylinositol-3-kinase/Akt-dependent, p70(S6k)-independent pathway to induce hypoxia inducible factor transactivation and Cap43 expression in mouse epidermal Cl41 cells. *Cancer Res* **64** 94-101.

Lidhar K, Korbonits M, Jordan S, Khalimova Z, Kaltsas G, Lu X, Clayton RN, Jenkins PJ, Monson JP, Besser GM, et al. 1999 Low expression of the cell cycle inhibitor p27Kip1 in normal corticotroph cells, corticotroph tumors, and malignant pituitary tumors. *J Clin Endocrinol Metab* **84** 3823-3830.

Liu XH, Kirschenbaum A, Yao S, Stearns ME, Holland JF, Claffey K & Levine AC 1999 Upregulation of vascular endothelial growth factor by cobalt chloride-simulated hypoxia is mediated by persistent induction of cyclooxygenase-2 in a metastatic human prostate cancer cell line. *Clin Exp Metastasis* **17** 687-694.

- Lloyd RV, Jin L, Tsumanuma I, Vidal S, Kovacs K, Horvath E, Scheithauer BW, Couce ME & Burguera B 2001 Leptin and leptin receptor in anterior pituitary function. *Pituitary* **4** 33-47.
- Lloyd RV, Scheithauer BW, Kuroki T, Vidal S, Kovacs K & Stefaneanu L 1999 Vascular endothelial growth factor (VEGF) expression in human pituitary adenomas and carcinomas. *Endocr Pathol* **10** 229-235.
- Lloyd RV, Vidal S, Horvath E, Kovacs K & Scheithauer B 2003 Angiogenesis in normal and neoplastic pituitary tissues. *Microsc Res Tech* **60** 244-250.
- Lohrer P, Gloddek J, Hopfner U, Losa M, Uhl E, Pagotto U, Stalla GK & Renner U 2001 Vascular endothelial growth factor production and regulation in rodent and human pituitary tumor cells in vitro. *Neuroendocrinology* **74** 95-105.
- Lohrer P, Gloddek J, Nagashima AC, Korali Z, Hopfner U, Pereda MP, Arzt E, Stalla GK & Renner U 2000 Lipopolysaccharide directly stimulates the intrapituitary interleukin-6 production by folliculostellate cells via specific receptors and the p38alpha mitogen-activated protein kinase/nuclear factor-kappaB pathway. *Endocrinology* **141** 4457-4465.
- Lombardero M, Quintanar-Stephano A, Vidal S, Horvath E, Kovacs K, Lloyd RV & Scheithauer BW 2006 Vascularization of rat pituitary autografts. *J Anat* **208** 587-593.
- Lyttle DJ, Fraser KM, Fleming SB, Mercer AA & Robinson AJ 1994 Homologs of vascular endothelial growth factor are encoded by the poxvirus orf virus. *J Virol* **68** 84-92.
- Madan A & Curtin PT 1993 A 24-base-pair sequence 3' to the human erythropoietin gene contains a hypoxia-responsive transcriptional enhancer. *Proc Natl Acad Sci U S A* **90** 3928-3932.
- Maeda K, Chung YS, Takatsuka S, Ogawa Y, Sawada T, Yamashita Y, Onoda N, Kato Y, Nitta A, Arimoto Y, et al. 1995 Tumor angiogenesis as a predictor of recurrence in gastric carcinoma. *J Clin Oncol* **13** 477-481.
- Maglione D, Guerriero V, Viglietto G, Delli-Bovi P & Persico MG 1991 Isolation of a human placenta cDNA coding for a protein related to the vascular permeability factor. *Proc Natl Acad Sci U S A* **88** 9267-9271.
- Maglione D, Guerriero V, Viglietto G, Ferraro MG, Aprelikova O, Alitalo K, Del Vecchio S, Lei KJ, Chou JY & Persico MG 1993 Two alternative mRNAs coding for the angiogenic factor, placenta growth factor (PlGF), are transcribed from a single gene of chromosome 14. *Oncogene* **8** 925-931.
- Mann B, Gelos M, Siedow A, Hanski ML, Gratchev A, Ilyas M, Bodmer WF, Moyer MP, Riecken EO, Buhr HJ, et al. 1999 Target genes of beta-catenin-T cell-factor/lymphoid-enhancer-factor signaling in human colorectal carcinomas. *Proc Natl Acad Sci U S A* **96** 1603-1608.
- Mantovani G, Bondioni S, Ferrero S, Gamba B, Ferrante E, Peverelli E, Corbetta S, Locatelli M, Rampini P, Beck-Peccoz P, et al. 2005 Effect of cyclic adenosine 3',5'-monophosphate/protein kinase a pathway on markers of cell proliferation in nonfunctioning pituitary adenomas. *J Clin Endocrinol Metab* **90** 6721-6724.

Masson N & Ratcliffe PJ 2003 HIF prolyl and asparaginyl hydroxylases in the biological response to intracellular O(2) levels. *J Cell Sci* **116** 3041-3049.

Masson N, Willam C, Maxwell PH, Pugh CW & Ratcliffe PJ 2001 Independent function of two destruction domains in hypoxia-inducible factor- α chains activated by prolyl hydroxylation. *EMBO J* **20** 5197-5206.

McCabe CJ, Boelaert K, Tannahill LA, Heaney AP, Stratford AL, Khaira JS, Hussain S, Sheppard MC, Franklyn JA & Gittoes NJ 2002 Vascular endothelial growth factor, its receptor KDR/Flk-1, and pituitary tumor transforming gene in pituitary tumors. *J Clin Endocrinol Metab* **87** 4238-4244.

McNicol AM 1986 A study of intermediate lobe differentiation in the human pituitary gland. *J Pathol* **150** 169-173.

Mehta A & Dattani MT 2008 Developmental disorders of the hypothalamus and pituitary gland associated with congenital hypopituitarism. *Best Pract Res Clin Endocrinol Metab* **22** 191-206.

Meyer M, Clauss M, Lepple-Wienhues A, Waltenberger J, Augustin HG, Ziche M, Lanz C, Buttner M, Rziha HJ & Dehio C 1999 A novel vascular endothelial growth factor encoded by Orf virus, VEGF-E, mediates angiogenesis via signalling through VEGFR-2 (KDR) but not VEGFR-1 (Flt-1) receptor tyrosine kinases. *EMBO J* **18** 363-374.

Morand I, Fonlupt P, Guerrier A, Trouillas J, Calle A, Remy C, Rousset B & Munari-Silem Y 1996 Cell-to-cell communication in the anterior pituitary: evidence for gap junction-mediated exchanges between endocrine cells and folliculostellate cells. *Endocrinology* **137** 3356-3367.

Mucha SA, Melen-Mucha G, Godlewski A & Stepien H 2007 Inhibition of estrogen-induced pituitary tumor growth and angiogenesis in Fischer 344 rats by the matrix metalloproteinase inhibitor batimastat. *Virchows Arch* **450** 335-341.

Muller S, Berger M, Lehembre F, Seeler JS, Haupt Y & Dejean A 2000 c-Jun and p53 activity is modulated by SUMO-1 modification. *J Biol Chem* **275** 13321-13329.

Musat M, Korbonits M, Kola B, Borboli N, Hanson MR, Nanzer AM, Grigson J, Jordan S, Morris DG, Gueorguiev M, et al. 2005 Enhanced protein kinase B/Akt signalling in pituitary tumours. *Endocr Relat Cancer* **12** 423-433.

Musat M, Vax VV, Borboli N, Gueorguiev M, Bonner S, Korbonits M & Grossman AB 2004 Cell cycle dysregulation in pituitary oncogenesis. *Front Horm Res* **32** 34-62.

Nakakura T, Yoshida M, Dohra H, Suzuki M & Tanaka S 2006 Gene expression of vascular endothelial growth factor-A in the pituitary during formation of the vascular system in the hypothalamic-pituitary axis of the rat. *Cell Tissue Res* **324** 87-95.

Neufeld G, Cohen T, Gengrinovitch S & Poltorak Z 1999 Vascular endothelial growth factor (VEGF) and its receptors. *FASEB J* **13** 9-22.

Nickoloff BJ, Mitra RS, Varani J, Dixit VM & Poverini PJ 1994 Aberrant production of interleukin-8 and thrombospondin-1 by psoriatic keratinocytes mediates angiogenesis. *Am J Pathol* **144** 820-828.

Niveiro M, Aranda FI, Peiro G, Alenda C & Pico A 2005 Immunohistochemical analysis of tumor angiogenic factors in human pituitary adenomas. *Hum Pathol* **36** 1090-1095.

Novella-Maestre E, Carda C, Noguera I, Ruiz-Sauri A, Garcia-Velasco JA, Simon C & Pellicer A 2009 Dopamine agonist administration causes a reduction in endometrial implants through modulation of angiogenesis in experimentally induced endometriosis. *Hum Reprod* **24** 1025-1035.

Nussey SS & Whitehead SA Eds 2001 *Endocrinology: An Integrated Approach*. London: Taylor & Francis group.

O'Brien ER, Garvin MR, Dev R, Stewart DK, Hinohara T, Simpson JB & Schwartz SM 1994 Angiogenesis in human coronary atherosclerotic plaques. *Am J Pathol* **145** 883-894.

Oberg-Welsh C, Sandler S, Andersson A & Welsh M 1997 Effects of vascular endothelial growth factor on pancreatic duct cell replication and the insulin production of fetal islet-like cell clusters in vitro. *Mol Cell Endocrinol* **126** 125-132.

Oberholtzer JC 1999 Tumors of the pituitary gland. *human pathol* **30** 485-486.

Ogino A, Yoshino A, Katayama Y, Watanabe T, Ota T, Komine C, Yokoyama T & Fukushima T 2005 The p15(INK4b)/p16(INK4a)/RB1 pathway is frequently deregulated in human pituitary adenomas. *J Neuropathol Exp Neurol* **64** 398-403.

Okada F, Rak JW, Croix BS, Lieubeau B, Kaya M, Roncari L, Shirasawa S, Sasazuki T & Kerbel RS 1998 Impact of oncogenes in tumor angiogenesis: mutant K-ras up-regulation of vascular endothelial growth factor/vascular permeability factor is necessary, but not sufficient for tumorigenicity of human colorectal carcinoma cells. *Proc Natl Acad Sci U S A* **95** 3609-3614.

Onofri C, Theodoropoulou M, Losa M, Uhl E, Lange M, Arzt E, Stalla GK & Renner U 2006 Localization of vascular endothelial growth factor (VEGF) receptors in normal and adenomatous pituitaries: detection of a non-endothelial function of VEGF in pituitary tumours. *J Endocrinol* **191** 249-261.

Orlandini M, Marconcini L, Ferruzzi R & Oliviero S 1996 Identification of a c-fos-induced gene that is related to the platelet-derived growth factor/vascular endothelial growth factor family. *Proc Natl Acad Sci U S A* **93** 11675-11680.

Pagotto U, Arzberger T, Theodoropoulou M, Grubler Y, Pantaloni C, Saeger W, Losa M, Journot L, Stalla GK & Spengler D 2000 The expression of the antiproliferative gene ZAC is lost or highly reduced in nonfunctioning pituitary adenomas. *Cancer Res* **60** 6794-6799.

Park JE, Keller GA & Ferrara N 1993 The vascular endothelial growth factor (VEGF) isoforms: differential deposition into the subepithelial extracellular matrix and bioactivity of extracellular matrix-bound VEGF. *Mol Biol Cell* **4** 1317-1326.

Patan S, Haenni B & Burri PH 1996 Implementation of intussusceptive microvascular growth in the chicken chorioallantoic membrane (CAM): 1. pillar formation by folding of the capillary wall. *Microvasc Res* **51** 80-98.

- Powell DF, Baker HL, Jr. & Laws ER, Jr. 1974 The primary angiographic findings in pituitary adenomas. *Radiology* **110** 589-595.
- Prezant TR, Levine J & Melmed S 1998 Molecular characterization of the men1 tumor suppressor gene in sporadic pituitary tumors. *J Clin Endocrinol Metab* **83** 1388-1391.
- Radhakrishnan SK & Kamalakaran S 2006 Pro-apoptotic role of NF-kappaB: implications for cancer therapy. *Biochim Biophys Acta* **1766** 53-62.
- Rasmussen AT 1930 Origin of the basophilic cells in the posterior lobe of the human hypophysis. *Am J Anat* **46** 461-475.
- Renner U, De Santana EC, Gerez J, Frohlich B, Haedo M, Pereda MP, Onofri C, Stalla GK & Arzt E 2009 Intrapituitary expression and regulation of the gp130 cytokine interleukin-6 and its implication in pituitary physiology and pathophysiology. *Ann N Y Acad Sci* **1153** 89-97.
- Renner U, Lohrer P, Schaaf L, Feirer M, Schmitt K, Onofri C, Arzt E & Stalla GK 2002 Transforming growth factor-beta stimulates vascular endothelial growth factor production by folliculostellate pituitary cells. *Endocrinology* **143** 3759-3765.
- Ribatti D, Conconi MT & Nussdorfer GG 2007a Nonclassic endogenous novel [corrected] regulators of angiogenesis. *Pharmacol Rev* **59** 185-205.
- Ribatti D, Nico B, Crivellato E, Roccaro AM & Vacca A 2007b The history of the angiogenic switch concept. *Leukemia* **21** 44-52.
- Richard DE, Berra E & Pouyssegur J 2000 Nonhypoxic pathway mediates the induction of hypoxia-inducible factor 1alpha in vascular smooth muscle cells. *J Biol Chem* **275** 26765-26771.
- Rinehart JF & Farquhar MG 1953 Electron microscopic studies of the anterior pituitary gland. *J Histochem Cytochem* **1** 93-113.
- Risau W 1997 Mechanisms of angiogenesis. *Nature* **386** 671-674.
- Roskoski R, Jr. 2007 Vascular endothelial growth factor (VEGF) signaling in tumor progression. *Crit Rev Oncol Hematol* **62** 179-213.
- Rosso L & Mienville JM 2009 Pituicyte modulation of neurohormone output. *Glia* **57** 235-243.
- Ruas JL, Poellinger L & Pereira T 2002 Functional analysis of hypoxia-inducible factor-1 alpha-mediated transactivation. Identification of amino acid residues critical for transcriptional activation and/or interaction with CREB-binding protein. *J Biol Chem* **277** 38723-38730.
- Saeger W, Ludecke DK, Buchfelder M, Fahlbusch R, Quabbe HJ & Petersenn S 2007 Pathohistological classification of pituitary tumors: 10 years of experience with the German Pituitary Tumor Registry. *Eur J Endocrinol* **156** 203-216.
- Saland LC 2001 The mammalian pituitary intermediate lobe: an update on innervation and regulation. *Brain Res Bull* **54** 587-593.

- Salnikow K, Blagosklonny MV, Ryan H, Johnson R & Costa M 2000 Carcinogenic nickel induces genes involved with hypoxic stress. *Cancer Res* **60** 38-41.
- Sandrini F, Kirschner LS, Bei T, Farmakidis C, Yasufuku-Takano J, Takano K, Prezant TR, Marx SJ, Farrell WE, Clayton RN, et al. 2002 PRKAR1A, one of the Carney complex genes, and its locus (17q22-24) are rarely altered in pituitary tumours outside the Carney complex. *J Med Genet* **39** e78.
- Sang N, Fang J, Srinivas V, Leshchinsky I & Caro J 2002 Carboxyl-terminal transactivation activity of hypoxia-inducible factor 1 alpha is governed by a von Hippel-Lindau protein-independent, hydroxylation-regulated association with p300/CBP. *Mol Cell Biol* **22** 2984-2992.
- Schechter J 1972 Ultrastructural changes in the capillary bed of human pituitary tumors. *Am J Pathol* **67** 109-126.
- Schechter J, Goldsmith P, Wilson C & Weiner R 1988 Morphological evidence for the presence of arteries in human prolactinomas. *J Clin Endocrinol Metab* **67** 713-719.
- Schechter J, Pattison A & Pattison T 1996 Basic fibroblast growth factor within endothelial cells during vascularization of the anterior pituitary. *Anat Rec* **245** 46-52.
- Schechter JE, Pattison A & Pattison T 1993 Development of the vasculature of the anterior pituitary: ontogeny of basic fibroblast growth factor. *Dev Dyn* **197** 81-93.
- Schlechte JA 2003 Clinical practice. Prolactinoma. *N Engl J Med* **349** 2035-2041.
- Schmidt D & Muller S 2002 Members of the PIAS family act as SUMO ligases for c-Jun and p53 and repress p53 activity. *Proc Natl Acad Sci U S A* **99** 2872-2877.
- Schofield CJ & Zhang Z 1999 Structural and mechanistic studies on 2-oxoglutarate-dependent oxygenases and related enzymes. *Curr Opin Struct Biol* **9** 722-731.
- Schulte HM, Oldfield EH, Allolio B, Katz DA, Berkman RA & Ali IU 1991 Clonal composition of pituitary adenomas in patients with Cushing's disease: determination by X-chromosome inactivation analysis. *J Clin Endocrinol Metab* **73** 1302-1308.
- Schwarz DS, Hutvagner G, Haley B & Zamore PD 2002 Evidence that siRNAs function as guides, not primers, in the Drosophila and human RNAi pathways. *Mol Cell* **10** 537-548.
- Schwarz SE, Matuschewski K, Liakopoulos D, Scheffner M & Jentsch S 1998 The ubiquitin-like proteins SMT3 and SUMO-1 are conjugated by the UBC9 E2 enzyme. *Proc Natl Acad Sci U S A* **95** 560-564.
- Semenza GL 1998 Hypoxia-inducible factor 1: master regulator of O₂ homeostasis. *Curr Opin Genet Dev* **8** 588-594.
- Semenza GL 2003 Targeting HIF-1 for cancer therapy. *Nat Rev Cancer* **3** 721-732.
- Senger DR, Galli SJ, Dvorak AM, Perruzzi CA, Harvey VS & Dvorak HF 1983 Tumor cells secrete a vascular permeability factor that promotes accumulation of ascites fluid. *Science* **219** 983-985.

Shao R, Zhang FP, Tian F, Anders Friberg P, Wang X, Sjoland H & Billig H 2004 Increase of SUMO-1 expression in response to hypoxia: direct interaction with HIF-1alpha in adult mouse brain and heart in vivo. *FEBS Lett* **569** 293-300.

Sharp PS 1995 The role of growth factors in the development of diabetic retinopathy. *Metabolism* **44** 72-75.

Shima DT, Deutsch U & D'Amore PA 1995 Hypoxic induction of vascular endothelial growth factor (VEGF) in human epithelial cells is mediated by increases in mRNA stability. *FEBS Lett* **370** 203-208.

Smith LE, Shen W, Perruzzi C, Soker S, Kinose F, Xu X, Robinson G, Driver S, Bischoff J, Zhang B, et al. 1999 Regulation of vascular endothelial growth factor-dependent retinal neovascularization by insulin-like growth factor-1 receptor. *Nat Med* **5** 1390-1395.

Snyder PJ 1985 Gonadotroph cell adenomas of the pituitary. *Endocr Rev* **6** 552-563.

Soker S, Takashima S, Miao HQ, Neufeld G & Klagsbrun M 1998 Neuropilin-1 is expressed by endothelial and tumor cells as an isoform-specific receptor for vascular endothelial growth factor. *Cell* **92** 735-745.

Sondell M, Lundborg G & Kanje M 1999 Vascular endothelial growth factor has neurotrophic activity and stimulates axonal outgrowth, enhancing cell survival and Schwann cell proliferation in the peripheral nervous system. *J Neurosci* **19** 5731-5740.

Srinivas V, Zhang LP, Zhu XH & Caro J 1999 Characterization of an oxygen/redox-dependent degradation domain of hypoxia-inducible factor alpha (HIF-alpha) proteins. *Biochem Biophys Res Commun* **260** 557-561.

Steinbrech DS, Mehrara BJ, Saadeh PB, Greenwald JA, Spector JA, Gittes GK & Longaker MT 2000 VEGF expression in an osteoblast-like cell line is regulated by a hypoxia response mechanism. *Am J Physiol Cell Physiol* **278** C853-860.

Stepien H, Grochal M, Zielinski KW, Mucha S, Kunert-Radek J, Kulig A, Stawowy A & Pisarek H 1996 Inhibitory effects of fumagillin and its analogue TNP-470 on the function, morphology and angiogenesis of an oestrogen-induced prolactinoma in Fischer 344 rats. *J Endocrinol* **150** 99-106.

Stiehl DP, Jelkmann W, Wenger RH & Hellwig-Burgel T 2002 Normoxic induction of the hypoxia-inducible factor 1alpha by insulin and interleukin-1beta involves the phosphatidylinositol 3-kinase pathway. *FEBS Lett* **512** 157-162.

Swearingen B & Biller BM Eds 2008a *Diagnosis and management of pituitary disorders: Molecular pathogenesis of pituitary adenomas*: Humana press.

Swearingen B & Biller BM Eds 2008b *Diagnosis and management of pituitary disorders: Pathology of pituitary adenomas*: Humana press.

Sztal-Mazer S, Topliss DJ, Simpson RW, Hamblin PS, Rosenfeld JV & McLean CA 2008 Gonadotroph adenoma in multiple endocrine neoplasia type 1. *Endocr Pract* **14** 592-594.

- Takechi A, Uozumi T, Kawamoto K, Ito A, Kurisu K & Sudo K 1994 Inhibitory effect of TNP-470, a new anti-angiogenic agent, on the estrogen induced rat pituitary tumors. *Anticancer Res* **14** 157-162.
- Talks KL, Turley H, Gatter KC, Maxwell PH, Pugh CW, Ratcliffe PJ & Harris AL 2000 The expression and distribution of the hypoxia-inducible factors HIF-1alpha and HIF-2alpha in normal human tissues, cancers, and tumor-associated macrophages. *Am J Pathol* **157** 411-421.
- Tanaka C, Kimura T, Yang P, Moritani M, Yamaoka T, Yamada S, Sano T, Yoshimoto K & Itakura M 1998 Analysis of loss of heterozygosity on chromosome 11 and infrequent inactivation of the MEN1 gene in sporadic pituitary adenomas. *J Clin Endocrinol Metab* **83** 2631-2634.
- Tashiro H, Katabuchi H, Ohtake H, Kaku T, Ushio Y & Okamura H 1999 A follicle-stimulating hormone-secreting gonadotroph adenoma with ovarian enlargement in a 10-year-old girl. *Fertil Steril* **72** 158-160.
- Teodoro JG, Evans SK & Green MR 2007 Inhibition of tumor angiogenesis by p53: a new role for the guardian of the genome. *J Mol Med* **85** 1175-1186.
- Terman BI, Dougher-Vermazen M, Carrion ME, Dimitrov D, Armellino DC, Gospodarowicz D & Bohlen P 1992 Identification of the KDR tyrosine kinase as a receptor for vascular endothelial cell growth factor. *Biochem Biophys Res Commun* **187** 1579-1586.
- Tetsu O & McCormick F 1999 Beta-catenin regulates expression of cyclin D1 in colon carcinoma cells. *Nature* **398** 422-426.
- Theodoropoulou M, Cavallari I, Barzon L, D'Agostino DM, Ferro T, Arzberger T, Grubler Y, Schaaf L, Losa M, Fallo F, et al. 2004 Differential expression of menin in sporadic pituitary adenomas. *Endocr Relat Cancer* **11** 333-344.
- Theodosios DT 2002 Oxytocin-secreting neurons: A physiological model of morphological neuronal and glial plasticity in the adult hypothalamus. *Front Neuroendocrinol* **23** 101-135.
- Tischer E, Mitchell R, Hartman T, Silva M, Gospodarowicz D, Fiddes JC & Abraham JA 1991 The human gene for vascular endothelial growth factor. Multiple protein forms are encoded through alternative exon splicing. *J Biol Chem* **266** 11947-11954.
- Tordjman K, Stern N, Ouaknine G, Yossiphov Y, Razon N, Nordenskjold M & Friedman E 1993 Activating mutations of the Gs alpha-gene in nonfunctioning pituitary tumors. *J Clin Endocrinol Metab* **77** 765-769.
- Tuffnell DJ, Cartmill RS & Lilford RJ 1991 Fetal movements; factors affecting their perception. *Eur J Obstet Gynecol Reprod Biol* **39** 165-167.
- Turner HE, Harris AL, Melmed S & Wass JA 2003 Angiogenesis in endocrine tumors. *Endocr Rev* **24** 600-632.
- Turner HE, Nagy Z, Gatter KC, Esiri MM, Harris AL & Wass JA 2000a Angiogenesis in pituitary adenomas - relationship to endocrine function, treatment and outcome. *J Endocrinol* **165** 475-481.

- Turner HE, Nagy Z, Gatter KC, Esiri MM, Harris AL & Wass JA 2000b Angiogenesis in pituitary adenomas and the normal pituitary gland. *J Clin Endocrinol Metab* **85** 1159-1162.
- Turner KJ, Moore JW, Jones A, Taylor CF, Cuthbert-Heavens D, Han C, Leek RD, Gatter KC, Maxwell PH, Ratcliffe PJ, et al. 2002 Expression of hypoxia-inducible factors in human renal cancer: relationship to angiogenesis and to the von Hippel-Lindau gene mutation. *Cancer Res* **62** 2957-2961.
- Vallar L, Spada A & Giannattasio G 1987 Altered Gs and adenylate cyclase activity in human GH-secreting pituitary adenomas. *Nature* **330** 566-568.
- Verger A, Perdomo J & Crossley M 2003 Modification with SUMO. A role in transcriptional regulation. *EMBO Rep* **4** 137-142.
- Viacava P, Gasperi M, Acerbi G, Manetti L, Cecconi E, Bonadio AG, Naccarato AG, Acerbi F, Parenti G, Lupi I, et al. 2003 Microvascular density and vascular endothelial growth factor expression in normal pituitary tissue and pituitary adenomas. *J Endocrinol Invest* **26** 23-28.
- Vidal S, Horvath E, Kovacs K, Kuroki T, Lloyd RV & Scheithauer BW 2003a Expression of hypoxia-inducible factor-1alpha (HIF-1alpha) in pituitary tumours. *Histol Histopathol* **18** 679-686.
- Vidal S, Horvath E, Kovacs K, Lloyd RV & Scheithauer BW 2003b Microvascular structural entropy: a novel approach to assess angiogenesis in pituitary tumors. *Endocr Pathol* **14** 239-247.
- Vidal S, Kovacs K, Cohen SM, Stefanescu L, Lloyd RV & Scheithauer BW 1999 Localization of vascular endothelial growth factor in nontumorous human pituitaries. *Endocr Pathol* **10** 109-122.
- Vidal S, Kovacs K, Horvath E, Scheithauer BW, Kuroki T & Lloyd RV 2001 Microvessel density in pituitary adenomas and carcinomas. *Virchows Arch* **438** 595-602.
- Vierimaa O, Georgitsi M, Lehtonen R, Vahteristo P, Kokko A, Raitila A, Tuppurainen K, Ebeling TM, Salmela PI, Paschke R, et al. 2006 Pituitary adenoma predisposition caused by germline mutations in the AIP gene. *Science* **312** 1228-1230.
- Vlotides G, Chen YH, Eigler T, Ren SG & Melmed S 2009 Fibroblast growth factor-2 autofeedback regulation in pituitary folliculostellate TtT/GF cells. *Endocrinology* **150** 3252-3258.
- Volarevic S & Thomas G 2001 Role of S6 phosphorylation and S6 kinase in cell growth. *Prog Nucleic Acid Res Mol Biol* **65** 101-127.
- Wang GL, Jiang BH & Semenza GL 1995 Effect of protein kinase and phosphatase inhibitors on expression of hypoxia-inducible factor 1. *Biochem Biophys Res Commun* **216** 669-675.
- Ward RD, Stone BM, Raetzman LT & Camper SA 2006 Cell proliferation and vascularization in mouse models of pituitary hormone deficiency. *Mol Endocrinol* **20** 1378-1390.
- Webb JD, Coleman ML & Pugh CW 2009 Hypoxia, hypoxia-inducible factors (HIF), HIF hydroxylases and oxygen sensing. *Cell Mol Life Sci* **66** 3539-3554.

- Weidner N, Carroll PR, Flax J, Blumenfeld W & Folkman J 1993 Tumor angiogenesis correlates with metastasis in invasive prostate carcinoma. *Am J Pathol* **143** 401-409.
- Weidner N, Folkman J, Pozza F, Bevilacqua P, Allred EN, Moore DH, Meli S & Gasparini G 1992 Tumor angiogenesis: a new significant and independent prognostic indicator in early-stage breast carcinoma. *J Natl Cancer Inst* **84** 1875-1887.
- Weidner N, Semple JP, Welch WR & Folkman J 1991 Tumor angiogenesis and metastasis--correlation in invasive breast carcinoma. *N Engl J Med* **324** 1-8.
- Wenbin C, Asai A, Teramoto A, Sanno N & Kirino T 1999 Mutations of the MEN1 tumor suppressor gene in sporadic pituitary tumors. *Cancer Lett* **142** 43-47.
- Wilkinson KA & Henley JM 2010 Mechanisms, regulation and consequences of protein SUMOylation. *Biochem J* **428** 133-145.
- Williamson EA, Ince PG, Harrison D, Kendall-Taylor P & Harris PE 1995 G-protein mutations in human pituitary adrenocorticotrophic hormone-secreting adenomas. *Eur J Clin Invest* **25** 128-131.
- Yamamoto H, Ihara M, Matsuura Y & Kikuchi A 2003 Sumoylation is involved in beta-catenin-dependent activation of Tcf-4. *EMBO J* **22** 2047-2059.
- Yamamoto T, Nishizawa Y, Tsuji M, Saitoh Y, Funai H, Hirai T, Sugihara A, Tsujimura T, Nakata Y, Tshiguro S, et al. 1999 Expression of vascular endothelial growth factor in normal pituitary cells and pituitary adenomas producing adrenocorticotrophic hormone *Endocrine Pathology* **10** 157-164.
- Yamasaki H, Mizusawa N, Nagahiro S, Yamada S, Sano T, Itakura M & Yoshimoto K 2003 GH-secreting pituitary adenomas infrequently contain inactivating mutations of PRKAR1A and LOH of 17q23-24. *Clin Endocrinol (Oxf)* **58** 464-470.
- Yoshida D, Kim K, Yamazaki M & Teramoto A 2005 Expression of hypoxia-inducible factor 1alpha and cathepsin D in pituitary adenomas. *Endocr Pathol* **16** 123-131.
- Yoshida D & Teramoto A 2007 Enhancement of pituitary adenoma cell invasion and adhesion is mediated by discoidin domain receptor-1. *J Neurooncol* **82** 29-40.
- Yoshino A, Katayama Y, Ogino A, Watanabe T, Yachi K, Ohta T, Komine C, Yokoyama T & Fukushima T 2007 Promoter hypermethylation profile of cell cycle regulator genes in pituitary adenomas. *J Neurooncol* **83** 153-162.
- Yu JL, Rak JW, Carmeliet P, Nagy A, Kerbel RS & Coomber BL 2001 Heterogeneous vascular dependence of tumor cell populations. *Am J Pathol* **158** 1325-1334.
- Yuan Y, Hilliard G, Ferguson T & Millhorn DE 2003 Cobalt inhibits the interaction between hypoxia-inducible factor-alpha and von Hippel-Lindau protein by direct binding to hypoxia-inducible factor-alpha. *J Biol Chem* **278** 15911-15916.
- Yuh WT, Fisher DJ, Nguyen HD, Tali ET, Gao F, Simonson TM & Schlechte JA 1994 Sequential MR enhancement pattern in normal pituitary gland and in pituitary adenoma. *Am J Neuroradiol* **15** 101-108.

- Zelzer E, Levy Y, Kahana C, Shilo BZ, Rubinstein M & Cohen B 1998 Insulin induces transcription of target genes through the hypoxia-inducible factor HIF-1alpha/ARNT. *EMBO J* **17** 5085-5094.
- Zhang SX, Gozal D, Sachleben LR, Jr., Rane M, Klein JB & Gozal E 2003 Hypoxia induces an autocrine-paracrine survival pathway via platelet-derived growth factor (PDGF)-B/PDGF-beta receptor/phosphatidylinositol 3-kinase/Akt signaling in RN46A neuronal cells. *FASEB J* **17** 1709-1711.
- Zhang X, Horwitz GA, Heaney AP, Nakashima M, Prezant TR, Bronstein MD & Melmed S 1999 Pituitary tumor transforming gene (PTTG) expression in pituitary adenomas. *J Clin Endocrinol Metab* **84** 761-767.
- Zhong H, De Marzo AM, Laughner E, Lim M, Hilton DA, Zagzag D, Buechler P, Isaacs WB, Semenza GL & Simons JW 1999 Overexpression of hypoxia-inducible factor 1alpha in common human cancers and their metastases. *Cancer Res* **59** 5830-5835.
- Zhuang Z, Ezzat SZ, Vortmeyer AO, Weil R, Oldfield EH, Park WS, Pack S, Huang S, Agarwal SK, Guru SC, et al. 1997 Mutations of the MEN1 tumor suppressor gene in pituitary tumors. *Cancer Res* **57** 5446-5451.

8 Abbreviations

2-OG	2-oxoglutarate
α -MSH	Alpha-melanocyte stimulating hormone
ACTH	Adrenocorticotropic hormone
AHR	Aryl hydrocarbon receptor
AIP	Aryl hydrocarbon receptor interacting protein
APL	Acute promyelocytic leukemia
ARD1	Arrest-defective-1
AVP	Arginine vasopressin
ARNT	Aryl hydrocarbon receptor nuclear translocator
bFGF	Basic fibroblast growth factor
bHLH	Basic helix-loop-helix
CD31	Platelet endothelial cell adhesion molecule
CDK	Cyclin-dependent kinase
CDKI	Cyclin-dependent kinase inhibitor
CRH	Corticotropin-releasing hormone
D2R	Dopamine 2 receptor
EC	Endothelial cell
ECM	Extracellular matrix
ER	Estrogen receptor
F8	Endothelial antigens factor eight-related antigen
FIH	Factor inhibiting HIF-1
FS	Folliculostellate cell
FSH	Follicle-stimulating hormone
GFPA	Glial fibrillary acidic protein
GH	Growth hormone
GHRH	Growth-hormone-releasing hormone
GnRH	Gonadotropin-releasing hormone
GR	Glucocorticoid receptor
HIF-1	Hypoxia inducible factor-1
HRE	Hypoxia response element

IGF-1	Insulin-like growth factor-1
IL-6	Interleukin-6
LH	Luteinizing hormone
LOH	Loss of heterozygosity
MAPK	Mitogen-activated protein kinase
MEN1	Multiple endocrine type 1
MMP	Matrix metalloproteinase
mTOR	Mammalian target of rapamycin
MVD	Microvessel density
NF- κ B	Nuclear factor- κ B
NGF	Nerve growth factor
ODDD	Oxygen-dependent degradation domain
PAS domain	Per-ARNT-Sim domain
PAS stain	Periodic acid-Schiff stain
PDGF	Platelet-derived growth factor
PHD	Prolyl hydroxylase
PI3K	Phosphatidylinositol 3-kinase
PIAS1	Protein inhibitor of activated STAT-1
Pit-1	Pituitary transcription factor 1
PKA	Protein kinase-A
PML	Promyelocytic leukemia protein
POMC	Pro-opiomelanocortin
pRb	Retinoblastoma protein
PRL	Prolactin
Prop1	Prophet of pituitary transcription factor 1
PTAG	Pituitary tumor apoptosis gene
PTTG	Pituitary tumor transforming gene
RAR	Retinoic acid receptor
SAE	SUMO-activating enzyme
SF-1	Steroidogenic factor-1
STAT	Signal transduction and transcription protein
SUMO	Small ubiquitin-related modifier

TAD	Transactivation domain
TGF- β	Transforming growth factor-beta
Tpit-1	T-box transcription factor
TR β	Thyroid hormone receptor β
TRH	Thyrotropin-releasing hormone
TSH	Thyroid-stimulating hormone
Ubc9	Ubiquitin-conjugating 9
UEA1	Ulex europaeus agglutinin 1
VEGF	Vascular endothelial growth factor
VHL	Von Hippel-lindau
VSMC	Vascular smooth muscle cell

9 Acknowledgements

This work was done under the supervision of Dr. Ulrich Renner in the Department of Clinical Neuroendocrinology (group leader: Prof. Dr. Günter. K. Stalla), Max Planck Institute of Psychiatry in Munich (Director: Prof. Dr. Dr. Dr. h. c. Florian Holsboer).

I would like to thank Prof. Dr. Dr. Dr. h. c. Florian Holsboer for giving me the opportunity to work in this institute.

I would also like to thank Prof. Dr. Günter. K. Stalla, the head of our group, for giving me the great chance of joining in his renowned group and conducting my doctoral research in the intriguing field of pituitary adenomas. He has provided vital support for me to get well trained in my discipline, and his generous encouragement was essential to me in completing this dissertation. His excellent outstanding achievements in scientific and clinical research are great inspirations to me and my research.

I would like to thank Prof. Dr. Rainer Landgraf for accepting me as his registered PhD student in Ludwig-Maximilians-Universität München. His help, support and encouragement have been indispensable for me to pursue the doctor's degree.

I also want to express my deep appreciation to Dr. Ulrich Renner, for his supervision on this project and his continuous help, support, patience, understanding, friendship, encouragement and concern during my stay. I highly appreciate the freedom he has always given me in the academic research and the valuable suggestions he has provided when I encountered difficulties on the project. His guidance was instrumental to my PhD study and would continue to benefit me in the future.

I would like to thank Prof. Dr. Eduardo Arzt from FCEN-Universidad de Buenos Aires, Argentina. He always provided me with constructive suggestions and strong encouragement. The previous study on RSUME in his outstanding group is the basis of this thesis.

I would like to thank Dr. Chiara Onofri for introducing me the techniques and getting me familiar with the lab at the beginning. She has given me a supportive, helpful hand when I started to work in the new environment.

I would like to sincerely thank Dr. Marily Theodoropoulou for her great help during my PhD study. She has always given me practical suggestions and helped me out in many problems. Her scientific thoughts have inspired me a lot. Her optimistic personality and energetic attitude in scientific career has influenced me and her concern has made me feel touched and warm.

I would like to thank Yonghe Wu for his enthusiastic help with the experiments of PCR and also for his substantial support during the last three years.

I would like to thank my dear friends Dr. Vesna Cerovac and Jose Luis Monteserin Garcia for their help, support and warm concern as well as for all the fun we had together during the tough PhD life.

I would like to thank all my colleagues in the lab for the friendly, cooperative environment they have provided me and also for their selfless and enthusiastic help. I would like to give many thanks to Monika Makrutzki, Johanna Stalla, Bärbel Wölfel, Dr. Marta Labeur, Dr. Eliane Correa de Santana, Christian Schaaf and Stjepan Curic. I have spent a lot of joyful time with all of them and this wonderful memory will never fade away.

Last but not least, I want to deliver my deepest gratitude to my beloved parents and grandparents in China, my brother in Australia, and my boyfriend Zhang Yaoyang who has kept me company in Munich during my graduate study. They have showed enormous love and support to me, which have been the greatest inspiration to my work. All that I am or ever have achieved, I owe to them.

Curriculum Vitae

Personal information

Name: Shan, Bing

Date of Birth: 19.07.1981

Place of Birth: Zhengzhou, province of Henan, P. R. China

Email: bing@mpipsykl.mpg.de

Education

- | | |
|---------------|--|
| 2007- Present | Ph.D. student
Department of Biology II
Ludwig-Maximilians-Universität München , Germany |
| 2004 - 2007 | M. Sc. (Immunology)
Department of Prion Disease
China center for Disease Control and Prevention , China |
| 2000 - 2004 | B. Sc. (Bioengineering)
School of Life Science and Technology
Beijing Institute of Technology , China |

Professional employment

- | | |
|----------------|--|
| 2007 - Present | Ph.D. student
Department of Neuroendocrinology (AG STALLA)
Max Planck Institute of Psychiatry , Germany |
|----------------|--|

Awards

Deutschen Gesellschaft für Endokrinologie Ernst and Berta Scharrer Prize 2010

Academic presentations

1. Shan B. The novel sumoylation enhancer RSUME is implicated in pituitary tumour pathogenesis. **Presentation of Deutschen Gesellschaft für Endokrinologie Ernst and Berta Scharrer Preis 2010**, 53. Symposion der Deutschen Gesellschaft für Endokrinologie und Jahrestagung der Slowakischen Gesellschaft für endokrinologie, Leipzig, Germany, 3-6 March 2010.

2. Shan B, Onofri C, Theodoropoulou M, Buchfelder M, Kreutzer J, Rachinger W, Losa M, Arzt E, Stalla GK, Renner U. Expression and regulation of HIF-1 α and RSUME in murine and human pituitary tumor cells. **Oral presentation**, 13. Jahrestagung der Sektion Neuroendokrinologie der Deutschen Gesellschaft für Endokrinologie (DGE), Hamburg, Germany, 27 November 2009.
3. Shan B, Onofri C, Theodoropoulou M, Buchfelder M, Kreutzer J, Rachinger W, Losa M, Arzt E, Stalla GK, Renner U. Expression and regulation of HIF-1 α and RSUME in murine and human pituitary tumor cells. **Poster presentation**, 11th European Congress of Endocrinology, Istanbul, Turkey, 25-29 April 2009.
4. Shan B, Onofri C, Theodoropoulou M, Buchfelder M, Kreutzer J, Rachinger W, Losa M, Arzt E, Stalla GK, Renner U. Expression and regulation of HIF-1 α and RSUME in murine and human pituitary tumor cells. **Oral presentation**, 52th Symposium der Deutschen Gesellschaft für Endokrinologie (DGE), Giessen, Germany, 4-7 March 2009.
5. Shan B, Onofri C, Theodoropoulou M, Buchfelder M, Kreutzer J, Rachinger W, Losa M, Arzt E, Stalla GK, Renner U. Expression and regulation of HIF-1 α and RSUME in murine and human pituitary tumor cells. **Poster presentation**, 12. Jahrestagung der Sektion Neuroendokrinologie der Deutschen Gesellschaft für Endokrinologie (DGE), Bamberg, Germany, 24 October 2008.

Publications

1. Schaaf C, **Shan B**, Onofri C, Stalla GK, Arzt E, Schilling T, Perone MJ, Renner U. Curcumin inhibits the growth, induces apoptosis and modulates the function of pituitary folliculostellate cells. *Neuroendocrinology*. 2010; 91(2):200-10. Epub 2010 Feb 17.
2. Schaaf C, **Shan B**, Buchfelder M, Losa M, Kreutzer J, Rachinger W, Stalla GK, Schilling T, Arzt E, Perone MJ, Renner U. Curcumin acts anti-tumourigenic and hormone-suppressive in murine and human pituitary tumour cells in vitro and in vivo. *Endocr Relat Cancer*. 2009 Dec; 16(4):1339-50.
3. Shi XH, Han J, Zhang J, Shi Q, Chen JM, Xia SL, Xie ZQ, Shen XJ, **Shan B**, Lei YJ, Shi S, Zhou W, Zhang BY, Gao C, Liu YH, Song J, Guo YJ, Wang DX, Xu BL, Dong XP. Clinical, histopathological and genetic studies in a family with fatal familial insomnia. *Infect Genet Evol*. 2010 Mar; 10 (2):292-7. Epub 2010 Jan 22.
4. Shi S, Dong CF, Wang GR, Wang X, An R, Chen JM, **Shan B**, Zhang BY, Xu K, Shi Q, Tian C, Gao C, Han J, Dong XP. PrP(Sc) of scrapie 263K propagates efficiently in

- spleen and muscle tissues with protein misfolding cyclic amplification. *Virus Res.* 2009 Apr; 141(1):26-33. Epub 2009 Jan 20.
5. Li P, Dong C, Lei Y, **Shan B**, Xiao X, Jiang H, Wang X, Gao C, Shi Q, Xu K, Tian C, Han J, Dong X. Doppel-induced cytotoxicity in human neuronal SH-SY5Y cells is antagonized by the prion protein. *Acta Biochim Biophys Sin (Shanghai)*. 2009 Jan; 41(1):42-53.
 6. Zhang J, Han J, Shi XH, Guo WS, Xia SL, Shi Q, Chen JM, Zhao WQ, Xie ZQ, Shen XJ, Li ML, Lei YJ, Shi S, Zhou W, Zhang BY, Gao C, **Shan B**, Guo YJ, Wang DX, Xu BL, Dong XP. Studies on heredity rule of the first genealogy regarding fatal familial insomnia in Henan province. *Zhonghua Liu Xing Bing Xue Za Zhi*. 2009 Jan; 30 (1):1-5. *Chinese*.
 7. Chen J, Gao C, Shi Q, Wang G, Lei Y, **Shan B**, Zhang B, Dong C, Shi S, Wang X, Tian C, Han J, Dong X. Casein kinase II interacts with prion protein in vitro and forms complex with native prion protein in vivo. *Acta Biochim Biophys Sin (Shanghai)*. 2008 Dec; 40 (12):1039-47.
 8. Chen JM, Gao C, Shi Q, Gao YJ, Lei YJ, **Shan B**, Dong CF, Wang GR, Shi S, Han J, Dong XP. PrP protein can bind to protein kinase CK2 both in native and recombinant forms in vitro. *Bing Du Xue Bao*. 2008 Sep; 24 (5):335-9. *Chinese*.
 9. Dong CF, Huang YX, An R, Chen JM, Wang XF, **Shan B**, Lei YJ, Han L, Zhang BY, Han J, Dong XP. Establishment of an assay for PrP(Sc) detection based on streptomycin precipitation. *Bing Du Xue Bao*. 2008 May; 24 (3):185-9. *Chinese*.
 10. Chen JM, Gao C, Shi Q, **Shan B**, Lei YJ, Dong CF, An R, Wang GR, Zhang BY, Han J, Dong XP. Different expression patterns of CK2 subunits in the brains of experimental animals and patients with transmissible spongiform encephalopathies. *Arch Virol*. 2008; 153 (6):1013-20. Epub 2008 Apr 11.
 11. **Shan B**, Gao C, Chen JM, Bi XY, Zhang BY, Guo Y, Dong CF, An R, Shi Q, Hu JQ, Zhao P, Han J, Dong XP. Establishment of a sandwich ELISA method for detection of vascular endothelial growth factor in serum samples of hepatocellular carcinoma patients. *Biomed Environ Sci*. 2008 Feb; 21(1):69-74.
 12. Dong CF, Wang XF, Wang X, Shi S, Wang GR, **Shan B**, An R, Li XL, Zhang BY, Han J, Dong XP. Molecular interaction between prion protein and GFAP both in native and recombinant forms in vitro. *Med Microbiol Immunol*. 2008 Dec; 197 (4):361-8. Epub 2007 Dec 18.

13. Wang XF, Dong CF, Zhang J, Wan YZ, Li F, Huang YX, Han L, **Shan B**, Gao C, Han J, Dong XP. Human tau protein forms complex with PrP and some GSS- and fCJD-related PrP mutants possess stronger binding activities with tau in vitro. *Mol Cell Biochem.* 2008 Mar; 310 (1-2): 49-55. Epub 2007 Nov 25.
14. Dong CF, Shi S, Wang XF, An R, Li P, Chen JM, Wang X, Wang GR, **Shan B**, Zhang BY, Han J, Dong XP. The N-terminus of PrP is responsible for interacting with tubulin and fCJD related PrP mutants possess stronger inhibitive effect on microtubule assembly in vitro. *Arch Biochem Biophys.* 2008 Feb 1; 470 (1):83-92. Epub 2007 Nov 17.
15. Dong CF, **Shan B**, Wang XF, Han J, Dong XP. Interaction between various PrP segments and GFAP in vitro. *Zhonghua Shi Yan He Lin Chuang Bing Du Xue Za Zhi.* 2007 Sep; 21(3):214-6. *Chinese.*
16. Li P, Han J, **Shan B**, Lei YJ, Zhou W, Jiang HY, Dong XP. Expression of recombinant human doppel protein and analysis of its cytotoxic activities. *Bing Du Xue Bao.* 2007 Jul; 23 (4):265-9. *Chinese.*
17. Dong CF, Wang XF, An R, Chen JM, **Shan B**, Han L, Lei YJ, Han J, Dong XP. Interaction analysis between various PrP fusion proteins and the tubulin in vitro. *Bing Du Xue Bao.* 2007 Jan; 23 (1):28-32. *Chinese.*